DISS. ETH No.: **20062**

Motor physiology and neural network anatomy in rats following incomplete cervical spinal cord injury

A dissertation submitted to

ETH ZURICH

for the degree

Doctor of Science

ETH Zurich

presented by

Linard Peider Filli

Master of Science ETH in Biology
12.03.1984
Val Müstair, GR

Accepted on the recommendation of

Prof. Dr. Martin E. Schwab

Prof. Dr. Volker Dietz

Prof. Dr. Kevan Martin

Prof. Dr. Fritjof Helmchen

2011

Table of content

Summary

Spinal cord injury and subsequent pathophysiological processes often lead to devastating and irreversible deficits in sensorimotor and autonomous functions in affected patients. Despite substantial progress in clinical care and rehabilitative training, spontaneous restoration of neurological functions after spinal injury is still limited. Extensive laboratory research over the last decades in animal models has shed new light on many of the mechanisms responsible for the restricted neuronal plasticity and functional recovery. Different growth-inhibitory components of the central nervous systems were identified and subsequently targeted by experimental treatment strategies to enhance neuronal plasticity and functional recovery in animal models of spinal cord injury. Indeed, multiple experimental strategies revealed significant improvements in neuroanatomical or sensorimotor properties of the injured animals. Nevertheless, the clinical translation of these experimental treatments emerged to be enormously challenging. The issue of translational research in the field of spinal cord repair is reviewed in chapter 1.

Chapter 2 of the thesis deals with a second important topic of translational spinal cord injury research, which is the accurate assessment of locomotor performance after different forms of neuropathologies. Behavioral analysis in animal research is frequently performed by tests which suffer from subjectivity, non-linearity and insensitivity. The subjectivity hinders the comparison of data across laboratories, and the insensitive tests impede the accurate analysis of, for instance, treatment-induced functional recovery. We constructed a behavioral testing battery including 4 different forms of locomotion, which allows a global, comprehensive and quantitative monitoring of locomotor functions in rodents. Transgenic mice and rats with different forms of spinal cord injury and ischemic stroke were investigated by kinematic analysis to validate the reliability and sensitivity of the testing system. The acquisition of multiple quantitative readouts during skilled locomotion, walking, wading and swimming allowed an accurate profiling of locomotor recovery after different types of central nervous system injury in adult rodents.

The most abundant type of spinal injury among humans is cervical incomplete spinal cord injury, resulting in sensorimotor impairments of upper and lower extremities. Nevertheless, studies investigating tetraplegic animal models and forelimb motor functions are rare. In Chapter 3 and 4 of the thesis, physiological and anatomical features of rats with a unilateral C4/C5 hemisection were investigated. This type of lesion leads to the Brown-Séquard syndrome revealing ipsilesional

weakness in motor and proprioceptive functions and contralesional loss of pain and temperature sensation.

Chapter 3 of the present work displays the physiological similarities between rats and humans with unilateral damage of the spinal cord. Similar to humans with incomplete cervical spinal cord injuries, rats with a unilateral C4/C5 hemisection recovered substantial locomotor functions of lower extremities, but only limited functional recovery of upper extremities. Potential reasons accounting for this disproportional recovery pattern were investigated in detail. Additionally, differential effects of monoaminergic agonists on fore- and hindlimb locomotor performance were demonstrated. Monoaminergic agonists, which have repeatedly shown to massively facilitate hindlimb stepping in different animal species with complete spinal cord transection, revealed minor and mostly negative effects on hindlimb locomotion, and no effects on forelimb functions in animals with a C4/C5 hemisection. Taken together, this chapter displayed remarkable differences in the functionality of fore- and hindlimb motor networks.

Anatomical plasticity following unilateral C4/C5 hemisection was examined in chapter 4. The combination of retrograde/anterograde neuroanatomical tracing with immunohistochemical stainings revealed spontaneous anatomical plasticity of different neuronal systems. Severed reticulospinal fibers originating from the nucleus reticularis gigantocellularis showed a massive fiber sprouting rostral to the spinal lesion, which persisted up to 43 days post injury. These fibers were colocalized with the presynaptic marker vGLUT2 and additionally formed close-appositions to C3-C4 propriospinal neurons. These neurons were shown to re-cross the lesion site and to innervate the ipsilesional cervical enlargement, thereby bridging supraspinal commands to the denervated spinal cord. The functional relevance of this propriospinal relay is currently investigated.

Finally, Chapter 5 of the thesis provides a general conclusion and outlook about the present doctoral thesis.

Summarized, this thesis provides detailed information about physiological and neuroanatomical aspects upon incomplete cervical spinal cord injury in adult rats. A new, comprehensive behavioral setup enabled a quantitative and sensitive profiling of locomotor functions. Basic differences between fore-and hindlimb spinal circuits and their functional dependence on descending inputs and pharmacological spinal excitation were displayed. Moreover, anatomical investigations resolved neuronal plasticity at different levels of the central nervous system. Descending reticulospinal fibers

and propriospinal neurons rostral to the lesion anatomically rearranged post injury in order to relay supraspinal information to the denervated cervical enlargement.

Zusammenfassung

Rückenmarksverletzungen und daraus resultierende Folgeprozesse führen oft zu bleibenden Schäden der motorischen, sensorischen und autonomen Funktionen in betroffenen Patienten. Trotz grosser Fortschritte in der medizinischen Betreuung und in rehabilitativen Behandlungsstrategien, erholen sich diese Leute nur geringfügig (z.B. motorisch oder sensorische Funktionen). Umfangreiche Tierversuche während der letzten Jahrzehnte haben viele der Mechanismen entschlüsselt, die für die geringe neuronale Plastizität und funktionelle Erholung verantwortlich sind. Verschiedene dieser wachstumshemmenden Bestandteile des Zentralnervensystems wurden gefunden und in späteren Tierexperimenten anviesiert, um die neuronale Plastizität und die funktionelle Erholung nach Rückenmarksverletzungen zu erhöhen. Mehrere dieser experimentellen Strategien haben tatsächlich deutliche Verbesserungen von neuroanatomischen oder sensorischen/motorischen Eigenschaften in verletzten Tieren hervorrufen können. Nichtsdestotrotz stellte sich die klinische Umsetzung dieser tierexperimentellen Behandlungen als äusserst schwierig heraus. Die Thematik der translationellen Forschung im Feld der Rückenmarksregeneration wird in Kapitel 1 besprochen.

Im Kapitel 2 dieser Doktorarbeit wird eine weitere wichtige Thematik in der Forschung von Neuropathologien besprochen. Es geht um die präzise Messung der Fortbewegungsfähigkeit nach verschiedenen Formen von neurologischen Pathologien. Verhaltensanalysen in Tierexperimenten sind immer noch häufig subjektiv, nicht-linear und unzureichend genau. Dies erschwert den Vergleich von Daten zwischen verschiedenen Laboratorien und die Erkennung von potentiellen Behandlungserfolgen in Tiermodellen. Wir haben in unserem Labor nun eine Verhaltensbatterie konstruiert, die 4 verschiedenen Fortbewegungsarten gleichzeitig untersucht. Dies ermöglicht eine vollständige, verständliche und quantitative Untersuchung der Fortbewegung in Tiermodellen. Transgene Mäuse und Ratten mit verschiedenen Arten von Rückenmarkverletzungen und einem Hirnschlags-Modell sind kinematisch untersucht worden, um die Verlässlichkeit und Sensitivität des Testapparates zu überprüfen. Die parallele Datenerhebung in den verschiedenen Tests (Leiterlaufen, normales Laufen, Waten und Schwimmen) ermöglichte eine genaue Profilerstellung und Defizitanalyse der Fortbewegung in Tiermodellen mit verschiedenen Formen von Verletzungen im zentralen Nervensystem.

Die am häufigsten auftretende Form von menschlichen Rückenmarksverletzungen ist die inkomplette Verletzung des zervikalen Rückenmarks. Diese Art der Rückenmarksverletzung erzeugt sensorische/motorische Schäden in Armen und Beinen. Trotz der Häufigkeit ihres Auftretens werden

diese Verletzung und die daraus folgenden Defizite in Armen und Händen nur selten in Tiermodellen untersucht. Kapitel 3 und 4 dieser Arbeit untersuchten die physiologischen und anatomischen Eigenschaften in Ratten mit einseitiger Verletzung des Rückenmarks auf der zervikalen Höhe C4/C5. Diese Verletzung führt zum Brown-Séquard Syndrome, das sich durch ipsiläsionale Schäden der Motorik und der propriozeptiven Sensorik, und durch den kontralateralen Verlust von Schmerz- und Temperaturempfinden äussert.

Kapitel 3 zeigt die physiologischen Ähnlichkeiten zwischen dem Ratten-Model und dem Menschen mit einseitigen Verletzungen des Rückenmarks auf. Ähnlich dem Menschen zeigten Ratten mit entsprechender Verletzung im zervikalen Rückenmark (C4/C5) starke motorische Verbesserungen der Beinbewegungen, aber nur wenig funktionelle Erholung im betroffenen Arm. Die möglichen Gründe für diese asymmetrische Erholung wurden detailliert untersucht. Zusätzlich wurde entdeckt, dass monoaminerge Agonisten sehr verschieden auf die Vorder- und Hinterbeine wirkten. In früheren Experimenten wurde wiederholt gezeigt, dass die Applikation von monoaminergen Agonisten zu erheblichen Verbesserungen der Hinterbeinfunktionen in Tieren mit kompletter Durchtrennung des Rückenmarks führen kann. Tiere in unserem Experiment, die inkomplette Verletzungen hatten, zeigten eine geringe und meist negative Beeinflussung der Hinterbeinfunktion, und keine Effekte in den Vorderarmen. Zusammengefasst zeigt dieses Kapitel, dass es erhebliche Unterschiede in der Funktionalität zwischen Vorder- und Hinterbeinen gibt.

Kapitel 4 beschäftigte sich mit der anatomischen Plastizität, die nach der unilateralen C4/C5 Hemisektion des Rückenmarks auftritt. Die Kombination von anterograden und retrograden Farbstoff-Techniken mit immunohistochemischen Färbungen hat gezeigt, dass spontane anatomische Plastizität in verschiedenen Teilen des Zentralnervensystems auftritt. Reticulospinalfasern, die aus dem nucleus reticularis gigantocellularis im Hirnstamm entspringen, zeigten ein massives Faserspriessen oberhalb der spinalen Läsion, das bis 43 Tage nach der Verletzung bestehen blieb. Die spriessenden Fasern wurden positiv auf den synaptischen Marker vGLUT2 gefärbt. Dies deutet darauf hin, dass diese Fasern sich in die spinalen Netzwerke verschaltet haben und neuronale Verknüpfungen bilden. Weiter wurde gezeigt, dass die Fasern Verbindungen zu propriospinalen Neuronen herstellten, die oberhalb der Läsion lokalisiert sind. Diese propriospinalen Neurone wiesen Fasern auf, die die Verletzung umgehen konnten und unterhalb der Verletzung wieder endeten. Das ganze System bildete somit einen Umweg um die Läsion, das einen Informationsfluss zwischen Hirn und abgeschnittenen

Rückenmarksteilen wieder ermöglichte. Die funktionelle Bedeutung dieser anatomischen Veränderungen wird in derzeitigen Experimenten erforscht.

Kapitel 5 der Dissertation liefert eine generelle Schlussfolgerung der Doktorarbeit und diskutiert mögliche zukünftige Experimente, um verbleibende Fragen zu klären.

Zusammengefasst liefert diese Doktorarbeit detaillierte Informationen über die physiologischen und neuroananatomischen Aspekte, die nach einer teilweisen zervikalen Rückenmarksverletzung in Ratten auftreten. Ein neuer Verhaltensapparat ermöglichte eine quantitative und genaue Fortbewegungsanalyse, welche für die genaue Verhaltensforschung gebraucht werden kann. Es wurde gezeigt, dass es starke Unterschiede in der Funktionalität zwischen Vorder- und Hinterbeinen gibt. Vorder- und Hinterbeine reagieren sehr verschieden auf Unterbrechungen von Hirnimpulsen und auf spezifische neuromodulatorische Medikamente. Weiter hat die Untersuchung der Anatomie erwiesen, das neuronale Plastizität auf verschiedenen Ebenen des Zentralnervensystems stattfindet. Reticulospinale Hirnstammbahnen haben vermehrt auf propriospinale Neuronen projiziert, die Fasern um die Verletzung wachsen liessen.

Chapter 1

A synopsis of translation in spinal cord repair

In preparation for submission

Abstract

The biological understanding of the central nervous system under intact and pathological circumstances has massively increased by mechanistic laboratory research over the last decades. This resulted in multiple treatment strategies with the collective aim to promote the limited spontaneous recovery occurring in animal models and humans suffering from spinal cord injury. Even though many of the developed laboratory treatments revealed beneficial effects in animal models of spinal cord injury, their translation into successful clinical treatments is difficult. The present review provides a short survey of the current status of spinal cord repair. It further aims to highlight shortcomings in the pre-clinical and clinical sector of translational research which hamper the progression of human spinal cord repair. Major shortcomings in the experimental research concern the often insufficient robustness and reproduction of data and the inaccurate modelling of human spinal cord injury. A major shortcoming in the clinical field of spinal cord repair is related to the lack of reliable and precise clinical outcome measures which allow sensitive monitoring of neurological functions in patients. Moreover, improved prognosis of the neurological outcome is critical for an appropriate patient stratification and for the detection of treatment effects despite of occurring spontaneous functional recovery.

Several networks for spinal cord repair were built with the goal to optimize the conduct of animal studies and human trials. Multiple promising human trials are under current investigation and, if lessons were learned from earlier trials, might be able to sufficiently validate the experimental data in patients. The time has arrived for translational spinal cord repair to convert its high mechanistic knowledge into robust and efficient treatment interventions which are able to induce beneficial neurological effects in humans suffering from spinal cord injury.

Introduction

The field of spinal cord injury (SCI) research as well as clinical care has shown unprecedented progress over the last decades. Clinically, advanced medical care and surgical techniques have decreased the mortality rate of SCI patients from more than 95% before 1940 to less than 5% nowadays [1] . Yet severely injured patients remain wheelchair bound, suffering from significant and permanent losses in their quality of life. In basic neuroscience research of the past 25 years, many important discoveries were made that helped to understand the biological processes following SCI and the mechanisms by which plasticity and re-growth of injured fibers is limited in the adult CNS. Thus, specific growth inhibitory constituents of scars, extracellular matrix and myelin of the spinal cord and brain were identified, and the intrinsic restrictions of growth of adult neurons are being unravelled [2-7],. Moreover, the complex processes of inflammation and secondary damage were intensely studied over the recent years [8,9].

Despite the regeneration- and growth-inhibiting environment of the adult CNS some degree of spontaneous functional recovery is usually observed in patients as well as in animal models of SCI [10-13]. Ambulatory function, for instance, can recover with the help of physiotherapy in incomplete SCI patients, where some spared white matter tracts still pass the lesion site. In contrast, functional recovery is minimal or absent in subjects with very large or total spinal cord lesions, illustrating the important role of descending supra- and proprio-spinal fiber tracts for the restoration of neurological functions.

Multiple experimental attempts have been undertaken to enhance the limited spontaneous recovery occurring after SCI in animal models. The main treatment strategies include (1) neuroprotective and anti-inflammatory treatments, (2) promotion of fiber regeneration and compensatory sprouting, (3) transplantation of ‘bridges’ or stem cells, (4) pharmacological or electrophysiological manipulation of residual sublesional spinal networks, (5) neurorehabilitative training. Results for most of these treatment strategies were able to disclose beneficial effects in animals either on the anatomical/histological level (e.g. increased fiber sprouting), on the level of neurological functions (e.g. improved hindlimb function), or both [14,15]. The current clinical situation with regard to novel treatments for SCI is much less advanced. Several pilot, clinical trials failed or were abandoned [14-17]. Even Methylprednisolone, which was applied as an accepted neuroprotective treatment for acute SCI in many countries is now being resigned due to low or insignificant efficacy and side effects [18]. The only therapeutic intervention which is standard-of-care and internationally applied to maximize functional

recovery in human SCI is rehabilitative training including e.g. weight supported treadmill training [19-21]. Still, large differences exist between clinics and countries with regard to the type and intensity of the rehabilitative therapies applied, and very few systematic and comparative analyses of the efficacy of given therapies and optimal treatment schedules exist.

When assessing the difficulties to translate the successful laboratory treatments into clinical trials and novel therapies for SCI, the desperate situation for neuroprotection in the field of cortical stroke has to be taken into account. There, animal experiments showed clear-cut neuroprotective effects of several agents which all failed to be confirmed in the clinical situation [17].The stroke community reacted by building the Stroke Therapy Academic Industry Roundtable (STAIR) which provides recommendations to improve the quality of pre-clinical studies before entering clinical trials [22]. Although useful, the compliance with the STAIR guidelines has been limited, however [23]. On the clinical level, meta-analyses of the different trials showed that inaccurate trial conduct (not randomized, unblinded), broad inclusion criteria and the unreliable, insensitive outcome measures used were the main reasons for their failure [24-26]. Several research and clinical SCI networks formulated and standardized guidelines for an optimized conduct of pre-clinical and clinical trials, which intend to prompt the clinical translation of experimental treatments [27-31]. The present review aims to provide a synopsis of the complex issue of translation spinal cord repair by reviewing the pre-clinical and clinical status of the field. This review discusses emerging shortcomings in the current experimental studies and the specific problems of clinical trials in the SCI field, which hamper the progression of human spinal cord repair. We feel that the time has arrived for translating the current neurobiological knowledge into efficient, new therapies for humans suffering from SCI.

ASIA Impairment Scale (AIS)	
A	**Complete:** No motor or sensory function is preserved in the sacral segments S4-S5
B	**Sensory Incomplete:** Sensory but not motor function is preserved below the neurological level and includes the sacral segment S4-S5. No motor function is preserved more than three levels below the motor level on either side of the body
C	**Motor Incomplete:** Motor function is preserved below the neurological level, and more than half of key muscles below the neurological level have a muscle grade less than 3
D	**Motor Incomplete:** Motor function is preserved below the neurological level, and at last half of key muscles below the neurological level have a muscle grade of 3 or more
E	**Normal:** Normal motor and sensory function

Table 1: Definition of the ASIA Impairment Scale (AIS) which belongs to the International Standards for Neurological Classification of Spinal Cord Injury (ISNCSCI). Adapted from the scale provided by the American Spinal Injury Association (www.asia-spinalinjury.org)

Current status of spinal cord repair

Experimental SCI research underwent a fast and fruitful progression in the past two decades. Laboratory research in different animal models yielded basic insights into neuroanatomy and neurophysiology and elucidated numerous biological mechanisms occurring in the intact and injured CNS. A frequently used model in experimental SCI research is the complete transection of the thoracic spinal cord, which allows to evaluate the functionality of intrinsic spinal networks in the presence of the sensory afferents, but in the absence of supraspinal and long-propriospinal inputs. Due to the high incidence of sensorimotor complete SCI (approximately 45% of total SCI cases) and its poor prognosis for spontaneous neurological improvement, the investigation of complete SCI models is relevant [10,20,32]. Early studies in spinalized cats revealed their astonishing ability to restore basic locomotor functions when trained on a treadmill, provided with lateral stability and with their forelimbs fixed on a non-moving platform [33]. This important finding has established the basis on which task-specific neurorehabilitative training developed, which is routinely used in clinics nowadays [14]. Furthermore, the impact of spinal excitability on restoration of stepping has impressively been demonstrated by application of monoaminergic agonists, by epidural spinal cord stimulations and especially by their combined application, which massively facilitated locomotor ability in several animal species after complete SCI [34-41]. The experiments in completely spinalized animals disclosed the astonishing capacity of the isolated spinal cord to elicit locomotion under conditions of artificially increased spinal excitability. These findings might provide the basis for a new promising treatment branch, of which epidural stimulation has already been implemented in a current clinical case study [42].

Incomplete models of SCI are used much more frequently, although they exhibit a clearly higher degree of complexity as there is a varying extent of undamaged supra- and proprio-spinal fibers from different systems performing different functions. Incomplete SCI, however, allows to study the role of fiber regeneration and anatomical plasticity of descending supra- and proprio-spinal fibers. Mechanisms including anatomical plasticity of spared fibers (compensatory sprouting) or severed fibers (regenerative sprouting) at different levels in the CNS were shown to be critical for restoration of motor functions. Divers spared tracts such as ascending sensory fibers, descending supraspinal fibers (cortico-, reticulo- and rubro-spinal fibers) and propriospinal fibers have been shown to sprout upon a spinal insult and to be partially associated with functional recovery [45-48]. As few as 10-15% preserved white matter tracts can be sufficient for spontaneous restoration of locomotor functions in animals and humans [43,44]. The knowledge about the spontaneously occurring plasticity and restoration of function is

crucial to develop therapeutic strategies which can further improve neurological outcomes. Therapeutic interventions enhancing the limited fiber regeneration and neuronal plasticity either by stimulating the neuronal growth-machinery (e.g. by neurotrophic factors) or by inactivating growth-inhibitory components (e.g. Nogo-A, PTEN or chondroitin sulfate proteoglycans) are highly promising strategies for future treatments in human SCI [49]. Recent publications also displayed the important role of spinal neural circuitries in restoring locomotor capacity in incomplete models of SCI [50-52].

Clinical SCI research progressed mainly in the sector of primary care and standard-of-care therapies (e.g. neurorehabilitation), where it has gone through optimization and standardization among different centers. Patients are rapidly hospitalized, life-sustaining internistic interventions have improved, and acute interventions such as surgical spinal cord decompression are, if needed, mostly standard nowadays [14]. In parallel, neurorehabilitation programs, which were proven necessary to maximize functional recovery, are routinely used and initiated early after injury. Conventional rehabilitation after SCI comprise training of supported standing and, depending on the motor deficits of the patient, some gait training supported by assistive devices such as walkers, parallel bars and canes [53]. The improved standard-of-care rehabilitation is certainly an important component responsible for the spontaneous functional recovery observed in human patients: around 75% of patients with motor incomplete SCI regain some form of ambulatory function [54-56]. In addition to conventional neurorehabilitation, task-specific training such as body weight supported treadmill training can further induce significant improvements in walking speed, endurance and specific everyday life functions when applied after incomplete SCI [20,21]. Optimal onset and amount of training are still under current investigation and not strictly standardized among centers [56].

Besides physical exercise, however, there have no further therapeutic interventions being translated into efficient treatments for human SCI. Most randomized controlled human trials were performed with neuroprotective drugs which were applied acutely after injury [56]. Neuroprotection-based treatments have, despite of its beneficial effects in animal models, not been proven to be successful in the field of stroke and SCI yet [17,57]. Methylprednisolone, a synthetic glucocorticoid, has been used as standard treatment for acute SCI in the US due to its marked neuroprotective effects in animal models [58]. Methylprednisolone has been subject of 5 prospective randomized acute SCI trials and thus is the most extensively studied agent in acute human SCI [14,59]. However, meager neuroprotective effects which were faced by potentially harmful side effects such as increased susceptibility to infections rendered the treatment controversial and less applied [15]. Ongoing clinical trials investigate the effects

of different neuroprotective drugs (e.g. Minocycline). An alternative strategy to improve neurological recovery is the promotion of fiber regeneration and sprouting in the otherwise growth-inhibiting environment of the CNS. The key role of the myelin-associated protein Nogo-A as growh-inhibitor of the CNS has been demonstrated by functional ablation of Nogo-A or its binding receptor NgR. Functional neutralization has revealed increased axonal regeneration and sprouting in various animal models including mice, rats and primates after different forms of SCI [60-65]. A multicenter trial with the anti-Nogo-A antibody ATI 355 is currently ongoing and has successfully conducted Phase I [66]. Cethrin, an antagonist of the growth-inhibiting mediator Rho, improved behavioural and/or histological/ anatomical outcomes in 9 pre-clinical studies including mice and rats [15]. A multicenter human trial was initiated applying Cethrin acutely after SCI. Several cell transplantation strategies based on macrophages, Schwann cells, olfactory ensheathing cells, bone marrow and human embryonic stem cells are currently undergoing clinical investigation [14,15]. Finally, strategies which aim to excite remaining spinal circuitries either pharmaceutically (monoaminergic agonists) or electrically (epidural spinal stimulation) have, despite promising results in animal models of SCI, not resulted in randomized clinical trials yet. A promising case report, in which a chronic ASIA B patient was implanted with a chronic epidural electrode array, has recently attracted attention. This particular patient achieved full-weight bearing standing, facilitated performance of manually assisted stepping, limited voluntary motor function and improved autonomic functions under present stimulation [42]. However, further technical development as well as experimental and clinical investigations are needed to validate this exciting treatment approach.

Despite promising treatment strategies raised in laboratory research, their translation did not reveal sufficient efficacy in clinical trials. Nonetheless, the performed trials yielded important information about the difficult and complex nature of such multicenter human trials. In the next section we emphasize the most important shortcomings which, at least partially, need to be overcome in order to improve and accelerate the progression of treatments for human SCI. High quality experimental research combined with an improved and standardized conduct of clinical trials are required to implement successful and efficient treatment strategies.

Shortcomings in experimental research of spinal cord injury

Control of variability

A major point hampering the progression of translational research is the fact that experimental and clinical research does often not pursue the same goals. Experimental research is in many cases not primarily directed towards close modelling of the clinical situation, but is rather driven by the goal to understand the complex mechanisms of spinal function before and after insult. Therefore, the study design aims to minimize the variability between animals (extent and location of the lesion; age, gender and strain of animals; application of medication ect.) which facilitates the investigation of specific biological processes under maximal exclusion of alternative parameters. This low variability is in severe contrast to the clinical situation, where the injured population is extremely heterogeneous with respect to the severity and location of injury, comorbidities, amount of rehabilitative training, concomitant medications et cetera. This implies that beneficial effects upon treatment in animal models have to be robust, functionally meaningful and clearly reproducible (preferentially by independent groups) in order to be confirmed under the condition of uncontrolled variability in clinical trials [14,22,26,67].

Animal model of spinal cord injury

A critical point of translational research concerns the accuracy of a particular animal to model human SCI. The primate model of SCI is clearly most accurate due to its appropriate body size (e.g. for distance of fiber regeneration, pharmacokinetics and –dynamics ect.), the higher similarity in neuroanatomy and neurophysiology of descending fiber tracts (mainly the corticospinal tract), and probably due to more similar metabolic, immunologic and inflammatory properties [68]. Unfortunately, the research on primate models has gotten increasingly constrained in many countries, rendering the use of primate models complicated and less frequent. Additionally, research on primates, even if permitted, is beyond the financial capacity of many research institutes. This might hinder primate studies to reach sufficient statistical power to prove treatment efficacy [69]. Large-animal models are often viewed to be clinically more relevant than rodent models of SCI [17]. The correlation between body size and clinical relevance is certainly oversimplified. It has been demonstrated that, besides the obvious difference of bipedalism and quadrupedalism between the gait of humans and mammalian models, there is a surprisingly high degree of conserved characteristics in gait physiology and the spinal and supraspinal neuronal programs controlling and modulating locomotion across species [24,70-

[73]. The advantage of using larger animals (such as cats, dogs, sheep etc.) over the use of rodents is debatable and depends on the experimental question. In terms of neurophysiology and motor recovery after SCI the rodent model (mainly the rat) is likely to more closely resemble the human situation than many of the larger animals (e.g. skilled forelimb function). Compared to motor functions, sensory and autonomic functions are more conserved among mammals, which simplifies their investigation in animal models [68,74]. In short, the rodent model is valid for most neurological readouts and rodents will remain the basic species of SCI research. Nonhuman primates, if available, are extremely valuable and important for the confirmation of clinically relevant rodent data and for an accurate safety testing of therapeutic interventions. It is highly recommended to validate an experimental treatment in different animal models before entering a clinical trial [17,67].

Spinal injury model: type of spinal lesion

Spinal injuries in humans are most frequently severe compression/contusion injuries in the cervical spinal cord affecting one or more spinal segments [8,9,14,75]. The compression of the spinal cord is most prominent in the ventral spinal cord with varying degree of damage in intermediate and dorsal areas of the cord [8]. Additional peripheral damage of the dorsal or ventral roots frequently occurs [75]. An exact modelling of traumatic human SCI with compression, dislocation and distraction of the cord in all spatial dimensions, as well as with frequently occurring comorbidities, is almost infeasible under experimental conditions. In experimental research, the spinal cord is usually approached by a dorsal laminectomy and damage is performed to the dorsal spinal cord. The probably most adequate lesion in regard to the human situation is a severe compression injury damaging also the ventral spinal tracts and the ventral horn motoneurons [67]. The lesion-of-choice for laboratory studies, however, depends on the experimental question. If the primary focus of the experiment lies on mechanistic questions (e.g. fiber regeneration, tract-specific sprouting) a knife-transection is suited best. In contrast to compression injuries, it is much clearer to predict and analyse which fiber tracts were transected. However, if the main focus of the study lies on neuroprotective investigations, the compression/ contusion injury is the more accurate model. These injuries produce post-traumatic processes such as spreading ischemia, haemorrhage, cavitation, demyelination and inflammatory responses which closely resemble the pathology of human SCI [8,14].

Spinal injury model: location and extent of spinal lesion

Spinal lesions in model organisms are most often performed in the thoracic spinal cord [76]. The most common focus of these studies lies on hindlimb locomotor function and potential anatomical and histological features associated with hindlimb recovery. This contrasts the human situation, where the most frequent type of spinal injury is incomplete cervical SCI leading to sensorimotor deficits in upper and lower extremities [77]. Although motor function of upper extremities is of highest priority for patients with cervical spinal insults [78], the investigation of forelimb deficits is clearly underrepresented in experimental SCI models. The preference of thoracic over cervical injuries might be due to milder lesion deficits which require less animal care and due to the simpler motor evaluation of animals with paraplegic deficits in comparison to tetraplegic animals [68]. Nevertheless, an increased modelling of cervical spinal cord injury and upper limb function is crucial for translational studies [17].

It is increasingly recognized that the extent of the lesion can critically influence the effect of a particular treatment. Some treatments achieve a beneficial effect in subjects with a particular lesion severity, but not in others with a different severity. Two popular treatment strategies illustrating this fact are weight supported treadmill training and application of monoaminergic agonists. Locomotor treadmill training resulted in ambulatory recovery in subjects with motor incomplete lesions (ASIA C or D), but not in motor complete subjects (ASIA A or B). On the other side, monoaminergic treatment has been demonstrated to strongly facilitate locomotor performance in different animal species with total spinal cord transection [34,35,38,79]. Application of the same monoaminergic agonists, however, led to minor or even adverse modulations of locomotor parameters in animals with incomplete spinal cord lesion [73,80,81]. These examples illustrate the importance to experimentally investigate the lesion severity where optimal treatment efficacy occurs. This knowledge will help to perform reasonable and specific patient stratification for particular clinical trials.

Assessment of functional recovery

The analysis of motor performance in experimental research has improved over the last years. Although subjective and non-linear scorings of motor function are still widespread, people recognize the importance of using standardized behavioral tests which lead to objective, sensitive and quantitative evaluation of motor function [82]. Mainly the introduction of kinematic analysis led to a certain standardization of functional testing and greatly improved the reliability of behavioral data across laboratories. This linear quantification is often supplemented by qualitative data, which is still

indispensable for a proper interpretation of motor performance. Besides motor assessments, there should be an increase in outcome measures routinely used in clinical studies to facilitate the interpretation of the experimental data. Neurophysiological recordings are used only rarely as standard measures in laboratory animals, although physiological data would be valuable to confirm the histological findings [68]. Moreover, examination of sensory and autonomic dysfunction is strongly underrepresented in laboratory studies, although it is of major clinical relevance [78,83].

Shortcomings in clinical research of spinal cord injury

Clinical outcome measures

Clinical outcome measures represent a major challenge of translational research. Many outcome measures used in current clinical trials suffer from meagre standardization and from poor objectivity and sensitivity [25,29,84]. The moderate incidence of human SCI and the applied exclusion criteria for clinical trials require multicenter trials in order to recruit a sufficient number of adequate patients. Thus the development of standardized, comprehensive and quantitative functional assessment across different clinical centres is an absolute requirement to reliably monitor motor recovery and to detect potentially successful therapeutic strategies [14,26,29]. Despite updates and training programs for scaling, scoring and classification, clinical outcome assessments often exhibit poor inter-rater reliability [85-87]. Different international networks and panels were built with the goal to optimize clinical outcome measures [14,29]. Functional outcome measures are especially important to report meaningful motor recovery as they assess specific motor performances associated with everyday life. In contrast to the well standardized ambulatory assessments (e.g. WISCI, 10-meter Walk Test ect.), tests for upper extremity function need further standardization and development [25]. Among functional outcomes, those revealing quantitative linear outcomes (e.g. walking speed, distance covered over time) are superior to non-linear scores with questionable objectivity and sensitivity. This is indicated in a study where weight supported locomotor training led to a significant improvement in walking, which was detected by quantitative outcomes (10-meter Walk Test, 6-minute walk test, Timed Up & Go test), but not by the ordinal walking index for spinal cord injury (WISCI-II) [20]. Such examples acknowledge the trend in laboratory research, where the use of objective computer-based analysis massively increased over the last years. Kinematic gait analysis during weight supported treadmill training recently demonstrated to achieve high sensitivity and to provide specific information about neuronal and

biomechanical mechanisms targeted by the treatment in humans [21,88]. Although depreciated as not useful technique for many years, neurophysiological recordings have gone through a revival and have been re-established as valuable and accurate tool to perform quantitative functional analysis of ascending and descending fiber tracts at very acute time points after injury [14,55,89,90]. Together with the existing standardized outcome measures (e.g. ASIA grade and score, WISCI etc.), quantitative gait analysis and neurophysiological recordings might provide a precious tool to enable a more accurate and sensitive analysis of potentially successful treatment strategies and to give some insights into mechanisms underlying this functional restoration (adaptive vs. restorative recovery) [56,91,92].

Prognosis of spontaneous neurological outcome

Incomplete SCI results in a highly variable degree of spontaneous functional recovery among different patients, which is further increased by variables such as the amount and intensity of physical neurorehabilitation among different clinical centers [26,93]. This complicates the interpretation of beneficial treatment effects occurring on top of the variable spontaneous recovery. Together with the fact that running of control/placebo groups in human trials is ethically not always allowed (e.g. surgical treatments), this requires clinical algorithms to provide robust and early prediction of neurological outcome in SCI patients. Early prognosis of functional outcome is not only necessary to extrapolate the extent of spontaneous functional recovery, but also for stratification of patients into accurate groups for clinical trials [14,55,94]. Although outcome prediction by neurological and functional outcome measures has been shown to provide accurate prognosis of ambulatory function [94], patient stratification for acute treatments is performed at very early time points after the lesion, where voluntary outcome measures can not be assessed. Mainly two techniques might be important to improve the accuracy of functional prognosis. **Neuroimaging** is a rapidly developing technique which will be crucial to improve the prediction of functional outcome after SCI. Magnetic resonance imaging (MRI) is the method of choice to investigate the spinal lesion and to display the extent of contusion, axonal tract damage, oedema and haemorrhage. MRI is already in use to perform inclusion criterions or as outcome measure in certain clinical trials [14,95]. MRI-diffusion weighted imaging (MRI-DWI) is a valuable tool to quantify the integrity of the white matter (axonal preservation, myelin disruption and axonal swelling). Both imaging techniques have shown to be good predictors of clinical outcome [27] and their combined application represents a promising prognostic tool for SCI [96,97]. Further technical

development is necessary to enable a standardized use of imaging techniques as a valuable prognostic assessment tool.

Neurophysiological recordings including sensory- and motor-evoked potentials and reflex measurements are an alternative tool to quantitatively assess very acute neurological deficits in human patients [89,90,94]. Supplementary to imaging techniques, neurophysiological recordings can give valuable information about the integrity of ascending and descending tract systems and even about damage of the peripheral nervous system [98]. Neurophysiological recordings are valuable predictors of functional outcome when assessed within the first weeks after the spinal injury [89]. The use of biomarkers as indicators for the lesion severity is an alternative strategy for prognosis, which is still in a developmental stage [17,99].

Inclusion criteria for severity and location of spinal cord injury

Sensorimotor complete patients (ASIA A) with thoracic spinal injury are most frequently chosen for clinical trials, although cervical incomplete SCI has the highest incidence among humans [77]. Thoracic patients are preferred to cervical ones since detrimental treatment effects impairing spinal segments adjacent to the lesion would cause less disastrous consequences in the thoracic than in the cervical cord. The same reason applies for selecting ASIA A patients, which would lose less functions in the case of deteriorating treatments than patients with less functional deficits (ASIA B to D) [14]. Moreover, the functional recovery of ASIA A patients is limited and more precisely predictable, which helps to detect treatment effects [28,93]. However, there are also multiple disadvantages of using thoracic ASIA A patients: First, functional recovery is usually most pronounced in spinal sections adjacent to the injury (zone of partial preservation) [100]. Clinical outcome assessments are not sensitive enough to monitor restored functions at thoracic spinal cord levels, what diminishes the chance to detect potential treatment effects [14]. Second, the treatment effect required to induce functional recovery in ASIA A patients might be much more pronounced as compared to less impaired patients. In addition, the bulk of pre-clinical studies are not performed in motor complete animal models. Thus, recruiting SCI subjects with lesion severities more similar to those investigated in pre-clinical studies might increase the chance to reproduce a treatment effect. It is therefore highly recommended that clinical trials involve patients with incomplete cervical SCI, who are more frequent and would increase the chance to detect beneficial treatment effects. Such trials, however, will need improved prognosis of outcome and a high number of participants in order to expose a treatment effect [30].

Prerequisites for successful state-of-the-art clinical trials

The meagre clinical translation of experimental treatments does not conform to the big effort and progress performed in the field of spinal cord repair. Laboratory technologies, for instance, undergo a steady and fast development which enables the investigation of more precise and isolated biological processes. This results in a deep biological understanding of neuropathological mechanisms upon SCI, which drives the development of new treatment strategies. In the clinical sector, multiple SCI networks were built with the goal to optimize the conduct of clinical trials, to recruit sufficient appropriate patients, to provide joined data bases of trials, as well as to standardize and sensitize clinical outcome measures. Despite progression in the pre-clinical and clinical sector, there are remaining obstacles which, combined with the enormous biological complexity of CNS pathology, are responsible for the still lacking implementation of successful treatments for human SCI.

One of the big discrepancies impeding the progression of translation research is the differing amount of variability in the pre-clinical and clinical setting. Controlled variability is the key for the mechanistic-driven part of laboratory research, but at the same time implies that treatment effects have to be robust and stably reproducible in different experiments, in independent laboratories and in different animal species in order to be of potential clinical relevance. In the clinical setting, the heterogeneity among patients must be decreased by performing superior patient stratification for trials. This requires further technical progress in diagnostic tools enabling acute and reliable prediction of neurological outcome. Mainly neuroimaging techniques and neurophysiological recordings are promising tools to achieve optimized outcome prediction and thus improved patient stratification. Improved prognosis of neurological outcome is also critical to predict the amount of spontaneous functional recovery in order to detect treatment-induced recovery.

Experimental studies have to provide a range of important information about a treatment before its clinical translation is initiated. First, treatment effects observed in animal models have to be functionally meaningful and significant. Minor functional effects or effects on the anatomical/ histological level only are unlikely to induce any functional effects in clinical trials, where the patient population is heterogeneous and the assessment of outcome is difficult. Second, animal experimentation should investigate the lesion level and severity, where the treatment can attain its optimal effects. This will help to stratify the patients and thus to optimize the chance of success. Third, pre-clinical studies should examine the optimal onset and duration of the treatment. Forth, the animal species and the type of the lesion used in an experimental study should be carefully chosen in respect

to the question which wants to be answered. Studies investigating the action of a neuroprotective agent should, for instance, perform contusion/compression injuries, as the resulting lesion pathology resembles more the human SCI as when performing transection injuries [8,9]. Studies investigating anatomical plasticity and regeneration after specific spinal tract injuries might prefer transection injuries. Fifth, the interpretation of neurological findings should also be performed in regard to human neurophysiology. Whereas the anatomy and function of conserved neuronal systems such as the autonomic system or bulbospinal projections can be similar across species, this is more delicate for evolutionary younger systems such as the corticospinal system [68].

A major shortcoming in the clinical sector of SCI is the lack of reliability, objectivity and sensitivity in the outcome measures. Given the highly heterogeneous population of SCI patients, the detection of clinical treatment effects requires accurate assessment of neurological functions. The use of a standardized tool box including comprehensive and quantitative outcome measures such as kinematic gait analysis and neurophysiologic measures is highly recommended. These quantitative measures not only provide higher reliability and sensitivity in the evaluation of treatments, but might be able to provide some insight into the biomechanical and neurobiolgical mechanisms of a particular treatment.

The formation of clinical panels is important to exchange and discuss experiences about the rare human SCI trials. Owing to these panels there is, for instance, the general consensus that randomized, controlled and double-blinded human trials with control groups provide most accurate and reliable data. The panels also formulate detailed guidelines for the optimized conduct of clinical trials. However, providing guidelines does not guarantee its implementation. This had to be recognized in the field of animal stroke research, where the STAIR guidelines, which aimed to improve the quality of pre-clinical research, are still poorly put into practice [23]. To enhance the compliance with these guidelines, they would need, for instance, to be appreciated as criteria used by clinically related journals to accept pre-clinical manuscripts. A further promising way to generate successful clinical treatments would be to encourage neutral and competent scientific panels to valuate the reproducibility, strength and overall quality of the pre-clinical data before they enter clinical trials. In contrast to regulatory authorities, which primarily ensure the protection of the patient during a trial (safety, rights, well being of patient), scientific panels would guarantee a controlled quality of animal research on which upcoming clinical trials are based.

Resources for the initiation of clinical SCI trials are limited in that financial costs to conduct a clinical trial are immense and the number of patients matching the inclusion criteria is constricted. Thus, an optimized selection and conduct of clinical trials is fundamental. It is time that the pre-clinical and clinical side of spinal cord repair pull together and improve the quality of their research e.g. by adhering to standardized guidelines. High quality animal experimentations leading to robust and reproducible data together with refined clinical outcome measures and prognostic algorithms will certainly support the translation of successful experimental treatments into standard clinical therapies for patients suffering from SCI.

References

1. Schwab, J.M., Brechtel, K., Mueller, C. A., Failli, V., Kaps, H. P., Tuli, S. K., Schluesener, H. J. Experimental strategies to promote spinal cord regeneration--an integrative perspective. *Prog Neurobiol* 78, 91-116 (2006).
2. Schwab, M.E. & Caroni, P. Oligodendrocytes and CNS myelin are nonpermissive substrates for neurite growth and fibroblast spreading in vitro. *J Neurosci* 8, 2381-2393 (1988).
3. Oohira, A., Matsui, F. & Katoh-Semba, R. Inhibitory effects of brain chondroitin sulfate proteoglycans on neurite outgrowth from PC12D cells. *J Neurosci* 11, 822-827 (1991).
4. Liu, B.P., Fournier, A., GrandPre, T. & Strittmatter, S.M. Myelin-associated glycoprotein as a functional ligand for the Nogo-66 receptor. *Science* 297, 1190-1193 (2002).
5. Kottis, V., Thibault, P., Mikol, D., Xiao, Z. C., Zhang, R., Dergham, P., Braun, P. E. Oligodendrocyte-myelin glycoprotein (OMgp) is an inhibitor of neurite outgrowth. *J Neurochem* 82, 1566-1569 (2002).
6. Silver, J. & Miller, J.H. Regeneration beyond the glial scar. *Nat Rev Neurosci* 5, 146-156 (2004).
7. Kwok, J.C., Dick, G., Wang, D. & Fawcett, J.W. Extracellular matrix and perineuronal nets in CNS repair. *Dev Neurobiol* 71, 1073-1089.
8. Norenberg, M.D., Smith, J. & Marcillo, A. The pathology of human spinal cord injury: defining the problems. *J Neurotrauma* 21, 429-440 (2004).
9. Bunge, R.P., Puckett, W.R., Becerra, J.L., Marcillo, A. & Quencer, R.M. Observations on the pathology of human spinal cord injury. A review and classification of 22 new cases with details from a case of chronic cord compression with extensive focal demyelination. *Adv Neurol* 59, 75-89 (1993).
10. Tator, C.H., Duncan, E.G., Edmonds, V.E., Lapczak, L.I. & Andrews, D.F. Neurological recovery, mortality and length of stay after acute spinal cord injury associated with changes in management. *Paraplegia* 33, 254-262 (1995).
11. Tator, C.H. Experimental and clinical studies of the pathophysiology and management of acute spinal cord injury. *J Spinal Cord Med* 19, 206-214 (1996).
12. Vilensky, J.A., Moore, A.M., Eidelberg, E. & Walden, J.G. Recovery of Locomotion in Monkeys With Spinal Cord Lesions. *J Mot Behav* 24, 288-296 (1992).
13. Rossignol, S. & Frigon, A. Recovery of locomotion after spinal cord injury: some facts and mechanisms. *Annu Rev Neurosci* 34, 413-440.
14. Tator, C.H. Review of treatment trials in human spinal cord injury: issues, difficulties, and recommendations. *Neurosurgery* 59, 957-982; discussion 982-957 (2006).
15. Hawryluk, G.W., Rowland, J., Kwon, B.K. & Fehlings, M.G. Protection and repair of the injured spinal cord: a review of completed, ongoing, and planned clinical trials for acute spinal cord injury. *Neurosurg Focus* 25, E14 (2008).
16. Baptiste, D.C. & Fehlings, M.G. Update on the treatment of spinal cord injury. *Prog Brain Res* 161, 217-233 (2007).

17. Kwon, B.K., Hillyer, J. & Tetzlaff, W. Translational research in spinal cord injury: a survey of opinion from the SCI community. *J Neurotrauma* 27, 21-33.
18. Hurlbert, R.J. & Hamilton, M.G. Methylprednisolone for acute spinal cord injury: 5-year practice reversal. *Can J Neurol Sci* 35, 41-45 (2008).
19. Finch, L., Barbeau, H. & Arsenault, B. Influence of body weight support on normal human gait: development of a gait retraining strategy. *Phys Ther* 71, 842-855; discussion 855-846 (1991).
20. Wirz, M., Zemon, D. H., Rupp, R., Scheel, A., Colombo, G., Dietz, V., Hornby, T. G. Effectiveness of automated locomotor training in patients with chronic incomplete spinal cord injury: a multicenter trial. *Arch Phys Med Rehabil* 86, 672-680 (2005).
21. Lucareli, P.R., Lima, M. O., Lima, F. P., de Almeida, J. G., Brech, G. C., D'Andrea Greve, J. M. Gait analysis following treadmill training with body weight support versus conventional physical therapy: a prospective randomized controlled single blind study. *Spinal Cord* 49, 1001-1007 (2011).
22. Recommendations for standards regarding preclinical neuroprotective and restorative drug development. *Stroke* 30, 2752-2758 (1999).
23. Philip, M., Benatar, M., Fisher, M. & Savitz, S.I. Methodological quality of animal studies of neuroprotective agents currently in phase II/III acute ischemic stroke trials. *Stroke* 40, 577-581 (2009).
24. Dietz, V. & Harkema, S.J. Locomotor activity in spinal cord-injured persons. *J Appl Physiol* 96, 1954-1960 (2004).
25. Alexander, M.S., Anderson, K. D., Biering-Sorensen, F., Blight, A. R., Brannon, R., Bryce, T. N., Creasey, G., Catz, A., Curt, A., Donovan, W., Ditunno, J., Ellaway, P., Finnerup, N. B., Graves, D. E., Haynes, B. A., Heinemann, A. W.. Jackson, A. B.. Johnston, M. V., Kalpakjian, C. Z., Kleitman, N., Krassioukov, A., Krogh, K., Lammertse, D., Magasi, S., Mulcahey, M. J., Schurch, B., Sherwood, A., Steeves, J. D., Stiens, S., Tulsky, D. S., van Hedel, H. J., Whiteneck, G. Outcome measures in spinal cord injury: recent assessments and recommendations for future directions. *Spinal Cord* 47, 582-591 (2009).
26. Steeves, J.D., Zariffa, J. & Kramer, J.L. Are you "tilting at windmills" or undertaking a valid clinical trial? *Yonsei Med J* 52, 701-716.
27. Lammertse, D., Tuszynski, M. H., Steeves, J. D., Curt, A., Fawcett, J. W., Rask, C., Ditunno, J. F., Fehlings, M. G., Guest, J. D., Ellaway, P. H., Kleitman, N., Blight, A. R., Dobkin, B. H., Grossman, R., Katoh, H., Privat, A., Kalichman, M. Guidelines for the conduct of clinical trials for spinal cord injury as developed by the ICCP panel: clinical trial design. *Spinal Cord* 45, 232-242 (2007).
28. Tuszynski, M.H., Steeves, J. D., Fawcett, J. W., Lammertse, D., Kalichman, M., Rask, C., Curt, A., Ditunno, J. F., Fehlings, M. G., Guest, J. D., Ellaway, P. H., Kleitman, N., Bartlett, P. F., Blight, A. R., Dietz, V., Dobkin, B. H., Grossman, R., Privat, A. Guidelines for the conduct of clinical trials for spinal cord injury as developed by the ICCP Panel: clinical trial inclusion/exclusion criteria and ethics. *Spinal Cord* 45, 222-231 (2007).

29. Steeves, J.D., Lammertse, D., Curt, A., Fawcett, J. W., Tuszynski, M. H., Ditunno, J. F., Ellaway, P. H., Fehlings, M. G., Guest, J. D., Kleitman, N., Bartlett, P. F., Blight, A. R., Dietz, V., Dobkin, B. H., Grossman, R., Short, D., Nakamura, M., Coleman, W. P., Gaviria, M., Privat, A. Guidelines for the conduct of clinical trials for spinal cord injury (SCI) as developed by the ICCP panel: clinical trial outcome measures. *Spinal Cord* 45, 206-221 (2007).
30. Fawcett, J.W., Curt, A., Steeves, J. D., Coleman, W. P., Tuszynski, M. H., Lammertse, D., Bartlett, P. F., Blight, A. R., Dietz, V., Ditunno, J., Dobkin, B. H., Havton, L. A., Ellaway, P. H., Fehlings, M. G., Privat, A., Grossman, R., Guest, J. D., Kleitman, N., Nakamura, M., Gaviria, M., Short, D. Guidelines for the conduct of clinical trials for spinal cord injury as developed by the ICCP panel: spontaneous recovery after spinal cord injury and statistical power needed for therapeutic clinical trials. *Spinal Cord* 45, 190-205 (2007).
31. Kwon, B.K., Okon, E. B., Tsai, E., Beattie, M. S., Bresnahan, J. C., Magnuson, D. K., Reier, P. J., McTigue, D. M., Popovich, P. G., Blight, A. R., Oudega, M., Guest, J. D., Weaver, L. C., Fehlings, M. G., Tetzlaff, W. A grading system to evaluate objectively the strength of pre-clinical data of acute neuroprotective therapies for clinical translation in spinal cord injury. *J Neurotrauma* 28, 1525-1543 (2011).
32. Tator, C.H., Duncan, E.G., Edmonds, V.E., Lapczak, L.I. & Andrews, D.F. Changes in epidemiology of acute spinal cord injury from 1947 to 1981. *Surg Neurol* 40, 207-215 (1993).
33. Barbeau, H. & Rossignol, S. Recovery of locomotion after chronic spinalization in the adult cat. *Brain Res* 412, 84-95 (1987).
34. Forssberg, H. & Grillner, S. The locomotion of the acute spinal cat injected with clonidine i.v. *Brain Res* 50, 184-186 (1973).
35. Barbeau, H. & Rossignol, S. Initiation and modulation of the locomotor pattern in the adult chronic spinal cat by noradrenergic, serotonergic and dopaminergic drugs. *Brain Res* 546, 250-260 (1991).
36. Fedirchuk, B., Nielsen, J., Petersen, N. & Hultborn, H. Pharmacologically evoked fictive motor patterns in the acutely spinalized marmoset monkey (Callithrix jacchus). *Exp Brain Res* 122, 351-361 (1998).
37. Feraboli-Lohnherr, D., Barthe, J.Y. & Orsal, D. Serotonin-induced activation of the network for locomotion in adult spinal rats. *J Neurosci Res* 55, 87-98 (1999).
38. Antri, M., Mouffle, C., Orsal, D. & Barthe, J.Y. 5-HT1A receptors are involved in short- and long-term processes responsible for 5-HT-induced locomotor function recovery in chronic spinal rat. *Eur J Neurosci* 18, 1963-1972 (2003).
39. Landry, E.S. & Guertin, P.A. Differential effects of 5-HT1 and 5-HT2 receptor agonists on hindlimb movements in paraplegic mice. *Prog Neuropsychopharmacol Biol Psychiatry* 28, 1053-1060 (2004).
40. Ichiyama, R.M., Gerasimenko, Y.P., Zhong, H., Roy, R.R. & Edgerton, V.R. Hindlimb stepping movements in complete spinal rats induced by epidural spinal cord stimulation. *Neurosci Lett* 383, 339-344 (2005).

41. Courtine, G., Gerasimenko, Y., van den Brand, R., Yew, A., Musienko, P.. Zhong, H., Song, B., Ao, Y., Ichiyama, R. M., Lavrov, I., Roy, R. R., Sofroniew, M. V., Edgerton, V. R. Transformation of nonfunctional spinal circuits into functional states after the loss of brain input. *Nat Neurosci* 12, 1333-1342 (2009).
42. Harkema, S., Gerasimenko, Y., Hodes, J., Burdick, J., Angeli, C., Chen, Y., Ferreira, C., Willhite, A., Rejc, E., Grossman, R. G., Edgerton, V. R. Effect of epidural stimulation of the lumbosacral spinal cord on voluntary movement, standing, and assisted stepping after motor complete paraplegia: a case study. *Lancet* 377, 1938-1947 (2011).
43. Nathan, P.W. Effects on movement of surgical incisions into the human spinal cord. *Brain* 117 (Pt 2), 337-346 (1994).
44. Kakulas, B.A. Neuropathology: the foundation for new treatments in spinal cord injury. *Spinal Cord* 42, 549-563 (2004).
45. Kerr, F.W. Neuroplasticity of primary afferents in the neo-natal cat and some results of early deafferentation of the trigeminal spinal nucleus. *J Comp Neurol* 163, 305-327 (1975).
46. Fouad, K., Pedersen, V., Schwab, M.E. & Brosamle, C. Cervical sprouting of corticospinal fibers after thoracic spinal cord injury accompanies shifts in evoked motor responses. *Curr Biol* 11, 1766-1770 (2001).
47. Ballermann, M. & Fouad, K. Spontaneous locomotor recovery in spinal cord injured rats is accompanied by anatomical plasticity of reticulospinal fibers. *Eur J Neurosci* 23, 1988-1996 (2006).
48. Courtine, G., Song, B., Roy, R. R., Zhong, H., Herrmann, J. E., Ao, Y., Qi, J., Edgerton, V. R., Sofroniew, M. V. Recovery of supraspinal control of stepping via indirect propriospinal relay connections after spinal cord injury. *Nat Med* 14, 69-74 (2008).
49. Maier, I.C. & Schwab, M.E. Sprouting, regeneration and circuit formation in the injured spinal cord: factors and activity. *Philos Trans R Soc Lond B Biol Sci* 361, 1611-1634 (2006).
50. Barriere, G., Leblond, H., Provencher, J. & Rossignol, S. Prominent role of the spinal central pattern generator in the recovery of locomotion after partial spinal cord injuries. *J Neurosci* 28, 3976-3987 (2008).
51. Barriere, G., Frigon, A., Leblond, H., Provencher, J. & Rossignol, S. Dual spinal lesion paradigm in the cat: evolution of the kinematic locomotor pattern. *J Neurophysiol* 104, 1119-1133.
52. Martinez, M., Delivet-Mongrain, H., Leblond, H. & Rossignol, S. Recovery of hindlimb locomotion after incomplete spinal cord injury in the cat involves spontaneous compensatory changes within the spinal locomotor circuitry. *J Neurophysiol* 106, 1969-1984.
53. Dobkin, B.H. Motor rehabilitation after stroke, traumatic brain, and spinal cord injury: common denominators within recent clinical trials. *Curr Opin Neurol* 22, 563-569 (2009).
54. Waters, R.L., Yakura, J.S. & Adkins, R.H. Gait performance after spinal cord injury. *Clin Orthop Relat Res*, 87-96 (1993).

55. Steeves, J.D., Kramer, J. K., Fawcett, J. W., Cragg, J., Lammertse, D. P., Blight, A. R., Marino, R. J., Ditunno, J. F., Jr., Coleman, W. P., Geisler, F. H., Guest, J., Jones, L., Burns, S., Schubert, M., van Hedel, H. J., Curt, A. Extent of spontaneous motor recovery after traumatic cervical sensorimotor complete spinal cord injury. *Spinal Cord* 49, 257-265 (2011).
56. Wirz, M., Bastiaenen, C., de Bie, R. & Dietz, V. Effectiveness of automated locomotor training in patients with acute incomplete spinal cord injury: a randomized controlled multicenter trial. *BMC Neurol* 11, 60.
57. O'Collins, V.E., Macleod, M. R., Donnan, G. A., Horky, L. L., van der Worp, B. H., Howells, D. W. 1,026 experimental treatments in acute stroke. *Ann Neurol* 59, 467-477 (2006).
58. Hall, E.D. The neuroprotective pharmacology of methylprednisolone. *J Neurosurg* 76, 13-22 (1992).
59. Hurlbert, R.J. The role of steroids in acute spinal cord injury: an evidence-based analysis. *Spine (Phila Pa 1976)* 26, S39-46 (2001).
60. Schnell, L. & Schwab, M.E. Axonal regeneration in the rat spinal cord produced by an antibody against myelin-associated neurite growth inhibitors. *Nature* 343, 269-272 (1990).
61. Liebscher, T., Schnell, L., Schnell, D., Scholl, J., Schneider, R., Gullo, M., Fouad, K., Mir, A., Rausch, M., Kindler, D., Hamers, F. P., Schwab, M. E. Nogo-A antibody improves regeneration and locomotion of spinal cord-injured rats. *Ann Neurol* 58, 706-719 (2005).
62. GrandPre, T., Li, S. & Strittmatter, S.M. Nogo-66 receptor antagonist peptide promotes axonal regeneration. *Nature* 417, 547-551 (2002).
63. Li, S. & Strittmatter, S.M. Delayed systemic Nogo-66 receptor antagonist promotes recovery from spinal cord injury. *J Neurosci* 23, 4219-4227 (2003).
64. Freund, P., Schmidlin, E., Wannier, T., Bloch, J., Mir, A., Schwab, M. E., Rouiller, E. M. Nogo-A-specific antibody treatment enhances sprouting and functional recovery after cervical lesion in adult primates. *Nat Med* 12, 790-792 (2006).
65. Freund, P., Wannier, T. Schmidlin, E., Bloch, J., Mir, A., Schwab, M. E., Rouiller, E. M. Anti-Nogo-A antibody treatment enhances sprouting of corticospinal axons rostral to a unilateral cervical spinal cord lesion in adult macaque monkey. *J Comp Neurol* 502, 644-659 (2007).
66. Zorner, B. & Schwab, M.E. Anti-Nogo on the go: from animal models to a clinical trial. *Ann N Y Acad Sci* 1198 Suppl 1, E22-34.
67. Blesch, A. & Tuszynski, M.H. Spinal cord injury: plasticity, regeneration and the challenge of translational drug development. *Trends Neurosci* 32, 41-47 (2009).
68. Courtine, G., Fawcett, J. W., Grossman, R. G., Kaas, J. H., Lemon, R., Maier, I., Martin, J., Nudo, R. J., Ramon-Cueto, A., Rouiller, E. M., Schnell, L., Wannier, T., Schwab, M. E., Edgerton, V. R. Can experiments in nonhuman primates expedite the translation of treatments for spinal cord injury in humans? *Nat Med* 13, 561-566 (2007).
69. Fisher, M., Feuerstein, G., Howells, D. W., Hurn, P. D., Kent, T. A., Savitz, S. I., Lo, E. H. Update of the stroke therapy academic industry roundtable preclinical recommendations. *Stroke* 40, 2244-2250 (2009).
70. Vilensky, J.A. Locomotor behavior and control in human and non-human primates: comparisons with cats and dogs. *Neurosci Biobehav Rev* 11, 263-274 (1987).

71. Duysens, J. & Van de Crommert, H.W. Neural control of locomotion; The central pattern generator from cats to humans. *Gait Posture* 7, 131-141 (1998).
72. Jahn, K., Deutschlander, A., Stephan, T., Kalla, R., Hufner, K., Wagner, J., Strupp, M., Brandt, T. Supraspinal locomotor control in quadrupeds and humans. *Prog Brain Res* 171, 353-362 (2008).
73. Filli, L., Zorner, B., Weinmann, O. & Schwab, M.E. Motor deficits and recovery in rats with unilateral spinal cord hemisection mimic the Brown-Sequard syndrome. *Brain* 134, 2261-2273 (2011).
74. Kastner, A. & Gauthier, P. Are rodents an appropriate pre-clinical model for treating spinal cord injury? Examples from the respiratory system. *Exp Neurol* 213, 249-256 (2008).
75. Dietz, V. & Curt, A. Neurological aspects of spinal-cord repair: promises and challenges. *Lancet Neurol* 5, 688-694 (2006).
76. Gensel, J.C., Tovar, C. A., Hamers, F. P., Deibert, R. J., Beattie, M. S., Bresnahan, J. C. Behavioral and histological characterization of unilateral cervical spinal cord contusion injury in rats. *J Neurotrauma* 23, 36-54 (2006).
77. McKinley, W., Santos, K., Meade, M. & Brooke, K. Incidence and outcomes of spinal cord injury clinical syndromes. *J Spinal Cord Med* 30, 215-224 (2007).
78. Anderson, K.D. Targeting recovery: priorities of the spinal cord-injured population. *J Neurotrauma* 21, 1371-1383 (2004).
79. Musienko, P., van den Brand, R., Marzendorfer, O., Roy, R. R., Gerasimenko, Y., Edgerton, V. R., Courtine, G. Controlling specific locomotor behaviors through multidimensional monoaminergic modulation of spinal circuitries. *J Neurosci* 31, 9264-9278 (2011).
80. Brustein, E. & Rossignol, S. Recovery of locomotion after ventral and ventrolateral spinal lesions in the cat. II. Effects of noradrenergic and serotoninergic drugs. *J Neurophysiol* 81, 1513-1530 (1999).
81. Hayashi, Y., Jacob-Vadakot, S., Dugan, E. A., McBride, S., Olexa, R., Simansky, K., Murray, M., Shumsky, J. S. 5-HT precursor loading, but not 5-HT receptor agonists, increases motor function after spinal cord contusion in adult rats. *Exp Neurol* 221, 68-78 (2010).
82. Zörner, B., Filli, L., Starkey, M. L., Gonzenbach, R., Kasper, H., Rothlisberger, M., Bolliger, M., Schwab, M. E. Profiling locomotor recovery: comprehensive quantification of impairments after CNS damage in rodents. *Nat Methods* 7, 701-708 (2010).
83. Nakae, A., Nakai, K.,Yano, K., Hosokawa, K., Shibata, M., Mashimo, T. The animal model of spinal cord injury as an experimental pain model. *J Biomed Biotechnol* 2011, 939023 (2011).
84. Curt, A., Schwab, M.E. & Dietz, V. Providing the clinical basis for new interventional therapies: refined diagnosis and assessment of recovery after spinal cord injury. *Spinal Cord* 42, 1-6 (2004).
85. Chafetz, R.S., Vogel, L.C., Betz, R.R., Gaughan, J.P. & Mulcahey, M.J. International standards for neurological classification of spinal cord injury: training effect on accurate classification. *J Spinal Cord Med* 31, 538-542 (2008).

86. Waring, W.P., 3rd, Biering-Sorensen, F., Burns, S., Donovan, W., Graves, D., Jha, A., Jones, L., Kirshblum, S., Marino, R., Mulcahey, M. J., Reeves, R., Scelza, W. M., Schmidt-Read, M., Stein, A. _ 2009 review and revisions of the international standards for the neurological classification of spinal cord injury. *J Spinal Cord Med* 33, 346-352.

87. Schuld, C., Wiese, J., Hug, A., Putz, C., van Hedel, H. J., Spiess, M. R., Weidner, N., Em-Sci, S. G., Rupp, R. Computer Implementation of the International Standards for Neurological Classification of Spinal Cord Injury for Consistent and Efficient Derivation of its Subscores including Handling of Data from not Testable Segments. *J Neurotrauma* (2011).

88. Wolf, S., Loose, T., Schablowski, M., Doderlein, L., Rupp, R., Gerner, H. J., Bretthauer, G., Mikut, R. Automated feature assessment in instrumented gait analysis. *Gait Posture* 23, 331-338 (2006).

89. Curt, A. & Dietz, V. Electrophysiological recordings in patients with spinal cord injury: significance for predicting outcome. *Spinal Cord* 37, 157-165 (1999).

90. Scivoletto, G. & Di Donna, V. Prediction of walking recovery after spinal cord injury. *Brain Res Bull* 78, 43-51 (2009).

91. Thomas, S.L. & Gorassini, M.A. Increases in corticospinal tract function by treadmill training after incomplete spinal cord injury. *J Neurophysiol* 94, 2844-2855 (2005).

92. Dietz, V., Grillner, S., Trepp, A., Hubli, M. & Bolliger, M. Changes in spinal reflex and locomotor activity after a complete spinal cord injury: a common mechanism? *Brain* 132, 2196-2205 (2009).

93. Burns, A.S., Lee, B.S., Ditunno, J.F., Jr. & Tessler, A. Patient selection for clinical trials: the reliability of the early spinal cord injury examination. *J Neurotrauma* 20, 477-482 (2003).

94. Zörner, B., Blanckenhorn, W.U., Dietz, V. & Curt, A. Clinical algorithm for improved prediction of ambulation and patient stratification after incomplete spinal cord injury. *J Neurotrauma* 27, 241-252.

95. Fehlings, M.G. & Tator, C.H. An evidence-based review of decompressive surgery in acute spinal cord injury: rationale, indications, and timing based on experimental and clinical studies. *J Neurosurg* 91, 1-11 (1999).

96. Cohen-Adad, J., Descoteaux, M. Rossignol, S., Hoge, R. D., Deriche, R., Benali, H. Detection of multiple pathways in the spinal cord using q-ball imaging. *Neuroimage* 42, 739-749 (2008).

97. Cohen-Adad, J., El Mendili, M. M., Lehericy, S., Pradat, P. F., Blancho, S., Rossignol, S., Benali, H. Demyelination and degeneration in the injured human spinal cord detected with diffusion and magnetization transfer MRI. *Neuroimage* 55, 1024-1033 (2011).

98. Rutz, S., Dietz, V. & Curt, A. Diagnostic and prognostic value of compound motor action potential of lower limbs in acute paraplegic patients. *Spinal Cord* 38, 203-210 (2000).

99. Lubieniecka, J.M., Streijger, F., Lee, J. H., Stoynov, N., Liu, J., Mottus, R., Pfeifer, T., Kwon, B. K., Coorssen, J. R., Foster, L. J., Grigliatti, T. A., Tetzlaff, W. Biomarkers for severity of spinal cord injury in the cerebrospinal fluid of rats. *PLoS One* 6, e19247 (2011).

100. Marino, R.J., Ditunno, J.F., Jr., Donovan, W.H. & Maynard, F., Jr. Neurologic recovery after traumatic spinal cord injury: data from the Model Spinal Cord Injury Systems. *Arch Phys Med Rehabil* 80, 1391-1396 (1999).

Aim of the thesis

Incomplete cervical spinal cord injury has the highest incidence among human spinal injuries (McKinley et al., 2007). The consequences associated with such injuries include sensorimotor deficits in upper and lower extremities as well as autonomic dysfunctions. Despite severe initial deficits, incomplete spinal cord injuries are often followed by some degree of spontaneous functional recovery (Tator et al., 1995). Tetraplegic animal models are only rarely used in experimental studies. Given the high priority to regain upper limb motor control in humans suffering from tetraplegia, it is crucial to investigate appropriate models in animal research targeting forelimb motor recovery (Anderson et al., 2005).

The aim of the present work was to use a combined approach of detailed behavioral analysis and state of the art neuroanatomical tracing and staining techniques to perform a physiological and anatomical investigation of cervical unilateral spinal cord hemisection in the rat model.

The first aim of the thesis was to achieve an accurate assessment of motor performance in rodent animal models by constructing a standardized and comprehensive behavioral setup consisting of different locomotor tests. Standardization of outcome measures is crucial to improve the inter-rater reliability and to compare results across different laboratories around the globe (Muir and Webb, 2000; Basso, 2004). The ambition was to obtain objective and quantitative behavioral readouts from different locomotor tests enabling accurate and sensitive monitoring of functional recovery in rodent models of different central nervous system injuries. Therefore, the first project provided the basis on which the detailed physiological investigations of the subsequent studies relied.

The second aim of the thesis was to use the sensitive kinematic analysis to study fore- and hindlimb locomotor performance in rats with incomplete cervical spinal cord injury. Based on human studies (Levi et al., 1996) and the rare animal models of incomplete cervical spinal cord injury (Webb and Muir, 2002 and 2005; Rosenzweig et al., 2010), it was expected that the upper limb revealed a more restricted motor restoration compared to the lower limb. Besides detailed locomotor assessment of rats with C4/C5 unilateral hemisection, we aimed to investigate reasons accounting for the potentially disproportionate recovery between fore-and hindlimbs upon this lesion. Moreover, we wanted to address the responsiveness of fore-and hindlimb spinal circuitries to neuromodulatory monoaminergic agonists. The goal was to enhance locomotor capabilities of fore- and hindlimbs in these rats by intrathecal application of agonists targeting the three monoaminergic systems.

The third aim of the thesis was to investigate neuroanatomical correlates of the spontaneously occurring motor improvements in rats with unilateral C4/C5 hemisections. In detail, we wanted to address the question of how axotomized fiber tracts react to a spinal trauma. It has been known for a long time that long-distance regeneration is absent in the central nervous system, but that axotomized axons can show a transient sprouting reaction (Ramon y Cajal, 1928). The aim was to examine if regenerative sprouting of severed supraspinal fibers occurs spontaneously after axotomy and if yes, how long the sprouting persists or if the fibers are retracted in a later phase after injury. Further we were interested in the potential function of these sprouting fibers. Previous publications demonstrated that transected corticospinal axons are able to spontaneously rewire to new intraspinal targets (Bareyre et al., 2004). The impact of intraspinal plasticity on functional recovery after incomplete spinal cord injury is increasingly recognized in the community of spinal cord repair (Bareyre et al., 2004; Vavrek et al., 2006; Courtine et al., 2008). This project aimed to resolve supra- and intra-spinal neuroanatomical changes using accurate neuroanatomical tract tracings and immunohistochemical stainings.

Chapter 2

Profiling locomotor recovery: Comprehensive quantification of impairments following CNS damage in rodents

Linard Filli[*], Björn Zörner[*], Michelle L. Starkey, Roman Gonzenbach, Hansjörg Kasper, Martina Röthlisberger, Marc Bolliger and Martin E. Schwab

Original article published in: Nature Methods. 2010; 7(9):701-8.

[*] LF and BZ contributed equally to this work.

Abstract

Rodents are frequently used to model damage and diseases of the central nervous system (CNS) that lead to functional deficits. Impaired locomotor function is currently evaluated by using scoring systems or biomechanical measures. These methods often suffer from limitations such as subjectivity, non-linearity and low sensitivity, or focus on a few, very restricted aspects of movement. Thus, full quantitative profiles of motor deficits after CNS damage are lacking. Here, we report the detailed characterization of locomotor impairments after applying common forms of CNS damage in rodents. Numerous objective and quantitative readouts were obtained from rats with either spinal cord injuries or strokes and transgenic mice (*Epha4*$^{-/-}$) during skilled walking, overground walking, wading and swimming resulting in model-specific locomotor profiles. Our testing and analysis method provides comprehensive assessment of locomotor function in rodents and has broad application in various fields of life science research.

Introduction

A common consequence of damage to the central nervous system (CNS) caused by trauma, ischemia, or neurodegenerative or inflammatory diseases is impairment of motor functions. In the corresponding animal models accurate and comprehensive functional testing is not only important to determine whether a novel therapeutic approach is successful but is also indispensable for understanding complex CNS processes such as the mechanisms leading to spontaneous recovery[1, 2]. In neuroscience research, models based on rodents are commonly used and locomotion is one of the most frequently investigated motor functions[3-5].

For evaluation of locomotor deficits, different readouts such as endpoint measures[6, 7] (scores), biomechanical measures[8-10] (kinematics, kinetics) or electromyography (EMG)[9, 11] are commonly used. However, these readouts suffer from several limitations. The most commonly used scores are neither linear nor objective and often have a low sensitivity especially with regards to treatment effects or compensatory strategies[4, 12]. Established scoring systems are generally developed for a particular type of injury and thus are not easily transferred to other models[7]. Highly sensitive biomechanical measurements or EMG recordings usually focus on a few, very specific aspects of a movement, for example joint angles or timing of muscle activity, whilst other aspects, like changes in body posture are rarely assessed. Since the overall functional status of the animal is often ignored, data obtained from these approaches can be difficult to interpret[12]. Furthermore, application of these methods is mainly limited to a few specialized laboratories. The use of several endpoint measures combined with quantitative biomechanical readouts has been emphasized in the literature as a priority and might help overcome some of the above mentioned problems, but this is usually expensive, time- and space-consuming and not standardized hindering comparison of results between laboratories[4, 12]. Adding an additional level of difficulty to the behavior analysis, rodents show various forms of locomotion depending on their environment. This includes skilled walking, normal walking on even ground or, in an aquatic environment, wading through shallow water or swimming. All of these types of locomotion differ considerably with regards to the motor pattern produced, sensory input and participating CNS networks [13-16] and, therefore, might be differentially affected by a given CNS injury. Thus, a comprehensive analysis of the animals' behavior, including different forms of locomotion, is necessary for a full assessment of the consequences of a lesion and is a prerequisite to link neuroanatomical changes to functional outcome. However, studies investigating the effects of a given CNS injury by assessing full, quantitative locomotor profiles are lacking.

The objective of this study was to undertake a systematic and comprehensive evaluation of the effects of various insults to the CNS using four motor tasks that test different aspects of locomotion in rats and mice. By assessing a number of objective and quantitative outcome measures, we generated locomotor profiles characteristic for the investigated models of CNS damage. Thus, the dataset presented here can guide the selection of the appropriate lesion paradigm and the corresponding outcome measures for future animal studies.

Results

Set-up for locomotor testing in rodents

We evaluated locomotor function in rats and mice in a rectangular Plexiglas basin (Supplementary Fig. 1a). By changing the conditions within the basin, we investigated four different types of locomotion (Fig. 1a). To test skilled locomotion, we used a horizontal ladder. For assessment of overground locomotion, we replaced the ladder by a Plexiglas runway. For wading, we filled the basin with water to 3 cm (rats) or 1 cm (mice) above the runway's surface, because we found that these water levels were adequate to provide weight support for impaired rats without eliciting swimming movements. Finally, we evaluated swimming after filling the entire basin with water. We were able to test of a single animal in all four locomotor tasks within 15 minutes. Three mirrors were arranged inside and outside of the basin such that the animals performance was recorded simultaneously from three sides (left, right and below) with one camera (Fig. 1b). We used a color-based tracking software for automatic tracking of markers tattooed on the animals' skin overlying anatomical landmarks (Fig. 1a). In addition, it was possible to perform EMG recordings during the locomotor tasks (Fig. 1c). A large number of parameters describing locomotor outcome could be assessed in the four different tasks, as summarized in Table 1. However, for efficient analysis of locomotor ability, we chose a set of the most reasonable and relevant parameters for each locomotor task (Table 1). Precise paw placement[17] and fore-hindlimb coordination[14] were evaluated on the horizontal ladder, whereas basic aspects of locomotor function were assessed during normal walking or wading. In addition, during wading, rats and mice tended to raise themselves as much as possible out of the water thus maximally extending their limbs. Therefore, we assessed body height and joint angles in this task and interpreted them as measures of strength. During swimming, rats and mice showed consistent, stereotypical hindlimb movements and wave-like tail movements, which allowed reliable kinematic assessment of different forms of coordination and movement patterns.

Evaluation of locomotor impairments

To model different types of CNS injury, adult female Lewis rats received surgical dorsal thoracic, ventral thoracic or unilateral right-sided cervical spinal cord injuries (SCI) or unilateral left-sided ischemic strokes in the motor cortex induced by stereotactic injections of endothelin-1, a potent vasoconstrictor (Fig. 1d). We also assessed locomotion in a genetically modified mouse line, EphA4-

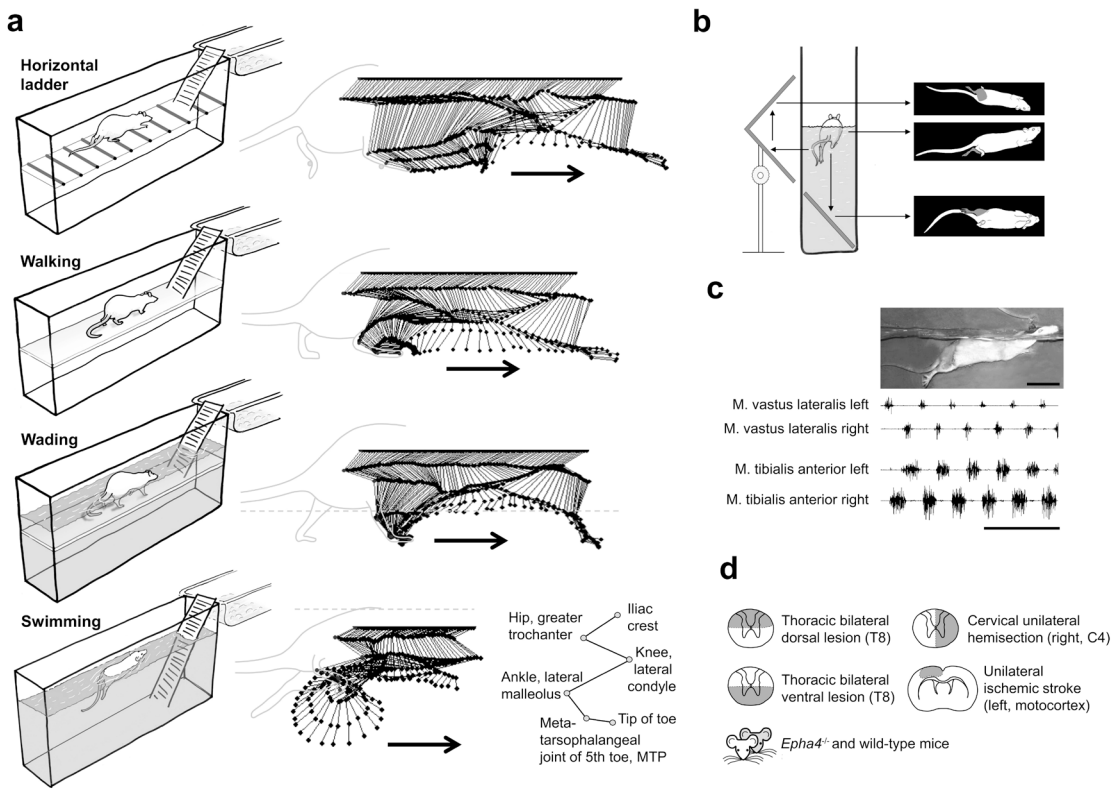

Figure 1: Experimental set-up for detailed evaluation of locomotor function in rodents after different forms of CNS damage. (**a**) We test locomotion in four different behavioral tasks by introducing different elements (horizontal ladder, shelf, water) into a basin. Tasks evaluated are "walking over an irregular horizontal ladder", "overground locomotion", "wading through shallow water" and "swimming". Stick diagrams of a single hindlimb step or swim cycle obtained from an uninjured animal illustrate that movement patterns differ considerably between tasks. Arrows indicate direction of movement and dashed line illustrates water level during wading and swimming**.** Bony landmarks for kinematic analysis of hindlimb movements are shown. (**b**) An arrangement of 3 mirrors enables recording of animals' performance with a high-speed camera from the left, right and bottom view, simultaneously. (**c**) Photograph of a swimming rat with head adapter for EMG recordings; scale bar, 5 cm. Sequences of amplified EMG illustrate hindlimb muscle activity of an uninjured animal during swimming; scale bar, 500 ms. (**d**) Schematic representations illustrate paradigms of CNS damage evaluated in this study, also used in **Figure 2-5**. CNS injuries are either bilateral dorsal spinal lesions at thoracic vertebral level 8 (T8), bilateral ventral spinal lesions at T8, unilateral right-sided spinal hemisections at cervical level 4 (C4) or ischemic strokes in the left motor cortex. *EphA4*-receptor knockout mice (*Epha4*$^{-/-}$) are compared to wild-type mice.

receptor knockout (*EphA4*$^{-/-}$), with a characteristic hopping gait[18] and compared them to wild-type mice.

In the horizontal ladder task, trained intact rats (Fig. 2a) crossed the ladder almost without slips or missteps, and hindlimbs were always placed on the rung that was previously occupied by the ipsilateral forepaw, indicating perfect coordination of fore- and hindlimbs. After bilateral dorsal thoracic SCI, rats demonstrated significant deficits in accurate hindpaw placement, typically owing to short targeting ($P < 0.0001$, one-way repeated-measures ANOVA, $n = 5$ animals; Fig. 2b,c). Rungs used by the ipsilateral forepaw were less frequently targeted by the respective hindlimb (49 ± 14%, 3 days after injury, animal group mean ± s.e.m., $n = 5$ animals) suggesting impaired fore-hindlimb coordination

(Fig. 2d). No substantial recovery of either skill was detected at 28 days after injury. Rats with thoracic bilateral ventral SCI or cervical hemisections had very low performance on the ladder; precise hindpaw placement and fore-hindlimb coordination were virtually absent post-injury (not shown). After cervical hemisection, the ipsilesional forelimb was strongly impaired and only passively dragged over the rungs. Left cortical strokes resulted in slight and transitory, but significant deficits in skilled placement of the right fore- and hindpaw (forepaw: P = 0.0122, hindpaw: P = 0.0344, one-way repeated-measures ANOVA, n = 3 animals) while left limbs were unimpaired (Fig. 2e). Fore-hindlimb coordination was unchanged after unilateral strokes (Fig. 2f). When crossing the horizontal ladder, precise paw placement was not impaired in the *Epha4*$^{-/-}$ mice (Fig. 2g). *Epha4*$^{-/-}$ mice demonstrated synchronous steps with both, forelimbs and hindlimbs whereas fore- hindlimb coordination was normal (Fig. 2h).

During overground walking (Fig. 3a), rats with dorsal thoracic SCI consistently showed weight bearing steps. However, the gait was unstable leading to a significantly increased base of support (P = 0.0275, one-way repeated-measures ANOVA, n = 5 animals; Fig. 3b) and increased hindpaw exorotation (P = 0.0002, one-way repeated-measures ANOVA, n = 5 animals; Fig. 3c). Kinematic analysis revealed a significant backwards shift of hindlimb excursions although the total extent of movement remained unchanged (protraction: P = 0.0008, retraction: P = 0.0041, total: P = 0.6693, one-way repeated-measures ANOVA, n = 5 animals; Fig. 3d). In addition, fore-hindlimb coordination (P = 0.0003, one-way repeated-measures ANOVA, n = 5 animals; Fig. 3e) and toe clearance (P < 0.0001, one-way repeated-measures ANOVA; 70 ± 12 % of steps with paw dragging, 3 days after injury, animal group mean ± s.e.m., n = 5 animals; Fig. 3f) was significantly impaired. Seven days after either ventral thoracic lesions or cervical hemisections the walking pattern of the hindlimbs were massively impaired. After ventral injury, weight bearing hindlimb steps were extremely rare, limbs were maximally extended with limb excursions reduced to about 1 cm (Fig. 3d). Animals dragged themselves with their forelimbs with minimal hindlimb movements over the runway thus making more detailed analysis of hindlimb function almost impossible. The flat position of the animals was reflected by a reduced height of the iliac crest (Fig. 3g). However, total hindlimb excursions and limb protraction substantially improved within 4 weeks (Fig. 3d). Animals with a stroke walked almost normally; with only a tendency towards an increased external rotation of the right hindpaw (not shown). Overground walking in *Epha4*$^{-/-}$ mice was characterized by synchronous hindlimb movements (Fig. 3h). Coupling between the forelimbs was also observed when animals walked at a constant speed but not during exploration (Fig. 3h).

Parameter	Measure	Horizontal ladder	Walking	Wading	Swimming
General locomotor function					
Velocity of locomotion	meters/second	+	+	+	+
Trunk instability	seconds, centimeters	+	+	+	+
Body height, body angle	centimeters, degrees	+	++ (Fig. 3g)	++ (Fig. 4b,e,g)	+
Duration of tail or abdominal dragging	seconds	+	+	+	-
Base of support (distance between paws)	centimeters	+	++ (Fig. 3b)	+	+
Forelimb activity during swimming	number of FL strokes/run	-	-	-	++ (Fig. 5b)
Tail position, tail height, tail movement pattern, tail oscillation, tail motion velocity	centimeters, second^{-1}, centimeters/second	+	+	+	++ (Fig. 5i,j)
Basic and skilled limb movement					
Correct stepping, accurate paw placement	percent of plantar or functional steps	++ (Fig. 2b,c,e,g)	+	+	-
Step or swim cycle duration, phase duration	seconds	+	+	+	+
Linear displacement (for example, limb pro- and retraction, step height)	centimeters	+	++ (Fig. 3d)	++ (Fig. 4d,f)	+
Angular displacement (for example, range of motion, minimal and maximal joint angles)	degrees	+	+	++ (Fig. 4b)	+
Velocity or acceleration of displacement	centimeters/second, radian/second, centimeters/second^2, radian/second^2	+	+	+	++ (Fig. 5c)
Toe clearance (paw dragging)	percent of steps with paw dragging, percent of step cycle duration	+	++ (Fig. 3f)	++ (Fig. 4c)	-
Paw position and rotation	centimeters, degrees	+	++ (Fig. 3c)	+	+
Coordination					
FL-HL coordination:					
Coordinated placement of fore- and hindpaws on ladder	percent of identical rungs targeted	++ (Fig. 2d,f,h)	-	-	-
Ratio of FL and HL cycle duration	seconds/seconds	+	++ (Fig. 3e)	+	-
Phase dispersion, footfall diagram	percent deviation	+	+	+	-
Left-right coordination:					
Ratio of left and right limb cycle duration	seconds/seconds	+	+	+	+
Phase dispersion, footfall or phase diagram, polar plot	percent deviation	+	++ (Fig.3h)	+	++ (Fig. 5d,e)
Timing of muscle activity (EMG recordings)	seconds	+	+	+	++ (Fig. 1c)
Intralimb coordination:					
Timing of joint excursions	seconds	+	+	+	+
Limb motion patterns (for example, stick diagram, spatial displacement plot, angle-angle plot)	centimeters, degrees	+	+	+	++ (Fig. 5f,g)
Timing of muscle activity (EMG recordings)	seconds	+	+	+	++ (Fig. 1c)
Tail-HL coordination:					
Timing of hindlimb excursions in relation to tail motion	seconds	+	+	+	++ (Fig. 5h)
Intratail coordination:					
Timing of motion of different tail segments	seconds	-	-	-	+

(-) parameter not applicable or measurable; (+) parameter measurable; (++) recommended outcome parameter

Table 1: Summary of parameters and possible measures for quantification of locomotor function in the different locomotor tasks. A large number of established quantitative parameters, as well as new readouts, can be assessed with the set-up. For locomotor profiling after CNS damage, we recommend a set of the most relevant outcome parameters and give references to the Figures illustrating them. We use the horizontal ladder for testing skilled locomotion and fore-hindlimb coordination. Parameters characterizing basic aspects of overground locomotion are assessed during walking and wading. During swimming, we evaluate intralimb and left-right coordination of hindlimbs and tail movements. HL, hindlimb; FL, forelimb.

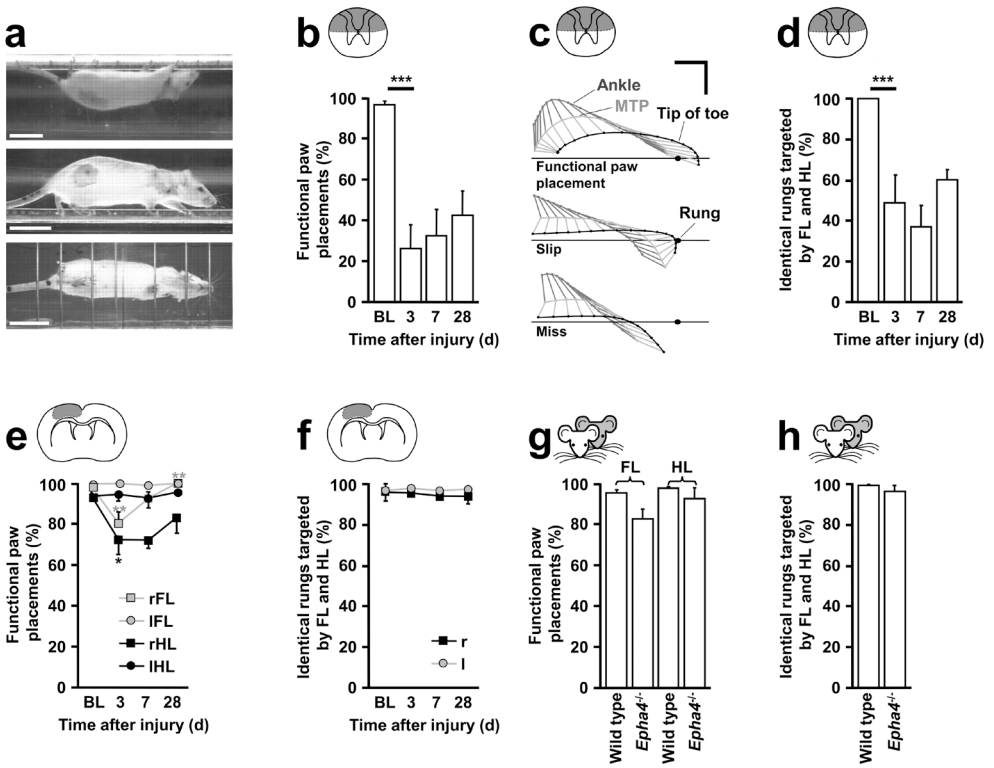

Figure 2: Skilled locomotion after CNS damage. (**a**-**f**) We evaluated skilled walking before (baseline, BL) and at several time points after dorsal thoracic SCI (*n* = 5 rats) or unilateral left-sided cortical stroke (*n* = 3 rats). (**a**) Image of intact rat crossing horizontal ladder; scale bars, 5 cm. (**b)** Precise placement of hindpaws after dorsal SCI. (**c**) Stick diagrams based on tracking of the ankle, MTP (metatarsophalangeal joint of 5th toe) and tip of toe illustrate typical hindpaw steps, classified as functional paw placement, slip or miss, after dorsal SCI; scale bars, 2 cm. (**d**) Fore-hindlimb coordination after dorsal SCI. (**e**) Precise placement of fore- and hindpaws and (**f**) fore-hindlimb coordination after stroke. (**g**) Precise placement of fore- and hindpaws and (**h**) fore-hindlimb coordination in wild-type (*n* = 3 animals) and *Epha4*$^{-/-}$ mice (*n* = 3 animals) assessed in a single testing session. (**b**,**d**-**h**) Bar and line graphs show animal group mean values for every testing session. (**b**,**d**,**g**,**h**) Values for left and right body side are averaged; (**e**,**f**) separate values for left (l) and right (r) side are presented. (**b**,**d**-**f**) For differences between time points, one-way repeated-measures ANOVA followed by *post hoc* Bonferroni tests were performed. (**g**,**h**) For differences between mice lines, data was subjected to Student's *t*-test (two-tailed, unpaired). ** $P < 0.01$, *** $P < 0.001$ indicate significantly different performances. Error bars, s.e.m.. FL, forelimb; HL, hindlimb.

During wading in intact animals, characteristic aspects of the locomotor pattern were a tiptoeing gait, elevated body position and increased limb excursions (Fig. 4a). After dorsal SCI and unilateral stroke, only minor lesion deficits were observed; the tiptoeing gait disappeared and heels touched the ground in the stance phase. Body height and joint angles of the knee and ankle, but not the hip, were transitorily reduced after dorsal SCI (Fig. 4b). Iliac crest height and joint angles of knee and ankle were strongly correlated (r_{knee}=0.87, r_{ankle}=0.91, Pearson's correlation coefficients, *n* = 88 steps of five animals, obtained 3, 7 and 28 days after injury). In contrast to normal overground walking, base of support was unchanged (not shown), paw dragging occurred only occasionally (38 ± 14 % of steps with paw dragging, 3 days after injury, animal group mean ± s.e.m., *n* = 5 animals; Fig. 4c) and hindlimb protraction was not significantly changed (*P* = 0.4883, one-way repeated-measures ANOVA,

n = 5 animals; Fig. 4d). Interestingly, animals with ventral thoracic lesions or with unilateral cervical injuries produced weight bearing hindlimb steps as early as 7 days after injury during wading, even though steps were characterized by increased retraction and reduced protraction (Fig. 4d). Following ventral injury, a gradual increase in iliac crest height during the recovery process was observed (Fig. 4e). After unilateral cervical hemisection, ipsilesional forelimb excursions were strongly impaired (Fig. 4f) paralleled by a strong reduction in the range of motion in the shoulder and elbow joint (data not shown). The *Epha4*$^{-/-}$ mice displayed a hopping gait also during wading. Other parameters like iliac crest height at mid-stance phase were unchanged in the mutant (Fig. 4g).

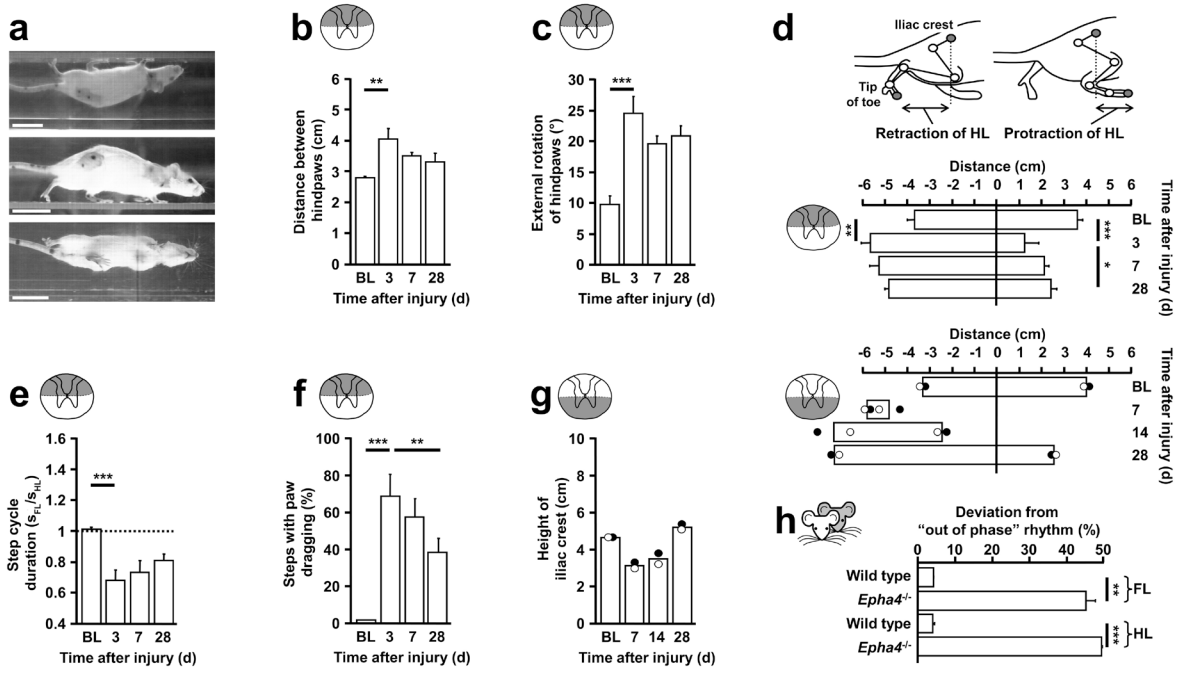

Figure 3: Overground walking after CNS damage. (**a**-**g**) Walking was tested before (baseline, BL) and at several time points after dorsal thoracic (*n* = 5 rats) or ventral thoracic SCI (*n* = 2 rats). (**a**) Image of intact rat walking over runway; scale bars, 5 cm. (**b**) Base of support and (**c**) external rotation of hindpaws at initial ground contact after dorsal SCI. (**d**) Horizontal hindlimb excursions described via the maximal protraction (maximal x-value) and retraction (minimal x-value) of the toe relative to the iliac crest after dorsal (upper panel) and ventral (lower panel) SCI. (**e**) Fore-hindlimb coordination and (**f**) toe clearance after dorsal SCI. (**g**) Height of iliac crest at mid-stance phase after ventral SCI. (**h**) Deviation from perfect left-right alternation (out-of-phase) of fore- and hindlimbs in wild-type (*n* = 3 animals) and *Epha4*$^{-/-}$ mice (*n* = 3 animals) assessed in one testing session. (**b**-**h**) Bars represent animal group mean values for every testing session. (**d** lower panel,**g**) Results for individual animals are shown; black and white dots represent individual animals. (**b**,**c**,**d** upper panel,**e**,**f**) For differences between time points, one-way repeated-measures ANOVA followed by *post hoc* Bonferroni tests were performed. (**d** lower panel,**g**) Data were not subjected to statistical testing. (**h**) For differences between mice lines, Student's *t*-test (two-tailed, unpaired) was applied. * $P < 0.05$, ** $P < 0.01$, *** $P < 0.001$ indicate significantly different performances. Error bars, s.e.m.. FL, forelimb; HL, hindlimb.

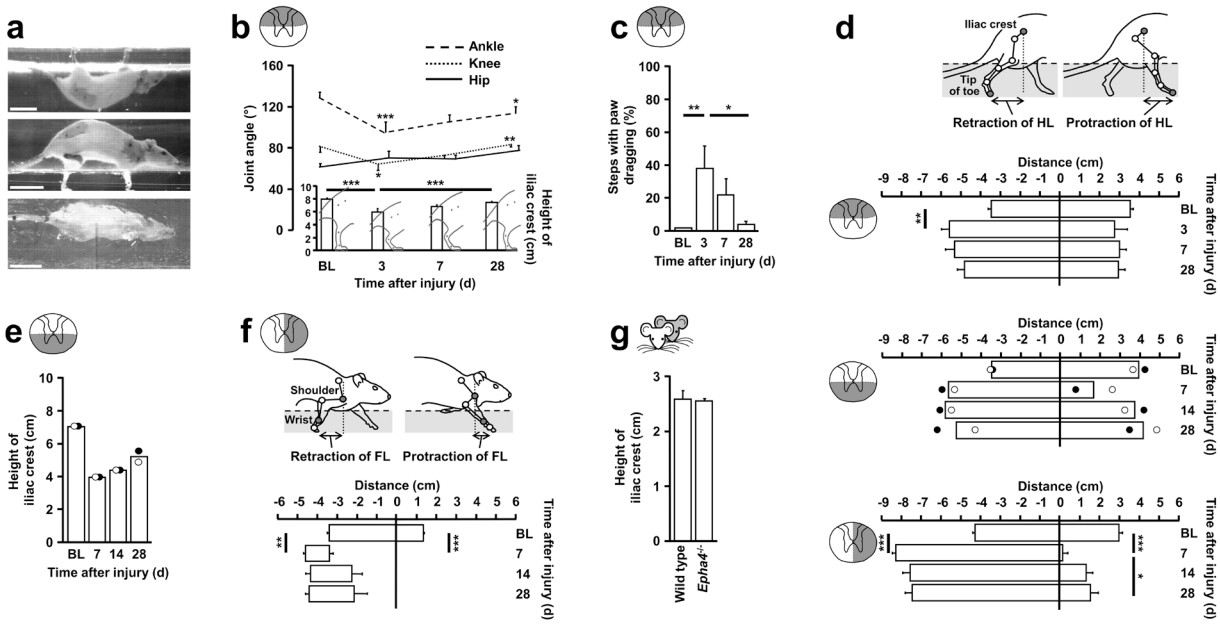

Figure 4: Wading after CNS damage. (**a**-**f**) Wading through shallow water was assessed before (baseline, BL) and at several time points after dorsal thoracic (*n* = 5 rats), ventral thoracic (*n* = 2 rats) or unilateral right-sided cervical SCI (*n* = 4 rats). (**a**) Image of intact rat wading; scale bars, 5 cm. (**b**) Hindlimb joint angles and iliac crest height at mid-stance phase after dorsal SCI. (**c**) Toe clearance in animals with dorsal SCI. (**d**) Horizontal hindlimb excursions during wading are presented as in **Figure 3d** for animals with dorsal (upper panel), ventral (middle panel) and unilateral cervical SCI (lower panel, ipsilesional hindlimb). (**e**) Height of iliac crest at mid-stance phase after ventral SCI. (**f**) Horizontal excursions of ipsilesional forelimb after unilateral cervical SCI. (**g**) Iliac crest height at mid-stance phase in wild-type (*n* = 3 animals) and *Epha4*$^{-/-}$ mice (*n* = 3 animals) measured at a single time point. (**b**-**g**) Bars represent animal group mean values for every testing session. (**d** middle panel,**e**) Results for individual animals are shown; black and white dots represent individual animals. (**b**,**c**,**d** upper and lower panel,**f**) For differences between time points, one-way repeated-measures ANOVA and *post hoc* Bonferroni tests were applied. (**d** middle panel,**e**) No statistical testing was performed. (**g**) For differences between mice lines, Student's *t*-test (two-tailed, unpaired) was used. * $P < 0.05$, ** $P < 0.01$, *** $P < 0.001$ indicate significantly different performances. Error bars, s.e.m.. FL, forelimb; HL, hindlimb.

Swimming is a stereotypical form of locomotor behavior characterized by powerful hindlimb strokes that are performed in a very consistent and well-coordinated manner providing the main drive for forward motion whilst forepaws are usually immobile below the chest (Fig. 5a)[19]. The horizontal sinusoidal oscillations of the tail and occasional forelimb strokes are probably important for navigation and stability during swimming. In infant rats[20] and SCI animals[21] extensive use of the forelimbs has been interpreted as a compensatory strategy for immature or impaired hindlimb function, respectively. Accordingly, we found that the number of forelimb strokes was significantly increased after dorsal thoracic SCI ($P = 0.0098$, one-way repeated-measures ANOVA, $n = 5$ animals; Fig. 5b). Hindlimb movements were slower as indicated by significantly reduced peak toe velocities ($P = 0.001$, one-way repeated-measures ANOVA, $n = 5$ animals) and longer stroke cycle durations with extended power and return stroke phases (Fig. 5c,d). A transient disturbance of the left-right coordination was present, and hindlimb excursions were initially smaller and of irregular shape (Fig. 5d-f).

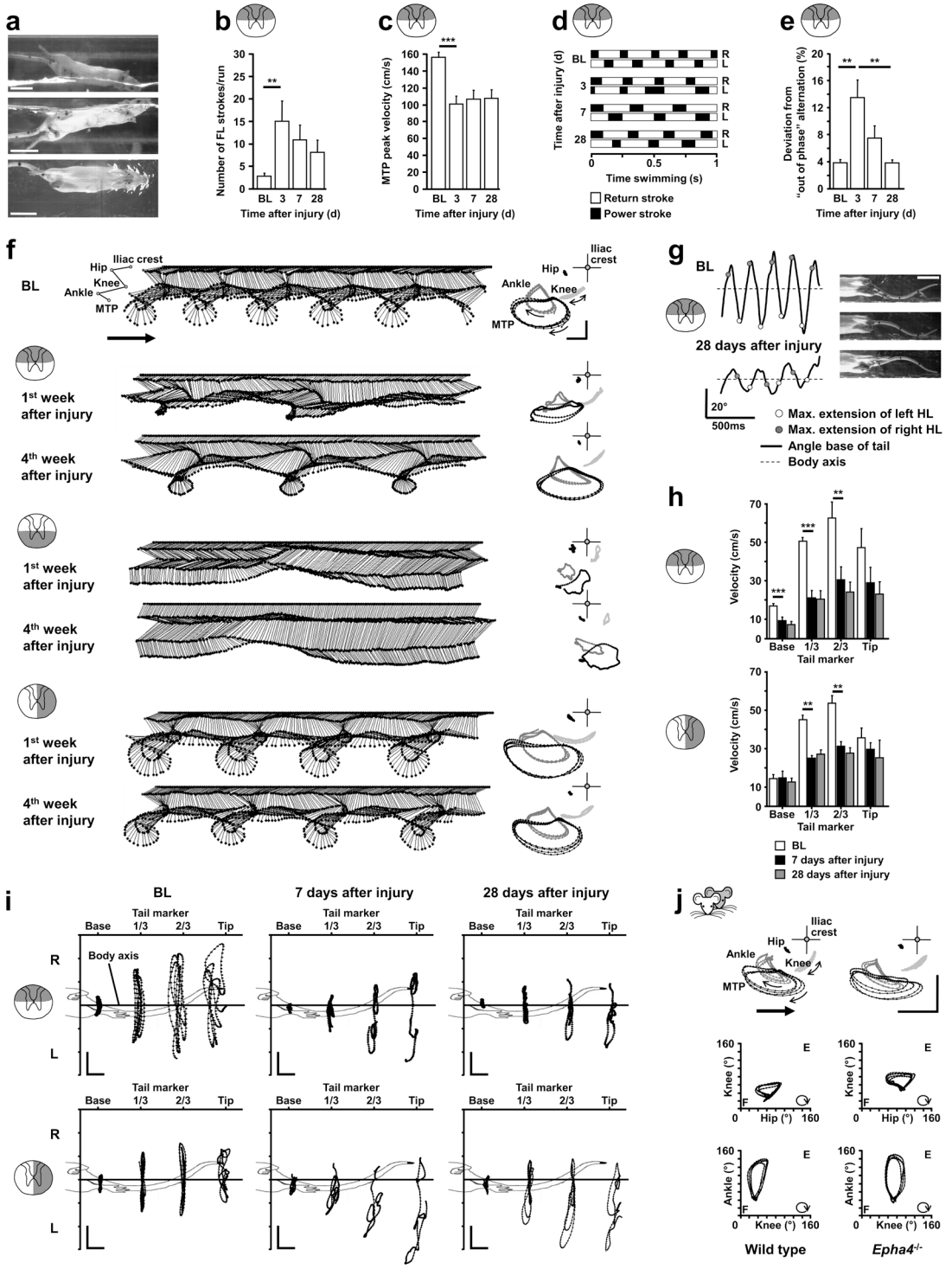

Figure 5: Swimming after CNS damage. (**a**-**i**) Swimming was tested before (baseline, BL) and at several time points after dorsal thoracic (*n* = 5 rats), ventral thoracic (*n* = 2 rats) or unilateral right-sided cervical SCI (*n* = 4 rats). (**a**) Intact rat swimming; scale bars, 5 cm. (**b**) Forelimb (FL) strokes and (**c**) peak velocity of metatarsophalangeal joint (MTP) after dorsal SCI. (**d**) Phase diagram illustrating left-right alternation of hindlimbs after dorsal SCI. (**e**) Deviation from perfect hindlimb alternation (out-of-phase) after dorsal SCI. (**f**) Stick diagrams and spatial displacement plots illustrate swimming performance after dorsal, ventral or unilateral SCI over a period of 1 s. Thick arrows, swimming direction; thin arrows, temporal progression of movements; scale bars, 2 cm. (**g**) Disturbed synchrony of tail base excursions and hindlimb (HL) extension after dorsal SCI. (**h**) Mean movement velocity of tail markers (base, first third, second third, tip of tail) after dorsal and unilateral SCI; scale bar, 5 cm. (**i**) Lateral movements of tail markers over a period of 1 s after dorsal and unilateral SCI; scale bars, 2 cm. R, right; L, left. (**j**) Spatial displacement and angle-angle plots of a *Epha4*$^{-/-}$ and wild-type mouse; scale bars, 2 cm. E, Extension; F, Flexion. (**b**,**c**,**e**,**h**) Bars represent animal group mean values for every testing session; one-way repeated-measures ANOVA and *post hoc* Bonferroni tests; ** $P < 0.01$, *** $P < 0.001$. Error bars, s.e.m.. (**d**,**f**,**g**,**i**,**j**) Results of single animals representative for their experimental group.

Hindlimb function during swimming recovered impressively, which was reflected in most of the parameters assessed. In contrast, the strongly impaired tail-hindlimb coordination, tail movement velocity and tail motion patterns did not improve over time (Fig. 5g-i). Throughout the testing period, animals with ventral thoracic SCI demonstrated massive impairments in hindlimb (Fig. 5f) and tail function (data not shown) and strong lateral instability in the swimming task. Forward motion was only achieved by excessive forelimb use. After cervical hemisection, kinematic analysis showed transiently exaggerated joint excursions of the ipsilesional hindlimb (Fig. 5f). Tail movements were slower and strongly deviated towards the uninjured side (Fig. 5h, i), suggesting an imbalance of tail muscle activity in favor of the intact side. Accordingly, animals with cervical hemisections suffered from lateral instability during swimming. After unilateral stroke, no deficits in swimming were detected (not shown). *Epha4*$^{-/-}$ mice showed consistent coupling of hindlimbs resulting in an uneven, bumpy swimming style that appeared less efficient than the regular left-right alternating pattern demonstrated by wild-type mice. A shift in the angle-angle plots towards higher degrees indicated increased extension of the hip and knee joint (Fig. 5j). In addition, *Epha4*$^{-/-}$ mice showed an extensive and coupled use of both forelimbs during swimming.

Discussion

We used a set of physiological, objective and quantitative parameters to generate comprehensive locomotor profiles for some of the most common models of CNS insult. We found that these profiles were highly dependent on lesion type and severity. Some parameters were more sensitive to or more affected by one particular lesion than another allowing for the selection of suitable combinations of locomotor task, readouts and lesion type in future studies.

After dorsal thoracic SCI, rats performed weight-bearing hindlimb steps and showed only transitory deficits in left-right and intralimb coordination during swimming, indicating that the lumbar spinal central pattern generator (CPG) networks and their main modulatory inputs were unaffected by the injury[22, 23]. However, damage to major components of the cortico- and rubrospinal tract and the gracile fasciculus led to strongly impaired paw placing, seen during skilled walking and overground locomotion, with respect to accuracy, strength and velocity. This suggests that these tracts play an important role in skilled and distal hindlimb motor function in rats[17]. In addition, after this lesion type fore-hindlimb coordination and tail movements were also impaired, possibly due to damage of components of the propriospinal system[24] and bulbospinal tracts, respectively. In line with these findings, unilateral strokes comprising the fore- and hindlimb sensorimotor region resulted in contralateral deficits in fine motor control without affecting other basic aspects of locomotion during swimming, walking or wading. Ventral thoracic SCIs disrupt, amongst others, vestibulospinal fibers and main portions of the reticulo- and raphespinal tracts. The latter are known to be crucial for the initiation and modulation of stepping movements via CPG networks[25, 26]. Accordingly, in the first week after injury rats were not able to perform hindlimb swimming strokes or stepping movements during normal overground walking. Interestingly, animals could generate hindlimb movements in the wading test since assistive weight support was provided by the water buoyancy. Although stepping ability improved significantly over time, animals were, even after several weeks, barely able to produce hindlimb strokes during swimming. In the absence of major bulbospinal input, it can be assumed that the rhythmic hindlimb movements generated by the lumbar CPGs rely on or are facilitated by proproiceptive input due to limb loading which is present during wading but not during swimming[27]. Thus, as both proproiceptive input and some weight support seem to be required for hindlimb movements after this lesion, wading is the most appropriate test to demonstrate and evaluate locomotor ability in these animals. Following cervical unilateral hemisection, fore- and hindlimbs as well as locomotion in the four different tasks were differently affected. Forelimb locomotor function was

extremely poor throughout the entire testing period in all locomotor tasks. In contrast, hindlimb movements were present during wading and swimming within the first week of injury followed by substantial functional recovery indicated by regular weight-bearing hindlimb steps and excellent intralimb coordination. However, animals remained poor in their ability to cross the ladder. These data suggest that the descending fiber tracts in the spared hemicord were at least partially sufficient to compensate for lost supraspinal input. This partial compensation allowed for good basic locomotor function of the affected hindlimb but not forelimb during walking, wading and swimming, however it did not enable skilled movements of either limb. The absence of EphA4, an important axon guidance receptor during development, led to anatomical alterations of corticospinal projections and locomotor networks in the lumbar spinal cord[18, 28]. These changes are considered responsible for the previously described synchronous hindlimb movements ('hopping') during walking[18]. Interestingly, we found additionally that forelimb movements were synchronously coupled during overground locomotion. No deficit in precise paw placement was detected on the horizontal ladder. These behavioral data suggest that important anatomical changes are also present on the level of cervical CPG networks[29], but that the anatomically altered corticospinal system is able to control precise targeted movements. These conclusions were based on testing in several locomotor tasks, highlighting the importance of broad screening.

Our data were comprehensive in several ways. We provided information about whether and how a task was performed after a variety of CNS insults in rats and mice. The battery of readouts used ranged from very basic to very specific. We assessed movements of all relevant body parts (forelimbs, hindlimbs, trunk and tail) as well as the most important characteristics of locomotion, for example different forms of coordination. In addition, our analysis was highly sensitive as it was able to detect compensatory strategies, such as the finding that during swimming, slower, less powerful and uncoordinated hindlimb strokes were compensated for by extensive forelimb use and exaggerated hindlimb movements in rats with SCI. A number of established as well as novel parameters were assessed. For the established parameters, our results are in line with data from earlier studies using comparable lesion types and testing conditions[16, 17, 21, 30]. In this study, we concentrated on commonly used CNS injury paradigms in adult rats and on one transgenic mouse line. However, our method is not limited to these situations and could also be used to study models of peripheral nerve injury, muscular diseases, and neuroinflammatory or neurodegenerative diseases.

Our results, derived from a systematic evaluation of different types of CNS damage in rodents, emphasize the importance of detailed locomotor profiling in animal research. Broad application of these sets of objective and quantitative readouts will improve and standardize behavioral assessment.

Online methods

Animals. We performed all experiments with the approval of and in accordance with the guidelines of the Veterinarian Office Zurich, Switzerland. CNS lesions and behavioral testing were performed on 14 adult female Lewis rats (200-250 g, R. Janvier). In addition, we evaluated locomotor function in three EphA4-receptor knockout (*Epha4*$^{-/-}$, C57BL/6 background, provided by R. Klein) and three wild-type C57BL/6 mice. Mice were 4-5 months old and of both sexes. Animals were housed in groups of 3-5 per cage, 12:12 h light:dark cycle with food and water *ad libitum*.

Surgery and animal care. We performed all surgeries (rats only) under general anesthesia achieved by subcutaneous injections of Hypnorm/Dormicum (Hypnorm: 120 µl per 200 g body weight, Janssen Pharmaceutics; Dormicum 0.75 mg per 200 g body weight, Roche Pharmaceuticals). Spinal cord injuries were either: a bilateral dorsal cut lesion at T8 vertebral level (*n* = 5 rats), a large bilateral ventral lesion at T8 (*n* = 2 rats), or a cervical unilateral right-sided complete hemisection at C4 (*n* = 4 rats). The lesions were performed as described previously[30, 31]. Animals with an ischemic lesion to the cortex (stroke, *n* = 3 rats) received 14 stereotactic injections of the vasoconstrictor endothelin-1 (ET-1, 0.3 □g/□,Sigma-Aldrich) into the left motor cortex (fore- and hindlimb areas). We injected a volume of 500 nl at a depth of 1.2 mm with a rate of 6 nl/sec. After each injection, we left the needle in place for 3 min before it was carefully removed. After the final injection of ET-1, or after SCI, the animals were sutured and returned to a heated blanket to recover from surgery. One day before and for two days after surgery, animals received subcutaneous injections of analgesic (Rimadyl, 2.5 mg per kg body weight, Pfizer AG). In addition, postoperative care included daily subcutaneous injections of antibiotics (Baytril, 5 mg per kg body weight, Bayer AG) for one week to prevent bladder or wound infections. We checked the animals' health twice daily for the entire experiment. After SCI, bladders were manually expressed until normal bladder function returned. As expected, stroke lesions did not affect bladder function.

Testing apparatus. For evaluation and analysis of locomotor function in rats and mice, we used a single custom designed set-up, the *MotoRater* (Supplementary Fig. 1a-e). The complete set-up is now commercially available at TSE-systems GmbH (www.tse-systems.com.). We tested the animals in a clear Plexiglas basin, 150 cm in length, 13 cm in width and 40 cm in height (Supplementary Fig. 1a). At one end a small footbridge allowed the animals to exit the basin into a cage. A temperature sensor

was installed to measure the water temperature. For testing skilled locomotion, we placed a horizontal ladder (for rats: length of 113 cm, width of 13 cm; for mice: length of 113 cm, width of 7 cm; 15 cm above ground) with regularly (training) or irregularly (testing) spaced, round metal rungs into the basin (Supplementary Fig. 1b). We used a Plexiglas runway (length of 123 cm, width of 13 cm, 15 cm above ground) to assess overground locomotion and wading (Supplementary Fig. 1b). For wading and swimming, the water temperature was 23 °C. Water depth for wading was 3 cm (rats) or 1 cm (mice) above the runway's surface; for swimming, water depth was 25 cm. For mice, we restricted the width of the testing corridor to 7 cm by two additional Plexiglas walls (Supplementary Fig. 1b). To allow evaluation of the animals` performance from the left and right side and from below at the same time, we placed one mirror (100 cm x 16 cm) on the basin's floor at an angle of ~ 90 ° and positioned two perpendicularly arranged mirrors (100 cm x 18 cm) behind the long side of the basin (Fig. 1b and Supplementary Fig. 1a, c). We used high frame rates to film the animals' performance in the testing basin (see below). This required an additional strong light source that was comprised of four commercially available 36 Watt fluorescent lamps emitting cool white light. During testing, the lighting rack was located between the camera and the testing apparatus illuminating the basin from above (one lamp) and below (three lamps). More detailed information is provided in the Supplementary Note 1.

Electromyographic recordings. For EMG recordings during the locomotor tasks, we placed a cableway system on top of the basin enabling a motile wire connection between a preamplifier and the animals' head adapter (Fig. 1c and Supplementary Fig. 1d). Bipolar Teflon-coated stainless steel wires (Cooner wires Inc.) were chronically implanted into the left and right m. tibialis anterior and m. vastus lateralis as described previously[32]. The distance between the electrode tips was between 1-2 mm. Implanted wires were led subcutaneously to the head and attached to a connector that was fixed on the animals' skull with dental cement. One wire served as a ground electrode and was placed subcutaneously in the neck region of the animal. Pre-amplified signals were digitized (sampling rate of 1 kHz), amplified (1000 x) and high-pass filtered (30 Hz). We processed the data with DIAdem academic 8.1 software (National Instruments Engineering GmbH & Co. KG).

Preparation of the animals. After acclimatization to the testing apparatus, we trained the animals in 5 daily sessions (every other day, about 10 passages per animal and task) until they crossed the testing

basin with a constant speed. Animals were trained on the ladder with a regular arrangement of metal rungs. For testing, rung sequences were irregular and varied to avoid habituation to a particular rung pattern. Before baseline recording, the skin overlying defined anatomical landmarks on the lateral side of the forelimbs and hindlimbs was shaved and tattooed with a commercially available tattooing kit (Hugo Sachs Elektronik, Harvard Apparatus GmbH). We marked the following bony structures of the forelimb: vertebral border of the scapula (shoulder blade); tip of the humerus (shoulder joint); wrist and the 5th metacarpal head (digit)[33]. We also labeled the following hindlimb structures: iliac crest; greater trochanter (hip); lateral malleolus (ankle); metatarsophalangeal joint of 5th toe (MTP) and the tip of toe[33]. On the ventral surface of the tail, we marked four points with tattoos, these were: the base of the tail, the first and second thirds of the tail and the tip of the tail.

Data acquisition and kinematic analysis. We tested animals with strokes and dorsal SCIs before (baseline) and 3, 7 and 28 days after injury. Locomotor performance of rats with ventral and cervical SCIs was evaluated at baseline and 7, 14 and 28 days following lesion. In these animals, we removed the early session (3 days) as animals are more severely impaired after ventral and cervical lesions than they are after stroke or dorsal SCI. We tested *Epha4*$^{-/-}$ and wild-type mice in a single session. Before every testing session, we reinforced visualization of the tattoos with a fluorescent dye (for example fluorescent, fast drying nail polish) or a black marker in case of albino rats. For each animal and each task, we recorded 3-10 passages and analyzed at least three of them. The analysis was based exclusively on video recordings captured with a high-speed color camera (Basler A504kc Color Camera, Basler AG, 1280 x 1024 pixels). We filmed animals at a frame rate of 50, 100 or 200 f/s (Hz) for skilled walking on the ladder, overground walking and wading or swimming, respectively.

To increase the number of pixels per marker, we placed the camera close to the basin (distance of 100-150 cm), thereby limiting the field of view to about one third of the length of the testing track. By moving the camera on a guide rail along the testing track, we recorded the full distance covered by the animals (Supplementary Fig. 1e). We attached a commercially available flashlight pointer to the camera that indicated the camera's field of view. This provided visual feedback to the experimenter who manually moved the camera thus allowing reliable recordings of moving animals. Locomotor behavior was only analyzed in a central, 60 cm long region of the testing apparatus to avoid artifacts due to acceleration and deceleration at the beginning and end of the track, respectively. For each task

only passages with similar and constant movement velocities and without lateral instability (see Supplementary Note 1) were used for kinematic analysis.

In collaboration with a software engineering company (ALEA Solutions GmbH), a color-based automated tracking software ClickJoint, V5.0 was developed (now commercially available at ALEA Solutions GmbH, www.aleasol.ch) and used for offline analysis of the video recordings. For calibration of the software, we placed three 5 cm long pieces of tape on the walls of the testing basin so they were visible from all perspectives (direct view and mirror images). As the camera was moved during recordings to follow the animals on their journey through the testing basin, normalization of the spatial measurements to the position of the iliac crest (for hindlimb analysis) or the shoulder blade (for forelimb analysis) was required. The software automatically tracked the markers on the animals' skin frame-by-frame and generated two-dimensional coordinates (x, y) for every marker and time point. Based on these coordinates, the software modeled body segments as rigid straight lines between markers. For kinematics, movements were automatically reconstructed from changes in the marker location between consecutive frames. Angles and distances were calculated directly by the software allowing the generation of stick diagrams and spatial displacement plots. For angle measurements, we used the smaller angle of the two alternatives; typically this was the angle at the flexor side of a limb joint. We analyzed the side and the bottom views of the animal separately. Data were smoothed by applying an integrated supplementary function of the ClickJoint software using a cubic-spline function. Data were then imported into Microsoft Office Excel 2007 and further analyzed with pre-assembled Excel sheets determining, for example joint angles or distances between joints at a given time point, range of motion, coordination parameters or movement velocities. To minimize artifacts due to divergent movements of the skin over the underlying bony structures[34], we defined the knee and elbow joints as virtual joints, that is their positions were indirectly computed by the ClickJoint software. For the knee, the calculation was based on both the position of the markers over the hip and ankle and the length of the femur (rat = 2.5 cm, mouse = 1.3 cm) and tibia (rat = 3.5 cm, mouse = 2 cm) bones. For the elbow joint, the shoulder and wrist positions and the length of humerus (rat = 2.5 cm, mouse = 1.1 cm) and the lower forelimb (rat = 2.8 cm, mouse = 1.2 cm) were used. For more detailed information about camera settings, software application and data processing see Supplementary Note 1.

Locomotor parameters. We defined the movement phases of a limb during locomotion in accordance with the literature[9, 19]. In brief, for walking and wading, a gait cycle was defined as the time period between two consecutive ground contacts of the paw of one limb. The time point of paw contact was identified visually. The stance phase lasted from the initial paw contact until lift off and this was followed by the swing phase which started with lift off and terminated with ground contact of the paw. We defined mid-stance as the time point in the middle of the stance phase. For swimming, we defined a stroke cycle as the time period between two consecutive hip angle minimums of one limb. This was determined based on kinematic joint angle measurements. Within a stroke cycle, two phases were distinguished, the "power stroke" and the "return stroke". The power stroke started with the minimum hip angle and ended when the maximum hip angle was reached. The onset and ending of the return stroke was determined by the maximum and minimum hip angle, respectively. We defined the body axis which was required for the tail kinematics as a virtual line connecting the nose, two virtual points midway between fore- and hindlimbs and the genital area.

Horizontal ladder: For evaluation of skilled walking over the horizontal ladder, steps were counted and classified as: functional paw placement (a weight-bearing step on a rung); slip (a step with initial contact of the rung followed by a slip off the rung) or miss (a step that missed the rung completely). We quantified fore-hindlimb coordination by assessing how often the same rung was targeted (touched) first by the forelimb and subsequently by the ipsilateral hindlimb; a pattern that is usually observed in intact rodents crossing a ladder (baseline)[14]. Numbers were expressed as a percentage of total steps or targeting attempts and were an average of at least three passes.

Wading and walking: We defined the base of support as the distance between the paws during the stance phase. For the hindlimbs, base of support was calculated by adding the distances measured between the MTP of the 3rd toe and the body axis for consecutive left-right hindlimb steps. We assessed external rotation of the hindlimb at the beginning of the stance phase by measuring the angle between the body axis and the paw axis defined by a virtual line connecting the 3rd MTP and the heel. For evaluation of base of support and external rotation, we used the bottom view of the animal. Based on the side views, horizontal pro- and retraction of hind- and forelimbs in the sagittal plane were quantified by measuring the maximal and minimal toe or wrist excursions relative to the iliac crest or shoulder, respectively. The number of steps with paw dragging (defined as digits touching the ground during the swing phase) were counted and expressed as a percentage of total steps. We determined

the height of the iliac crest by measuring the vertical distance between the iliac crest and the surface of the runway during mid-stance.

Swimming: The number of forelimb strokes was assessed manually. Forelimb strokes that touched the walls of the Plexiglas basin and thus were mainly used for navigation were excluded from the analysis. We evaluated left-right coordination by measuring the time interval between the onset of the stroke cycle of the ipsilateral and contralateral hindlimb. This time interval was then normalized to the duration of the complete stroke cycle of one of the hindlimbs, usually the right, and expressed as a percentage[9, 35]. Thus, 0 % indicates simultaneous hindlimb movements whilst 50 % suggests a perfect, alternating "out-of-phase" rhythm. Deviation from the perfect "out-of-phase" rhythm was used as readout of left-right coordination. Stick diagrams, spatial displacement plots and angle-angle plots were typically generated for a time period of 1sec (4-5 stroke cycles in intact rats) per pass. We evaluated tail-hindlimb coordination by determining the temporal relation between the time point of the most extreme angular displacement of the base of tail to the left or the right side and that of the maximal hindlimb extension.

Statistics. We performed the statistical analysis with the SPSS software package for Windows (V14.0; SPSS, Inc.) and GraphPad Prism 5 for Windows (V5.01; GraphPad Software, Inc.). For the behavioral data obtained from rats with a CNS injury, one-way repeated-measures ANOVA followed by *post hoc* Bonferroni tests were used to assess lesion effects (baseline vs. 3 or 7 days after injury) and functional recovery (3 or 7 vs. 28 days after injury). To detect correlations between parameters, we calculated Pearson's correlation coefficients. For animals with a ventral SCI, only descriptive statistics were applied due to the fact that only two animals were evaluated. In these cases, results for individual animals are shown with black and white dots representing individual animals in the Figures. To test differences between *Epha4*$^{-/-}$ mice and wild-type mice, we performed Student's *t*-test (two-tailed, unpaired). Data are presented as animal group mean values for every testing session and error bars represent s.e.m.. The level of statistical significance for all tests was determined *a priori* at $P < 0.05$.

Preparation of Figures

We generated the data graphs in Microsoft Office Excel 2007. Stick diagrams were generated by the ClickJoint software, V5.0 (ALEA Solutions GmbH). Photographs, diagrams and all data graphs were processed in Microsoft Office PowerPoint 2007 and Adobe Photoshop CS3 Extended.

References

1. Basso, D.M. Neuroanatomical substrates of functional recovery after experimental spinal cord injury: implications of basic science research for human spinal cord injury. *Phys Ther* 80, 808-817 (2000).
2. Raineteau, O. & Schwab, M.E. Plasticity of motor systems after incomplete spinal cord injury. *Nat Rev Neurosci* 2, 263-273 (2001).
3. McEwen, M.L. & Springer, J.E. Quantification of locomotor recovery following spinal cord contusion in adult rats. *J Neurotrauma* 23, 1632-1653 (2006).
4. Muir, G.D. & Webb, A.A. Mini-review: assessment of behavioural recovery following spinal cord injury in rats. *Eur J Neurosci* 12, 3079-3086 (2000).
5. Metz, G.A., Merkler, D., Dietz, V., Schwab, M.E. & Fouad, K. Efficient testing of motor function in spinal cord injured rats. *Brain Res* 883, 165-177 (2000).
6. Kunkel-Bagden, E., Dai, H.N. & Bregman, B.S. Methods to assess the development and recovery of locomotor function after spinal cord injury in rats. *Exp Neurol* 119, 153-164 (1993).
7. Basso, D.M., Beattie, M.S. & Bresnahan, J.C. A sensitive and reliable locomotor rating scale for open field testing in rats. *J Neurotrauma* 12, 1-21 (1995).
8. Hamers, F.P., Lankhorst, A.J., van Laar, T.J., Veldhuis, W.B. & Gispen, W.H. Automated quantitative gait analysis during overground locomotion in the rat: its application to spinal cord contusion and transection injuries. *J Neurotrauma* 18, 187-201 (2001).
9. Courtine, G., Garasimenko, Y., van den Brand, R., Yew, A., Musienko, P., Zhong, H. Song, B., Ao, Y., Ichiyama, R. M., Lavrov, I., Roy, R. R., Sofroniew, M. V., Edgerton, V. R. Transformation of nonfunctional spinal circuits into functional states after the loss of brain input. *Nat Neurosci* 12, 1333-1342 (2009).
10. Magnuson, D.S., Smith, R.R., Brown, E.H., Enzmann, G., Angeli, C., Quesada, P.M., Burke D. Swimming as a model of task-specific locomotor retraining after spinal cord injury in the rat. *Neurorehabil Neural Repair* 23, 535-545 (2009).
11. Gorska, T., Chojnicka-Gittins, B., Majczynski, H. & Zmyslowski, W. Recovery of overground locomotion following partial spinal lesions of different extent in the rat. *Behav Brain Res* 196, 286-296 (2009).
12. Basso, D.M. Behavioral testing after spinal cord injury: congruities, complexities, and controversies. *J Neurotrauma* 21, 395-404 (2004).
13. Roy, R.R., Hutchison, D.L., Pierotti, D.J., Hodgson, J.A. & Edgerton, V.R. EMG patterns of rat ankle extensors and flexors during treadmill locomotion and swimming. *J Appl Physiol* 70, 2522-2529 (1991).
14. Bolton, D.A., Tse, A.D., Ballermann, M., Misiaszek, J.E. & Fouad, K. Task specific adaptations in rat locomotion: runway versus horizontal ladder. *Behav Brain Res* 168, 272-279 (2006).
15. Garnier, C., Falempin, M. & Canu, M.H. A 3D analysis of fore- and hindlimb motion during locomotion: comparison of overground and ladder walking in rats. *Behav Brain Res* 186, 57-65 (2008).
16. Kanagal, S.G. & Muir, G.D. Task-dependent compensation after pyramidal tract and dorsolateral spinal lesions in rats. *Exp Neurol* 216, 193-206 (2009).

17. Metz, G.A. & Whishaw, I.Q. Cortical and subcortical lesions impair skilled walking in the ladder rung walking test: a new task to evaluate fore- and hindlimb stepping, placing, and co-ordination. *J Neurosci Methods* 115, 169-179 (2002).
18. Dottori, M., Hartley, L., Galea, M., Paxinos, M., Polizzotto, M., Kilpatrick, T., Bartlett, P.F., Murmpy, M., Köntgen, F., Boyd, A.W. EphA4 (Sek1) receptor tyrosine kinase is required for the development of the corticospinal tract. *Proc Natl Acad Sci U S A* 95, 13248-13253 (1998).
19. Gruner, J.A. & Altman, J. Swimming in the rat: analysis of locomotor performance in comparison to stepping. *Exp Brain Res* 40, 374-382 (1980).
20. Schapiro, S., Salas, M. & Vukovich, K. Hormonal effects on ontogeny of swimming ability in the rat: assessment of central nervous system development. *Science* 168, 147-150 (1970).
21. Liebscher, T., Schnell, L., Schnell, D., Scholl, J., Schneider, R., Gullo, M., Fouad, K., Mir, A., Rausch, M., Kindler, D., Hamers, F. P., Schwab, M. E. Nogo-A antibody improves regeneration and locomotion of spinal cord-injured rats. *Ann Neurol* 58, 706-719 (2005).
22. Kiehn, O. Locomotor circuits in the mammalian spinal cord. *Annu Rev Neurosci* 29, 279-306 (2006).
23. Goulding, M. Circuits controlling vertebrate locomotion: moving in a new direction. *Nat Rev Neurosci* 10, 507-518 (2009).
24. Juvin, L., Simmers, J. & Morin, D. Propriospinal circuitry underlying interlimb coordination in mammalian quadrupedal locomotion. *J Neurosci* 25, 6025-6035 (2005).
25. Grillner, S., Wallen, P., Saitoh, K., Kozlov, A. & Robertson, B. Neural bases of goal-directed locomotion in vertebrates--an overview. *Brain Res Rev* 57, 2-12 (2008).
26. Hagglund, M., Borgius, L., Dougherty, K.J. & Kiehn, O. Activation of groups of excitatory neurons in the mammalian spinal cord or hindbrain evokes locomotion. *Nat Neurosci* 13, 246-252.
27. Frigon, A. & Rossignol, S. Experiments and models of sensorimotor interactions during locomotion. *Biol Cybern* 95, 607-627 (2006).
28. Butt, S.J., Lundfald, L. & Kiehn, O. EphA4 defines a class of excitatory locomotor-related interneurons. *Proc Natl Acad Sci U S A* 102, 14098-14103 (2005).
29. Yamaguchi, T. The central pattern generator for forelimb locomotion in the cat. *Prog Brain Res* 143, 115-122 (2004).
30. Ghosh, A., Sydekum, E., Haiss, F., Peduzzi, S., Zörner, B., Schneider, R., Baltes, C., Rudin, M., Weber, B., Schwab, M. E. Functional and anatomical reorganization of the sensory-motor cortex after incomplete spinal cord injury in adult rats. *J Neurosci* 29, 12210-12219 (2009).
31. Schucht, P., Raineteau, O., Schwab, M.E. & Fouad, K. Anatomical correlates of locomotor recovery following dorsal and ventral lesions of the rat spinal cord. *Exp Neurol* 176, 143-153 (2002).
32. Kaegi, S., Schwab, M.E., Dietz, V. & Fouad, K. Electromyographic activity associated with spontaneous functional recovery after spinal cord injury in rats. *Eur J Neurosci* 16, 249-258 (2002).
33. Fischer, M.S., Schilling, N., Schmidt, M., Haarhaus, D. & Witte, H. Basic limb kinematics of small therian mammals. *J Exp Biol* 205, 1315-1338 (2002).

34. Filipe, V.M., Pereira, J.E., Costa, L.M., Mauricio, A.C., Couto, P.A., Melo-Pinto, P., Varejao, A.S. Effect of skin movement on the analysis of hindlimb kinematics during treadmill locomotion in rats. *J Neurosci Methods* 153, 55-61 (2006).

35. Kloos, A.D., Fisher, L.C., Detloff, M.R., Hassenzahl, D.L. & Basso, D.M. Stepwise motor and all-or-none sensory recovery is associated with nonlinear sparing after incremental spinal cord injury in rats. *Exp Neurol* 191, 251-265 (2005).

Supplementary information to Chapter 2

Supplementary Figure 1: Different components of the locomotor testing system.

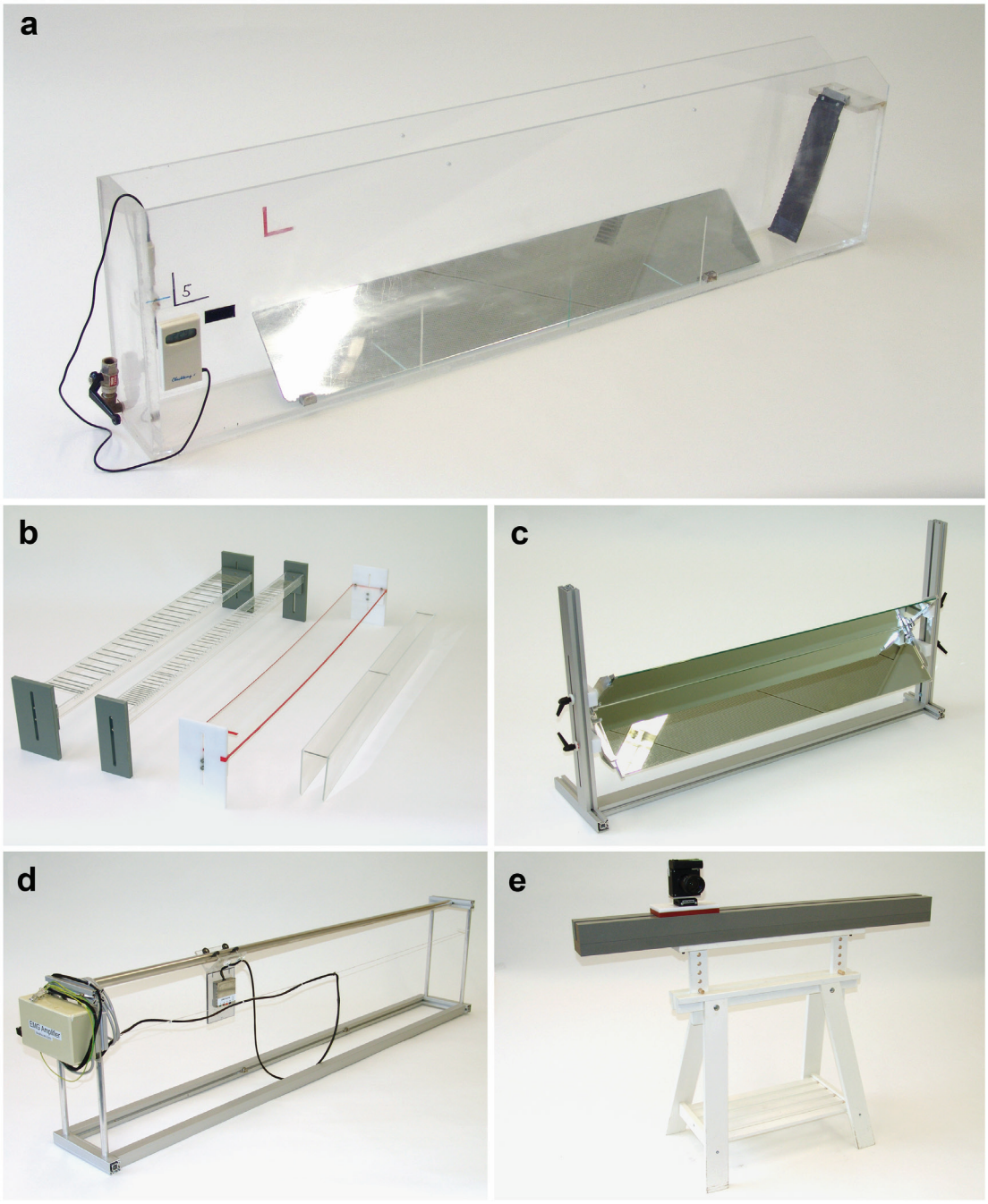

(**a**) Testing box. (**b**) Horizontal ladders for rats and mice, runway, Plexiglas corridor for mice. (**c**) Mirror system. (**d**) EMG set-up. (**e**) Camera mounted on a guide rail.

1. Testing apparatus

1.1 Testing box

The testing box (basin) was entirely made of Plexiglas and 150 cm in length, 13 cm in width (inside) and 40 cm in height. The walls (thickness: 0.8 cm) and the floor plate (thickness: 1.5 cm) of the box were attached to each other using an adhesive solution (Acrifix 106, Röhm GmbH).

At one side, the wall was 10 cm lower and a small footbridge (rigid PVC with rough surface) was attached to a ledge (Supplementary Fig. 1a) so that the animals could exit the testing box and enter a cage placed next to the testing box. On the opposite side of the box, a hole was drilled in the Plexiglas wall close to the floor plate and a ball valve was installed for water drainage (Supplementary Fig. 1a). A temperature sensor was installed to measure water temperature.

1.2 Elements to test different types of locomotion

The horizontal ladder (rats: length of 113 cm, width of 13 cm; mice: length of 113 cm, width of 7 cm) was composed of thin Plexiglas side rails (thickness of 0.5 cm), metal rungs (round, length of 13 cm (rats), 7 cm (mice); diameter of 0.3 cm (rats), 0.2 cm (mice)) and two PVC plates (height of 22 cm, width of 13 cm, thickness of 1.5 cm) as supporting legs (Supplementary Fig. 1b). Side rails were attached to the PVC plates at both ends so that the ladder was at least 15 cm above ground. A number of small holes separated by 1 cm were drilled into both stringers to insert the metal rungs. Therefore, it was possible to change the sequence of the metal rungs before every testing session. Animals were trained on the ladder with a regular arrangement of metal rungs (rung in every 4^{th} hole). For testing, rung sequences were irregular and varied (rungs in every 3^{rd}-5^{th} hole) to avoid habituation to a particular rung pattern and, thus, to ensure correct testing of skilled walking[1, 2]. During training and testing on the horizontal ladder, the box was filled with water to approximately 1 cm below the rungs, to prevent the animals from climbing underneath the ladder.

The runway used to test overground walking and wading consisted of a clear Plexiglas shelf (length of 123 cm, width of 13 cm, thickness of 0.5 cm) which was attached at both ends to PVC plates (height of 22 cm, width of 13 cm, thickness of 1 cm) holding the runway 15 cm above ground (Supplementary Fig. 1b). When inserting the runway into the testing box, sagging of the Plexiglas shelf was prevented by placing two small, but robust, PVC plates attached to each other by a double ended screw onto the floor of the testing box, just between the supporting elements of the runway and the walls of the testing box. By turning the screw, the total length of the two attached PVC plates could be altered

thereby changing the pressure exerted on the lowest parts of the supporting stands. This simple tool allowed us to adapt the tension of the runway and thus avoid sagging of the shelf.

For mice, passages were altered to 7 cm in width by two additional Plexiglas walls (length of 100 cm, height of 14 cm, thickness of 0.5 cm; Supplementary Fig. 1b). The upper sides of the walls were fixed to each other with three metal bars (length of 7 cm) used as spacer pieces to form a 7 cm wide Plexiglas corridor. For swimming, the bars served as suspension point for hooks to hang the Plexiglas corridor into the water. For walking and wading, the corridor was simply placed on top of the runway. The corridor was not used for the evaluation of skilled locomotion in mice since the width of the mouse ladder was already 7 cm.

1.3 Arrangement of mirrors

The arrangement of the three mirrors used in this study allowed recording and evaluation of the animals performance in the testing box simultaneously from three sides (left, right and below) with only one camera. The first mirror (100 cm x 16 cm, thickness of 0.4 cm) was placed on the basin's floor at an angle of ~ 90° (bottom view). The other two mirrors (100 cm x 18 cm, thickness of 0.4 cm) were connected via an adjustable hinge-joint and fixed to an aluminum rack (extrusion connecting system**,** Kanya AG) that was placed directly behind the long side of the testing box to visualize the side of the animals hidden from the camera (Fig.1 in the manuscript). One mirror was placed at the level at which the animals performed the locomotor task, while the other one was higher and positioned almost perpendicular to the lower mirror (Supplementary Fig. 1c).

1.4 Light system

The high frame rates used to record the animals required an additional strong light source (see below). We built a light system that was comprised of four commercially available 36 Watt fluorescent lamps emitting cool white light. The lamps were attached to an aluminum rack (extrusion connecting system**,** Kanya AG). To direct the light onto the testing box and diminish light loss, reflecting foils were placed behind the lamps. During testing, the rack was located between the camera and the testing apparatus illuminating the basin from above (one lamp) and below (three lamps). Since the light was directed onto the testing box, the escape cage at the end of the box was less strongly illuminated. The additional light did not seem to affect the animals' motivation to cross the testing box nor their locomotor behavior. In contrast, they were rather animated to cross the basin in order to enter the

darker escape cage at the end of the apparatus. This side effect of the light system emerged as a rather positive feature for locomotor function testing.

1.5 EMG setup

For EMG measurements, an aluminum frame that was 159 cm in length, 15 cm in width and 36 cm in height (extrusion connecting system**,** Kanya AG) was built. This frame could be plugged on top of the walls of the testing box and served as suspension for a round and smooth aluminum beam (Supplementary Fig. 1d). A mobile preamplifier was attached to a hanger unit running on four small wheels over the beam. This assembly resulted in minimal friction so that rats, connected to the preamplifier via wires to their head adapter, were easily able to pull the preamplifier with them when crossing the testing box. The preamplifier was connected to a second amplifier fixed to the frame. The second amplifier relayed the data to a working station for further processing with DIAdem academic 8.1 software (National Instruments Engineering GmbH & Co. KG).

2. Camera and recording

Based on pilot experiments, we decided to film the animals with a color high-speed camera (Basler A504kc Color Camera, Basler AG), because for successful automated tracking of the markers, several prerequisites had to be fulfilled by the camera and, in addition, also by the set-up.

First, a color camera was required, since marker tracking by the software was based on the color of the markers. This was crucial to enable the software to distinguish between markers that can come close to each other during a given movement and between the markers and the background. Before every testing session, visualization of the tattoos was reinforced with a fluorescent dye (for example fluorescent, fast drying nail polish) or a black marker, in case of albino rats, to increase the contrast and thus optimize tracking.

Second, sufficient temporal resolution was essential since movements of the animals during locomotion can be fast. For instance, the peak velocity of the toe during swimming can reach 160 cm/s in an intact rat. Therefore, recording at high frame rates up to 200 f/s (Hz) was necessary. During swimming, we found that occasionally the automated tracking of markers placed on the distal hindlimbs failed because changes in marker position between one frame and the next were too large even with recordings at 200 f/s. In these cases, manual frame-by-frame tracking was required. In addition, for recordings at high frame rates, an extra light source emitting cool white light in addition to

the daylight illumination was essential to ensure good image quality, that is in terms of brightness, and so that the depth of field could be extended by using smaller diaphragm openings of the lens. Depth of field was important for the evaluation of the mirror images. The different locomotor tasks required recordings at different minimal frame rates (see Methods in the manuscript) and so lens openings of f/4, f/5.6 or f/8 were used. Another option would be filming under UV illumination. In our hands, this approach was not satisfying because the light reflected by the markers was not sufficient for filming at high frame rates and most of the animals' body, apart from the markers placed on the skin, was almost invisible making the assessment of other endpoint measures impossible.

Third, good spatial resolution was crucial for the automated tracking. The dimensions of the digital color images obtained with the Basler camera were 1280 x 1024 pixels. To increase the number of pixels per marker, the camera was placed close to the basin (distance of 100-150 cm), thereby limiting the field of view to about one third of the length of the testing track. By moving the camera on a guide rail (Supplementary Fig. 1e), the full distance covered by the animal could be recorded. A commercially available laser pointer (light or flashlight pointer) was attached to the camera indicating the camera's field of view. This provided visual feedback to the experimenter who was manually moving the camera thus allowing reliable recordings of moving animals.

In summary, automated tracking of markers was feasible by using a high-speed color camera with excellent spatial resolution, intensive, colored markers, an additional illumination provided by the light system, small lens openings and high temporal resolution. However, manual tracking was occasionally necessary.

3. Software

Analysis of video recordings was performed offline with the color-based, automated tracking software ClickJoint (V5.0; ALEA Solutions GmbH, www.aleasol.ch). After the video files were imported into the software, the settings including the number of markers to be tracked, color of markers, size of search field for markers, the virtual joint and a representative distance for calibration (see below) were defined in two separate configuration windows. The knee and elbow joints were defined as virtual joints so that their positions were indirectly computed by the software. For the knee, the calculation was based on both the position of the markers over the hip and ankle and the length of the femur (rat = 2.5 cm, mouse = 1.3 cm) and tibia (rat = 3.5 cm, mouse = 2 cm) bones. For the elbow joint, the shoulder and

wrist positions and the length of humerus (rat = 2.5 cm, mouse = 1.1 cm) and the lower forelimb (rat = 2.8 cm, mouse = 1.2 cm) were used.

Before automated tracking could be started, the experimenter had to identify the markers on the animals' skin manually on the first frame of the video file. Then, by automatically tracking the markers frame-by-frame, the software generated two-dimensional coordinates (x, y) for every marker and time point. Movements could be reconstructed based on the changes of the xy-coordinates over time. Based on the xy-coordinates, the software directly calculated angles and distances and generated stick diagrams and spatial displacement plots. For angle measurements, usually the smaller angle of the two alternatives was used, typically this was the angle at the flexor side of a limb joint. The side and the bottom views of the animals were analyzed separately. For one run, tracking the markers during, for example swimming, took approximately 10-15 minutes per limb (4-5 stroke cycles). During wading and swimming, occasionally interference caused by disturbed water or light reflections on the water surface hindered automated tracking of the markers. In these cases, manual corrections by the experimenter were necessary. All data including the frame, xy-coordinates, angles and distances for every marker was exported, saved and imported into Microsoft Excel. Applying an integrated supplementary function of the ClickJoint software, raw data could be smoothed using a cubic-spline function (internal software value of 50). Data were then further analyzed with pre-assembled Microsoft Excel sheets determining joint angles or distances between joints at a given time point, range of motion, coordination parameters or movement velocities. Currently, the software is being further developed to provide a more comprehensive and convenient data analysis package independent of Microsoft Excel. This new version will be available with the full MotoRater setup at TSE-systems GmbH (www.tse-systems.com).

4. Practical considerations for animal testing and analysis

To test a single animal in all four locomotor tasks approximately 15 minutes is required. Depending on the task, 3-10 passages were recorded and usually three representative runs were analyzed for every task. Sample selection was based on objective criteria, i.e. comparable locomotion velocity between animals, removal of runs where animals stopped and explored the testing box and, for analysis of limb kinematics, removal of passages in which the animals demonstrated massive lateral instability during locomotion (see below).

5. Special locomotor parameters: Lateral stability during locomotion

Lateral stability is clearly an important component of all forms of locomotion in rodents and also in humans[3, 4]. In this study, lateral stability served on the one hand as a selection criterion for those passages that were used for limb kinematics and on the other hand as a readout of locomotor function. In order to assess lateral stability, both side views of the animal (mirror and direct view) were used. For instance, stability was assumed when both iliac crests were visible during swimming. Here, the time (in percent) that an animal moved under stable conditions could serve as a functional outcome measure. Other readouts for lateral stability during overground locomotion include the measurement of the animals' base of support[5] (distance between limbs; Fig. 3 in the manuscript) or, possibly more accurately, the variability of pelvis (iliac crest) oscillations in different planes[6].

References for Supplementary information

1. Metz, G.A. & Whishaw, I.Q. Cortical and subcortical lesions impair skilled walking in the ladder rung walking test: a new task to evaluate fore- and hindlimb stepping, placing, and co-ordination. *J Neurosci Methods* 115, 169-179 (2002).
2. Metz, G.A. & Whishaw, I.Q. The ladder rung walking task: a scoring system and its practical application. *J Vis Exp* (2009).
3. de Seze, M., Falgairolle, M., Viel, S., Assaiante, C. & Cazalets, J.R. Sequential activation of axial muscles during different forms of rhythmic behavior in man. *Exp Brain Res* 185, 237-247 (2008).
4. Ceccato, J.C., de Seze, M., Azevedo, C. & Cazalets, J.R. Comparison of trunk activity during gait initiation and walking in humans. *PLoS One* 4, e8193 (2009).
5. McEwen, M.L. & Springer, J.E. Quantification of locomotor recovery following spinal cord contusion in adult rats. *J Neurotrauma* 23, 1632-1653 (2006).
6. Courtine, G., Garasimenko, Y., van den Brand, R., Yew, A., Musienko, P., Zhong, H. Song, B., Ao, Y., Ichiyama, R. M., Lavrov, I., Roy, R. R., Sofroniew, M. V., Edgerton, V. R. Transformation of nonfunctional spinal circuits into functional states after the loss of brain input. *Nat Neurosci* 12, 1333-1342 (2009).

Chapter 3

Motor deficits and recovery in rats with unilateral spinal cord hemisection mimic the Brown-Séquard syndrome

L. Filli, B. Zörner, O. Weinmann, M. E. Schwab

Original article published in: Brain. 2011 134:2261-73.

Abstract

Cervical incomplete spinal cord injuries often lead to severe and persistent impairments of sensorimotor functions and are clinically the most frequent type of spinal cord injury. Understanding the motor impairments and the possible functional recovery of upper and lower extremities is of great importance. Animal models investigating motor dysfunction following cervical spinal cord injury are rare. We analyzed the differential spontaneous recovery of fore- and hindlimb locomotion by detailed kinematic analysis in adult rats with unilateral C4/5 hemisection, a lesion that leads to the Brown-Séquard syndrome in humans. The results showed disproportionately better performance of hindlimb compared to forelimb locomotion; hindlimb locomotion showed substantial recovery, whereas the ipsilesional forelimb remained in a very poor functional state. Such a differential motor recovery pattern is also known to occur in monkeys and in humans after similar spinal cord lesions. On the lesioned side, corticospinal, rubro-, vestibulo- and reticulospinal tracts and the important modulatory serotonergic, dopaminergic and noradrenergic fibre systems were interrupted by the lesion. In an attempt to facilitate locomotion, different monoaminergic agonists were injected intrathecally. Injections of specific serotonergic and noradrenergic agonists in the chronic phase after the spinal cord lesion revealed remarkable, although mostly functionally negative modulations of particular parameters of hindlimb locomotion. In contrast, forelimb locomotion was mostly unresponsive to these agonists. These results therefore show fundamental differences between fore- and hindlimb spinal motor circuitries and their functional dependence on remaining descending inputs and exogenous spinal excitation. Understanding these differences may help to develop future therapeutic strategies to improve upper and lower limb function in patients with incomplete cervical spinal cord injuries.

Introduction

Cervical incomplete spinal cord injury (SCI) leading to sensorimotor deficits in the upper and lower extremities has a high incidence among SCI patients (McKinley *et al.,* 2007). Despite this, animal studies focusing on functional recovery after SCI mostly use experimental models of thoracic spinal cord lesions, thereby neglecting the problem of intractable motor dysfunction of the forelimbs. Rats use their forelimbs extensively for many tasks including locomotion as well as fine motor skills such as reaching, grasping, seed manipulation and sensory perception of the environment (Webb and Muir 2005). Despite obvious differences in locomotion between bipedal humans and quadrupedal vertebrates like rats, several remarkable similarities in gait physiology and the neuronal program controlling locomotion could be found (Vilensky, 1987; Duysens and Van de Crommert, 1998; Dietz and Harkema, 2004; Courtine *et al.,* 2005). Recent fMRI studies revealed a surprising resemblance of the supraspinal locomotor control between humans and quadrupedal mammalians, indicating a conservation of locomotor control in humans despite their transition to bipedalism (Jahn *et al.,* 2008). Sensory integration during locomotion and activity of locomotor-related brain regions (subthalamic, cerebellar, and mesencephalic locomotor region etc) in humans strongly resembled the locomotor network found in the feline system. Primates and humans also have a spinal central pattern generator (CPG), as extensively shown for cats, rodents and other vertebrates (Grillner and Wallen, 1985; Dietz and Harkema, 2004). The CPG network is a self-sustained spinal system producing locomotor-like neural activity, which is controlled and modulated by sensory afferents and supraspinal commands (Grillner and Wallen, 1985). Moreover, quadrupedal interlimb coordination between upper and lower extremities has been shown to also occur in humans during bipedal locomotion (Dietz *et al.,* 2001; Balter and Zehr, 2007). Lastly, electrophysiological assessment of reflexes suggested a basic similarity in spinal locomotor circuitry between humans and quadrupeds (Duysens and Van de Crommert, 1998). These conserved characteristics of neuronal control of locomotion qualify quadrupedal animals as well suited models for many aspects of human spinal cord injury.

Unilateral spinal cord lesions produce a Brown-Séquard syndrome characterized by ipsilesional motor weakness or paralysis and loss of proprioception with contralesional deficits in pain and temperature sensation (Little and Halar, 1985; Roth *et al.,* 1991). Interestingly, patients with Brown-Séquard syndrome often recover good leg control and locomotion (Taylor and Gleave, 1957; Little and Halar, 1985; Roth *et al.,* 1991; Wirz *et al.,* 2010). Whereas Wirz and colleagues reported considerable recovery of upper extremity function (Wirz *et al.,* 2011), others, however, observed that arm and hand

functions recover only marginally and often remain severely impaired or fully paralysed in these patients (Levi *et al.,* 1996). Only a few studies have investigated motor functions after lateral spinal hemisection in rats and monkeys. They showed a similar discrepancy in fore- and hindlimb recovery (Webb and Muir, 2002 and 2005; Martinez *et al.,* 2009 and 2010; Rosenzweig *et al.,* 2010). The underlying mechanisms for such dissimilar functional recovery of upper and lower motor functions are not understood.

Local spinal circuits including central pattern generator (CPG) networks remain mostly intact below a spinal cord lesion, but loose their descending inputs, both the specific commands running mostly over the corticospinal, rubro-, vestibulo- and reticulospinal tracts, and the unspecific modulatory bulbospinal inputs carried by the serotonin, dopamine and noradrenaline fibres. Local pharmacological application of dopamine, noradrenaline, serotonin, or their agonists has been shown to partially substitute for these missing global excitatory inputs. Completely spinalised animals of different species (including mice, rats, cats and monkeys) showed remarkable transient activation of hindlimb CPGs and locomotion under these conditions (Forssberg and Grillner, 1973; Barbeau and Rossignol, 1991; Fedirchuk *et al.,* 1998; Feraboli-Lohnherr *et al.,* 1999; Antri *et al.,* 2003 and 2005; Guertin, 2004; Landry and Guertin, 2004). Monoaminergic bulbospinal projections are important for initiation and modulation of locomotion from fish to men (Grillner, 2003). After severe SCI, upregulation of various monoaminergic receptors occurs, which then can be pharmacologically targeted by locally applied monoaminergic drugs (Giroux *et al.,* 1999; Lee *et al.,* 2007; Hayashi *et al.,* 2010). Although application of monoaminergic agonists has powerful physiological effects in the hindlimb of animals with complete SCI, only very little is known about their potential in animals with partial SCI. After severe thoracic contusion injury in rats, voluntary hindlimb locomotion was not improved by injection of direct serotonergic agonists, which highly facilitate locomotion in spinalised rats (Feraboli-Lohnherr *et al.,* 1999; Antri *et al.,* 2003 and 2005), but locomotor improvement was achieved by application of the serotonin precursor 5-hydroxytryptophan (Hayashi *et al.,* 2010). In cats, responses to monoaminergic agonists seem to depend on the type and extent of the lesion (Brustein and Rossignol, 1999). Effects of monoaminergic drugs on impaired forelimb functions have not been studied so far.

The purpose of the present study was to investigate locomotor recovery of fore- and hindlimbs in adult rats with precise C4/5 unilateral spinal cord hemisections and to study the effects of intrathecally applied monoaminergic agonists on locomotor performance. Detailed kinematic assessment of locomotion revealed large differences between the hindlimbs, which rapidly developed robust and

regular locomotion, and the ipsilesional forelimb, which showed massive and persisting functional deficits. Specific monoaminergic agonists applied in the chronic phase after SCI induced considerable modulation of distinct parameters of hindlimb locomotion. In contrast, forelimb locomotor networks showed almost no responsiveness to the same agonists. This study highlights remarkable differences between fore- and hindlimb motor circuitries in response to the strong reduction of supraspinal input and to monoaminergic drug treatment.

Methods

Experimental setup

Adult female Lewis rats (180-220 g) received a precise and complete unilateral C4/5 hemisection. 5 animals were used for locomotor assessment. Spontaneous locomotor recovery was analysed during the first 28 days after SCI, whereas pharmacologically-induced locomotor modulations were studied in the same animals in the chronic phase (starting on post-operative day 31). 11 animals were used to investigate the monoaminergic innervation of the spinal cord in the intact situation, and 4 and 28 days after the lesion. Animals were housed in groups of 3-4 per cage and kept at a 12:12h light:dark cycle with food and water *ad libitum*. All experimental procedures were approved by the veterinary office of the canton of Zurich, Switzerland.

Surgical procedures

Spinal cord injury and postoperative care

Animals were anesthetized with a mixture of hypnorm (0.125 mg per 200 g body weight, Janssen Pharmaceutics) and dormicum (0.75 mg per 200 g body weight, Roche Pharmaceuticals). After laminectomy at C4 vertebral level, the right cervical spinal hemicord was transected with a surgical sapphire knife. The dorsal roots were spared from the transection. After surgery the animals received postoperative care including analgesics (Rymadil, 2.5 mg per kg body weight, Pfitzer AG) for 3 days following surgery and antibiotics (Baytril, 5mg per kg body weight, Bayer AG) for 7 days.

Intrathecal catheter implantation

A subdural catheter enabling intrathecal application of monoaminergic agonists was implanted 28 days after SCI. After partial laminectomy at T3 vertebral level, a thin catheter (32 gauge, Recathco, Allison Park, USA) was inserted into the subarachnoid space and pushed rostrally to the spinal segment C7. The catheter was sutured to the paravertebral musculature to avoid dislocation of the tube. The distal end of the catheter was attached to a subcutaneous connector/backmount (Plastics One Inc., USA), which was sutured to the lower back musculature of the rat. The connector system was accessible from outside and allowed intrathecal bolus injections of defined volumes in awake animals. Catheter implantation did not lead to any obvious impairment of locomotion.

Pharmacological treatment

All drugs were dissolved in sterile H_20. Monoaminergic agonists were applied in the period from 31 to 49 days after SCI. The injected volume for each drug solution was 20 µl, followed by 20 µl of NaCl 0.9% (B. Braun Medical AG, Germany) to flush the drug into the cerebrospinal fluid. The dead space of the catheter/backmount system was 12 µl. Each drug was injected only once (except for drugs used in combined injections) to avoid pharmacological tolerance. Drug injections were separated by at least 48 hours to avoid possible interactions with previously applied drug. Depending on the particular drug, actions (if observed) peaked within the first 10 minutes and generally declined gradually over a period of minutes to few hours. The cannula system was flushed daily with 20 µl saline solution to prevent clogging. Dosages of individual drugs were derived from earlier publications and were first tested in intact animals to avoid undesirable side effects. For each drug, two different dosages were tested, of which the higher was behaviorally evaluated. The different drugs were injected at the following dosage: apomorphine (67 µg/animal), clonidine (25 µg/animal), methoxamine (90 µg/animal), quipazine (40 µg/animal), 8-OHDPAT (52 µg/animal), combined quipazine and 8-OHDPAT (20 µg quipzaine and 26 µg 8-OHDPAT/animal), combined apomorphine and quipazine and 8-OHDPAT (22 µg apomorphine, 13 µg quipazine and 17 µg 8-OHDPAT/animal). Due to similar body weights of the animals (222-238 g), the dosages were not adapted to the body-weight.

Locomotor quantification

Kinematic analysis

Kinematic assessment of locomotor performance was analysed as described in detail previously (Zörner *et al.,* 2010). In brief, the animals had to walk through shallow water (3 cm water height) while their performance was recorded with a frame rate of 200 Hz by a mobile high-speed camera (Basler A504kc Color Camera, Basler AG). As shown earlier, the additional weight support provided by the water massively facilitated locomotion of animals with severe motor deficits (Kuerzi *et al.,* 2010; Zörner *et al.,* 2010). This enabled locomotor quantification of acutely injured animals, which otherwise would not have been able to bear their full body weight. It should be mentioned that, due to differing biomechanics, locomotor parameters during wading should not directly be compared to walking, although several basic locomotor features seem to be conserved. A mirror-system allowed simultaneous locomotor quantification of different body sites by providing the ventral and both lateral views of the animal. 4-6 runs were recorded per animal and condition. Only sequences with

continuous locomotor velocity between 0.2 and 0.3 m/s and sufficient lateral stability were selected for quantitative locomotor analysis. Pre-drug conditions were recorded immediately before drug application. Post-drug recordings were performed 10 min after drug application. The skin overlying prominent anatomical landmarks (hindlimb: iliac crest, hip, ankle, metatarsophalangeal joint (MTP); forelimb: shoulder blade, shoulder, wrist) was tattooed with a commercially available tattoo device (Hugo Sachs Elektronik, Harvard Apparatus GmbH) to allow permanent identification of the joints. Kinematic analysis of locomotion was performed by a color-based, semi-automated tracking software (Clickjoint V5.0; ALEA Solutions GmbH, www.aleasol.ch).

Locomotor parameters

Paw dragging was defined as contact of the paw with the runway during the swing phase of the step cycle and was expressed as ratio of the number of steps without dragging per total steps (Fig 3A/4A). Body weight support of the respective limbs was determined by measuring the height of the shoulder or the iliac crest relative to the runway. The height of the iliac crest was measured during its mid-stance phase (temporal middle of the stance phase). The ipsilesional shoulder height was quantified at the time point just before the contralesional forelimb touched the floor and started its stance phase, since there was often no defined swing phase in the ipsilesional forelimb (persistent paw dragging). At this time, the ipsilesional shoulder height is maximally dependent on the weight support of the ipsilesional forelimb. Left-right coordination was defined by calculating the phase dispersion between the particular limbs (Kloos *et al.,* 2005). In a perfectly locomoting animal, one limb starts the step cycle exactly in the middle of the step cycle of its contralateral limb, thus resulting in a phase dispersion of 0.5. In Fig 3C/4C, interlimb coordination was quantified by measuring the deviation from a perfect “out of phase” rhythm in percent. For evaluation of diagonal forelimb/hindlimb coordination, the deviation from a perfect “in phase” rhythm was calculated (Supplementary data). Since there was not always an obvious off-ground swing phase (mainly in the ipsilesional forelimb), step cycles were defined by the onset of limb protraction (initiation of swing phase) and the onset of limb retraction (initiation of the stance phase). Protraction of the ipsilesional limbs was expressed as maximal positive distance of the wrist or toe tip relative to the shoulder or iliac crest, respectively (Fig 3D/4D). Maximal protraction is found at the transition from swing to stance phase. Analogous to protraction, retraction of the ipsilesional fore- or hindlimb was defined as maximal negative distance of the wrist or toe tip relative to the shoulder or iliac crest, respectively (Fig 3E/4E). Maximal retraction is found at the transition from

stance to swing phase. Total limb excursion was derived from the sum of the absolute values of protraction and retraction of a particular step cycle (Fig 3F/4F).

Tissue processing

Animals were transcardially perfused with 50 ml Ringer`s solution containing heparin (B. Braun Medical AG, Germany) followed by 300 ml of a 4% phosphate-buffered formalin solution containing 5% sucrose. Animals used for immunohistochemical analysis were perfused with a formalin solution additionally containing 0.1% glutaraldehyde. The tissue was cryoprotected in a phosphate-buffered 30% sucrose solution for 3 days at 4°C. The spinal cords were embedded in Tissue-Tek O.C.T. Compound and frozen at -40°C. Spinal cords were cut in 40 µm thick transverse sections and mounted on slides. Transverse sections used for immunohistochemistry were collected free-floating in 24-well-plates filled with cold 0.1M PB and were stored in an anti-freeze medium (15% sucrose and 30% ethylene glycol in 50mM PB, pH 7.4) at -20°C.

Analysis of lesion extent and quantification of motoneurons

Lesion extent and number of motoneurons were analysed in Nissl-stained transverse spinal cord sections. For the lesion size, the maximal lesion extent was determined for each animal (Fig 1b). Motoneurons in the cervical spinal cord were counted in 35 transverse sections symmetrically distributed over the cervical spinal segments C1 to C8 in 3 animals. The criteria for motoneuron identification were a clearly Nissl-stained cell body with a diameter of at least 30 µm located in Rexed's lamina VIII or IX.

Immunostaining

Free-floating sections of different spinal segments were incubated for 3 days at 4°C with the primary rabbit antibody against serotonin (5-HT, 1 : 12000, rabbit, Immunostar) or tyrosine hydroxylase (TH, 1:250, rabbit, Millipore). Primary antibodies were detected with a biotinylated antibody (1:300, goat, Jackson ImmunoResearch Laboratories, USA) over night at 4°C. After washing with PB, the sections were probed with streptavidin Cy2 (1:500; Jackson ImmunoResearch Laboratories, USA) for 45 min at 25°C. For cytoarchitectonic identification of spinal segments and motoneuron pools, the sections were counterstained with NeuroTrace 640/660, a deep-red fluorescent Nissl stain (Invitrogen). After final

washing steps in PB, sections were mounted, air-dried over night, and coverslipped with Mowiol (Calbiochem).

Densitometric quantification

3-4 animals were analysed for each time point (intact, 4 days and 28 days after unilateral hemisection). Confocal image acquisition was performed using the spectral confocal microscope TCS SP2 AOBS (Leica Microsystems) with a 40x oil immersion objective (HCX PL APO Oil, 1.25 numerical aperture) at maximal antibody penetration depth. Image size was defined as 1024 x 1024 pixels. Gain voltage based pixel intensity of the immunoreactive fibres was set using LUT Glow (O) function to the optimal signal-to-noise ratio. Only areas exhibiting 2 or more fluorescent Nissl-stained motoneurons (in Rexed's lamina VIII or IX) were used for quantification of optical fibre density. The obtained images were background-corrected and their optical densities were quantified using ImageJ software (NIH, Bethesda, MD). Bilateral averaged optical density of all intact animals at spinal segment C2 was set as 1.0 relative optical density for the respective marker. Representative images were only processed by identical minimal contrast enhancement.

Statistics

Immunohistochemical (Fig 2a, c) and behavioural data of spontaneous locomotor recovery (Fig 3a-f) were analysed using one-way ANOVA followed by *post hoc* Bonferroni test (with repeated-measures for Fig 3a-f). For comparison of pre- and post-drug conditions (Fig 4a-f), we used Student`s *t*-test (two-tailed, paired). Data are presented as animal group mean values for every testing session and error bars represent s.e.m.. * $P < 0.05$; ** $P < 0.01$, *** $P < 0.001$.

Results

Analysis of lesion extent

Lesion size was analysed for all animals by determining the maximal lesion extent in Nissl stained spinal cord sections. The largest and smallest lesions among the animal groups (behavioral and immunohistochemical group) are shown in Fig 1A and B. Except for one animal which had additional damage in the dorsal quadrant of the contralateral hemicord, all lesions were unilateral with no or minor damage of contralesional fibre tracts. To assess the damage of cervical motoneurons by the lesion, the number of motoneurons in Rexed's lamina VIII and IX of the cervical spinal cord was quantified in 3 animals. The lesion was highly localized; motoneurons disappeared over a total rostrocaudal distance of 1 mm, which corresponds to around half a cervical segment (Fig 1C and D). Adjacent cervical spinal segments and the contralesional hemicord did not show any decrease in the number of motoneurons (Fig 1D). The majority of the motoneurons demonstrated normal morphology with granular Nissl staining. Only a few motoneurons, located in close proximity of the lesion site, revealed abnormal dense Nissl staining (data not shown).

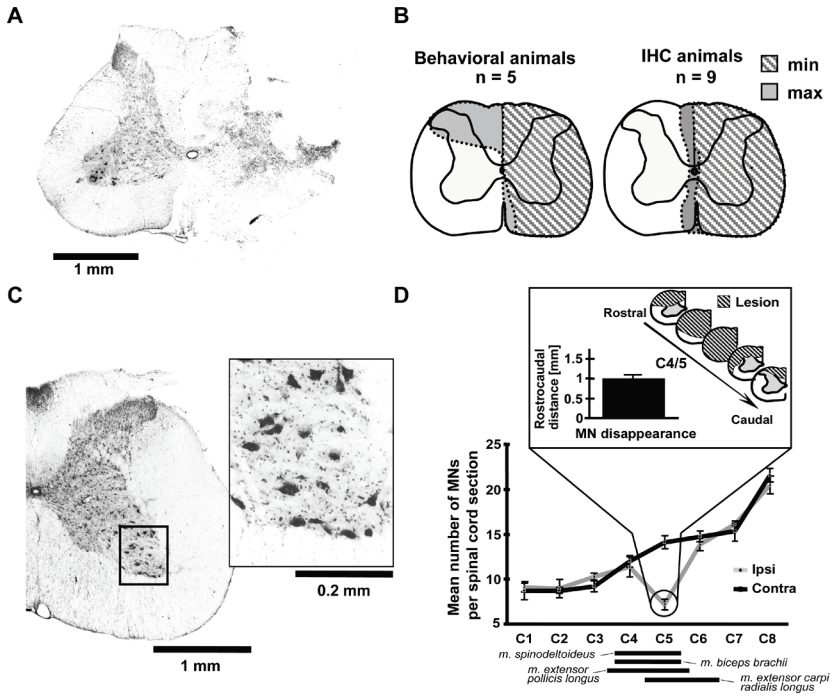

Figure 1 Histological analysis of the spinal cord lesion. (A) Nissl-stained transverse section through the lesion centre at C4/5. (B) Minimal and maximal lesion extent of animals used for functional evaluation of locomotion (left) and animals used for immunohistochemical investigations (right). (C) Nissl-stained section illustrating the intact motoneurons (MNs) in the ventral horn of spinal segment C6/7. (D) MN counts on ipsilesional (Ipsi, grey line) and contralesional (Contra, black line) hemicord in 3 animals 7 weeks after unilateral hemisection. The increased number of MNs in the caudal cervical segments is due to paw and digit MN pools. The ipsilesional hemicord revealed a dip in MNs at level C5, where the lesion was located. MNs disappeared over a total rostrocaudal distance of approximately 1 mm (top panel). MN pools of specific forelimb muscles (m. spinodeltoideus, m. biceps brachii, m. extensor pollicis longus and m. extensor carpi radialis longus), which span 2 or more spinal segments (from McKenna *et al.,* 2010), were only partially damaged by the restricted SCI. Adjacent spinal segments were not affected. Data are presented as mean ± SEM.

Depletion of 5-HT and TH-positive fibres in the cervical and lumbar spinal cord after injury

To assess the depletion of bulbospinal monoaminergic projections after cervical unilateral hemisection, immunohistochemical stainings for serotonin (5-HT) and tyrosine hydroxylase (TH) were performed at different spinal levels of intact animals, and animals 4 days and 28 days after SCI. 5-HT and TH antibodies revealed highly specific staining of axons and boutons with only minimal background noise.

In intact adult rats, the spinal 5-HT innervation was approximately twice as dense at the lumbar levels L2-4 than at the cervical levels C2 and C6-8. The sublesional 5-HT fibre density in the contralesional hemicord was unaffected at all time points after SCI (Fig 2A and B). Ipsilesional 5-HT fibres caudal to the lesion were strongly reduced by the injury, resulting in a reduction of 5-HT fibre density by 68% at C6-8 and by 92% at the spinal levels L2-4 at 28 days after the injury. The further decline of the 5-HT fibre density from postoperative day 4 to 28 argues against a significant compensatory sprouting of serotonergic fibres in the sublesional spinal cord within 28 days after SCI.

Similar results were obtained for dopaminergic/noradrenergic fibres visualized by TH immunohistochemistry. In intact animals, a higher density of TH fibres was found at spinal segments C6-8 than at C2, and the fibre density was again higher in the lumbar enlargement (Fig 2C). The ipsilesional TH fibres were reduced by 61% in the cervical and by 89% in the lumbar enlargement at 28 days after injury (Fig 2C and D). In contrast to 5-HT, TH-positive fibres demonstrated a partial depletion in the contralesional hemicord caudal to the lesion at 28 days after injury when compared to intact animals (C6-8: -40%; L2-4: -33%). As observed for 5-HT, there was no restitution of TH-positive fibre density up to 28 days after SCI.

Spontaneous locomotor recovery in rats with Brown-Séquard syndrome

The spontaneous locomotor performance in the absence of drug treatment was investigated weekly over a period of 28 days after SCI. Locomotion was analysed during walking through shallow water (3cm depth). The specific locomotor parameters analysed were paw dragging, parameters of interlimb coordination (phase dispersion), and detailed kinematic evaluations of fore- and hindlimb movements, i.e., body height, maximal positive and negative excursion (pro-/retraction), and total limb excursion. During the first few days after SCI, the animals showed partial to complete paresis of the ipsilesional forelimb and of both hindlimbs with frequent spastic-like periods of high muscle tonus (particularly in the hindlimbs). After postoperative day 7, the hindlimbs recovered at a fast rate and allowed the

animal to regain mobility within a few days. In contrast, the ipsilesional forelimb remained in a rigid condition with only minimal weight support function and a small range of motion.

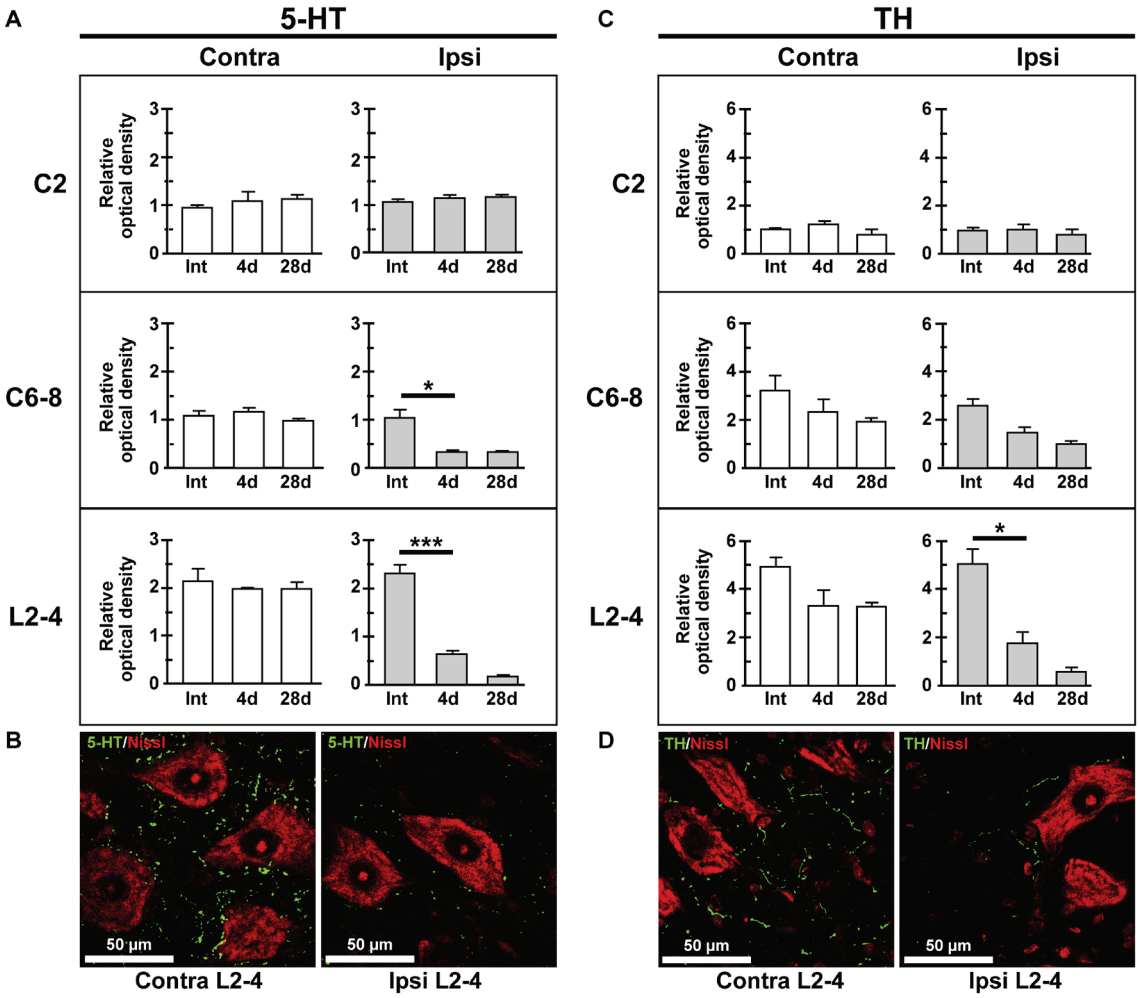

Figure 2 Analysis of 5-HT- and TH-positive fibres at different levels of the spinal cord. For quantification, densitometric values of all spinal segments were normalized to the average values obtained for intact animals at spinal segment C2. (A) Fibre density of 5-HT at spinal level C2, C6-8 and L2-4. 5-HT fibre density was higher in the lumbar than the cervical spinal cord in intact animals (Int). 5-HT fibres were progressively lost in the ipsilesional (Ipsi) hemicord 4 and 28 days after injury. The contralesional (Contra) innervation was unaffected below the lesion. (B) Representative images of lumbar 5-HT innervation of the MN pool in an animal 28 days after unilateral hemisection. Note the strong reduction of 5-HT fibre density in the ipsilesional hemicord (right panel). (C) TH fibre density at spinal levels C2, C6-8 and L2-4 showed increased lumbar versus cervical levels in intact animals. Caudal to the lesion, the TH innervation was mainly reduced in the ipsilesional hemicord, but also partially on the contralesional side. (D) Lumbar ventral horn motoneurons and TH innervation showing dense contralesional TH fibre innervation compared to the strongly reduced fibre plexus in the ipsilesional hemicord (28 days after the lesion). Data in (a) and (c) are presented as mean ± SEM. Statistical evaluation was done with One-way ANOVA with Bonferroni *post hoc* test comparing BL with 4d (lesion deficit) and 4d with 28d (recovery). * $P < 0.05$; ** $P < 0.01$; *** $P < 0.001$.

Paw dragging did not occur in fore- and hindlimbs during wading in intact animals. 7 days after injury, proper stepping was abolished and steps without paw dragging were rare or absent for the ipsilesional forelimb. Forelimb dragging persisted over the whole experimental period (Fig 3A). For the ipsilesional

hindlimb, proper steps without paw dragging decreased from 100% to 29% of total steps at 7 days after the lesion. Paw dragging of the ipsilesional hindlimb significantly recovered up to 28 days post injury (Fig 3A).

Body weight support provided by the fore- and hindlimbs was analysed by measuring the height of the shoulder and the iliac crest, respectively. The ipsilesional shoulder height decreased to 33% of the intact weight support 7 days after SCI (Fig 3B). There was no significant recovery of weight support in the ipsilesional forelimb during the experimental period. The height of the iliac crest was significantly reduced to 50% of the intact height 7 days after the lesion, and also showed no significant recovery by 28 days post injury (Fig 3B).

Left-right coordination was analysed by calculating the deviation from a perfect “out of phase” rhythm of the fore- and hindlimbs (see Zörner et al., 2010). In intact animals, this “out of phase” deviation was very low (3.5% for the fore- and hindlimbs; Fig 3C). The alternating stepping pattern in forelimb locomotion was highly distorted 7 days after injury (23.1% deviation). There was a trend towards functional recovery in inter-forelimb coordination, but this did not reach significance. Very different from the forelimbs, the inter-hindlimb coordination was only slightly impaired after SCI and reached an almost normal deviation of 5.8% at 28 days post injury (Fig 3C). To investigate coordination between forelimbs and hindlimbs, diagonal forelimb-hindlimb coupling was analysed by calculating the deviation from a perfect “in phase” rhythm (synchronous step cycle). Intact animals demonstrated a nearly perfect coupling between the diagonal fore- and hindlimb (Supplementary Fig 1A). There was a strong impairment of forelimb-hindlimb coupling, which did not recover up to 28 days post injury. This was due to a nearly doubled stepping frequency of the forelimbs as compared to the hindlimbs, which made a proper forelimb-hindlimb coordination impossible (Supplementary Fig 1B).

Protraction is found during the swing phase of the step cycle, when the limb advanced in reference to the body. Protraction of the ipsilesional forelimb was abolished by the lesion (intact: 1.4 cm; 7 days post lesion: -3.3 cm) without any recovery over time (Fig 3D). Hindlimb protraction was initially strongly affected (intact: 2.8 cm; 7 days post lesion: 0.1 cm), but in contrast showed a profound functional recovery from postoperative day 7 to 14 (14 days post lesion: 1.35 cm). Nonetheless, hindlimb protraction did not recover completely (Fig 3D).

Retraction is found during the stance phase of the step cycle, when the body advances in reference to the limbs. Retraction of the ipsilesional forelimb significantly increased 7 days after injury (intact: -3.4 cm; 7 days after SCI: -4.7 cm). There was no recovery of forelimb retraction by 28 days after the injury

(Fig 3E). The hindlimb retraction was also significantly increased after injury (intact: -4.8 cm; 7 days post lesion: -8.5 cm), but showed significant recovery up to 28 days after SCI (-7.0 cm), without, however, reaching baseline values (Fig 3E).

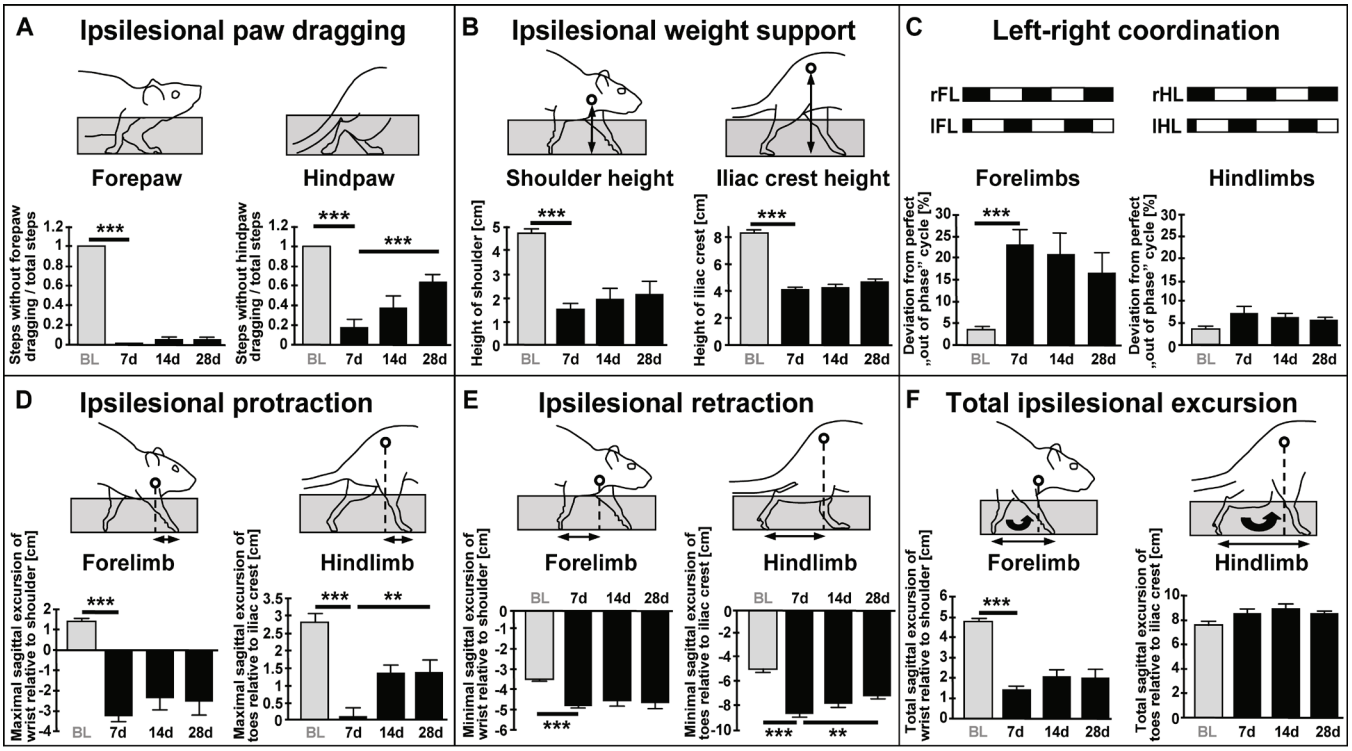

Figure 3 Assessment of spontaneous locomotor performance of fore- and hindlimbs at 7, 14 and 28 days after unilateral cervical hemisection. (A) Ipsilesional limbs showed a strong impairment in stepping resulting in severe paw dragging 7 days after injury. Forepaw dragging constantly persisted over the entire experimental period, whereas ipsilesional hindlimb stepping and dragging recovered significantly after the initial lesion deficit. (B) Body weight support of the ipsilesional fore- and hindlimb was significantly decreased 7 days after injury. There was no significant recovery of weight support in both limbs. (C) Inter-forelimb coordination was distorted acutely after the lesion and showed no significant recovery with time. Inter-hindlimb coordination revealed no significant lesion effect and was close to normal 28 days after SCI. (D) Protraction of the ipsilesional forelimb was strongly diminished 7 days post lesion and did not recover with time. Hindlimb protraction showed a severe initial decrease 7 days after SCI, which was followed by significant functional recovery up to 28 days after injury. (E) Retraction of the ipsilesional forelimb was significantly increased and did not recover up to 28 days post lesion. The ipsilesional hindlimb showed a significantly increased retraction acutely after the lesion, which decreased towards baseline by 28 days post injury. (F) Total excursion of the ipsilesional forelimb was significantly decreased by the lesion and did not recover. Total excursion of the ipsilesional hindlimb was not affected by the lesion. 5-10 representative step cycles were analysed per animal and per condition. Data are presented as mean ± SEM. Statistical evaluation was done with One-way ANOVA repeated measures with Bonferroni *post hoc* test comparing BL with 7d (lesion deficit) and 7d with 28d (functional recovery). * $P < 0.05$; ** $P < 0.01$; *** $P < 0.001$.

Total limb excursion is composed of the sum of pro- and retraction. Total ipsilesional forelimb excursion strongly decreased after the injury, which was mainly due to the inability of the lesioned animals to protract their forelimb. The forelimb persisted in a rigid state with a low range of movement (Fig 3F). The total excursion of the ipsilesional hindlimb was unaffected by the lesion (Fig 3F). This is

due to the fact that reduced protraction was associated with increased retraction leading to a backward shift of the movement with unchanged total values of total limb excursion.

In summary, the spontaneous locomotor performance of rats with unilateral C4/5 hemisection showed a very unequal recovery for the fore- and hindlimbs. The ipsilesional forelimb showed very severe deficits in all locomotor parameters evaluated, even under conditions where the body weight was optimally supported (wading), and only minor or no recovery occurred with time after the lesion. In contrast, the ipsilesional hindlimb demonstrated a remarkable degree of locomotor performance in most parameters up to 28 days after the lesion, in spite of large initial deficits. The locomotor parameters of the fore- and hindlimbs are at least partially influenced by each another. Mainly the poor locomotor function of the ipsilesional forelimb is likely to have an impact on the locomotor pattern of the hindlimbs.

Locomotor responses of fore- and hindlimbs to monoaminergic drugs

The responsiveness of fore- and hindlimb locomotor circuits to dopaminergic, serotonergic and noradrenergic agonists was analysed in the same animals already quantified for spontaneous locomotion, starting at 31 days after SCI. Agonists acting on the different monoaminergic systems were intrathecally applied via a subdural catheter implanted 4 days prior to injections. Apomorphine was used as a non-selective agonist of the dopaminergic system (agonist of D1 and D2 receptors), clonidine and methoxamine as selective agonists of the α2- or α1- noradrenergic receptors respectively, and quipazine (non-specific agonist of 5-HT_2 receptor) and 8-OHDPAT (selective agonist of 5-HT_1 receptor) were used as serotonergic agonists.

Paw dragging of the ipsilesional forelimb was not responsive to any of the applied drugs and constantly persisted throughout the experimental period (Fig 4A). Conversely, hindlimb dragging became significantly worse with noradrenergic agonists methoxamine and particularly clonidine. The 5-HT_2 receptor agonist quipazine also significantly increased hindpaw dragging (Fig 4A).

Body weight support was modulated by different monoaminergic agonists (Fig 4B). The shoulder height of the ipsilesional forelimb was significantly and selectively increased by apomorphine. This effect was not accompanied by a simultaneous increase of weight support in the hindlimbs, indicating a specific modulation of cervical locomotor networks by apomorphine. The height of the ipsilesional iliac crest was negatively affected by clonidine and 8-OHDPAT, both of them significantly decreased the weight support of the ipsilesional hindlimb (Fig 4B).

Left-right coordination of the forelimbs was largely unaltered by application of any drug (Fig 4C). Hindlimb left-right coordination was significantly distorted by clonidine. The animals frequently demonstrated stumbling and irregular locomotion. However, combined application of the serotonergic agonists quipazine and 8-OHDPAT tended to stabilize locomotion and improved rhythmic alternation of hindlimb stepping (Fig 4C). Diagonal forelimb/hindlimb coordination was not altered by drug application (Supplementary Fig 1C).

Protraction of the ipsilesional forelimb was unaffected by application of any monoaminergic agonist (Fig 4D). However, protraction of the ipsilesional hindlimb was strongly diminished after application of clonidine (from 1.3 cm to 0.3 cm). The 5-HT_1 receptor agonist 8-OHDPAT alone and combined injections containing 8-OHDPAT demonstrated a non-significant reduction of the hindlimb protraction (Fig 4D).

Retraction and total limb excursion did not show significant modulation for the ipsilesional fore- or hindlimb after application of any agonist (Fig 4E/F).

Taken together, the fore- and hindlimb locomotor networks revealed a very different responsiveness to monoaminergic agonists after unilateral cervical spinal cord injury. The ipsilesional hindlimb showed significant modulation of particular locomotor parameters after application of specific drugs, which in the majority of cases, however, negatively interfered with spontaneously recovered hindlimb function. In contrast, the ipsilesional forelimb showed almost no locomotor responsiveness to monoaminergic agonists.

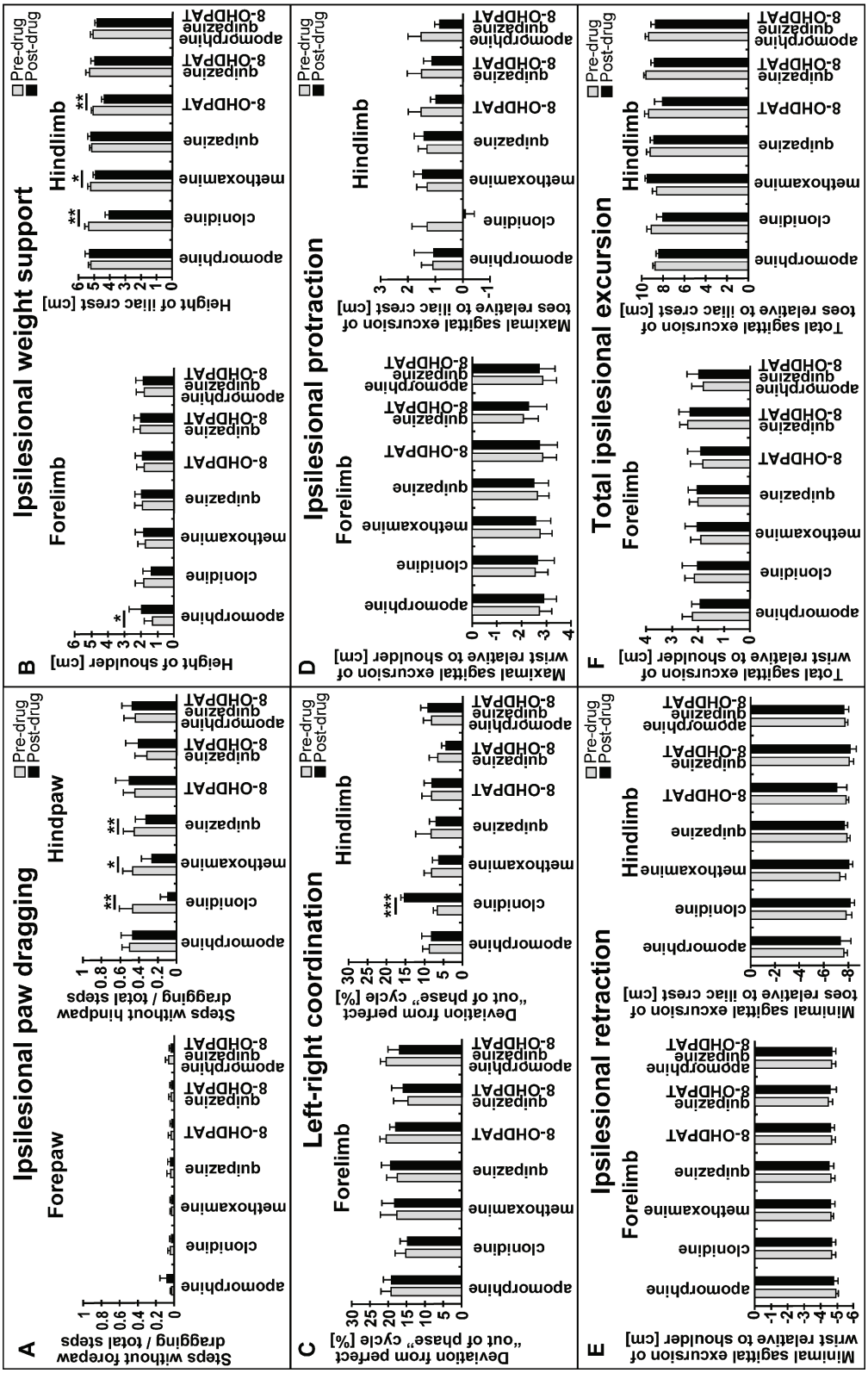

Figure 4 Locomotor responses of fore- and hindlimbs to monoaminergic drugs. (A) Ipsilesional forepaw dragging was unaltered by any monoaminergic agonist. Hindpaw dragging was significantly increased after application of clonidine, methoxamine and quipazine. (B) Injection of apomophine significantly increased weight support of the ipsilesional forelimb. Clonidine, methoxamine and 8-OHDPAT significantly reduced weight support in the ipsilesional hindlimb. (C) Inter-forelimb coordination was not impaired by monoaminergic drugs. Clonidine significantly perturbed coordination of hindlimbs during locomotion. Combined application of quipazine and 8-OHDPAT revealed non-significant improvement of hindlimb coordination. (D)-(F) Neither protraction (D), retraction (E), nor total limb excursion (F) of the ipsilesional fore- and hindlimb showed significant modulations by single or combined monoaminergic drug injections. 5-10 representative step cycles were analysed per animal and per condition. Data are presented as mean ± SEM. Statistical evaluation was done with Student`s *t*-test (two-tailed, paired) comparing pre-drug with post-drug condition of a particular drug. * $P < 0.05$; ** $P < 0.01$; *** $P < 0.001$.

Discussion

High cervical unilateral spinal cord hemisection in adult rats massively impairs fore- and hindlimb functions. Detailed kinematic analysis revealed a highly disproportional recovery of fore- versus hindlimb locomotor performance. The ipsilesional forelimb remained rigid and essentially non-functional, whereas the ipsilesional hindlimb showed substantial functional recovery and performance at 14 to 28 days post lesion. Dopaminergic, noradrenergic and serotonergic receptor agonists, some of them significantly improving the hindlimb function in complete thoracic SCI models, were without effect on forelimb locomotion in our hemisection model and had minor, mostly negative effects on hindlimb circuits.

Since acutely after injury, the ipsilesional forelimb and both hindlimbs were severely impaired, wading with partial body weight support was the most appropriate paradigm to study locomotor recovery in these rats. Over 2 to 4 weeks, the hindlimbs regained a well controlled locomotor pattern with movement parameters that were close to normal. In contrast, the ipsilesional forelimb remained paretic and rigid, with constant dragging often combined with a closed paw. Weight support of the ipsilesional forelimb was permanently reduced and interlimb coordination remained impaired over the entire experimental period. These findings parallel the clinical observations in humans with incomplete cervical SCI (including patients with Brown-Séquard syndrome); they often recover leg function (including walking), but only poor arm and hand functions (Levi *et al.,* 1996). Unilateral cervical hemisection at C7 spinal level in primates revealed an analogous motor recovery between fore- and hindlimbs; hindlimb locomotion recovered extensively, whereas forelimb locomotion and hand function recovered to a lesser extent (Rosenzweig *et al.,* 2010). Thus, the functional outcome after cervical lateral hemisection in rats (especially locomotion) strongly resembles the primate and human situation. This resemblance in lesion outcome across species with lateral spinal hemisection could rely on two main reasons:

First, there is a high functional and anatomical conservation of supraspinal and intraspinal motor systems among vertebrates. The classical studies by Kuypers and colleagues in macaques showed that the ventromedial (reticulo- and vestibulospinal tract) and the lateral system (rubrospinal tract) reveal similar anatomy and implement analogous motor function as observed in rodents and cats (Lawrence and Kuypers, 1968; Drew, 1991; Küchler *et al.,* 2002; Lemon, 2008). The corticospinal tract has a more prominent role in motor function in primates/humans as compared to non-primate quadrupeds (Nathan, 1994; Levi *et al.,* 1996; Courtine *et al.,* 2007). Experimental studies agree that

interruption of the corticospinal tract in rodents and cats only minimally impairs locomotor function (Alstermark *et al.,* 1989; Muir and Whishaw, 1999). The role of the corticospinal system in human locomotion is less clear, probably due to little restricted damage of this system in clinical cases. Whereas Nathan postulated that the corticospinal system in humans is the most prominent system for locomotion (Nathan, 1994), other researchers claim that, besides the corticospinal tract, mainly the ventromedial and –lateral reticulospinal fibres are critical for locomotion (Lawrence and Kuypers, 1968; Eidelberg, 1981; Levi *et al.,* 1996). There are also parallels in the propriospinal system between species, especially with regard to the C3-C4 propriospinal pool serving as relay for supraspinal information in cats and in monkeys (Alstermark *et al.,* 1981; Pettersson *et al.,* 2007). Evidence for a corresponding C3-C4 propriospinal system in rats is still lacking.

Second, a unilateral hemisection leads to a full unilateral ablation of commands in the spinal cord from each supraspinal system, independent of its specific function. Given the similar anatomy of most descending tracts (Lawrence and Kuypers, 1968; Lemon, 2008), this would result in a similar outcome across species, assuming that supraspinal inputs have a similar role on locomotion.

Motor recovery after unilateral hemisection is thought to result from compensatory sprouting of descending fibres from the intact side of the spinal cord (Weidner *et al.,* 2001; Ballermann and Fouad, 2006; Rosenzweig *et al.,* 2010), from propriospinal relay circuits (Alstermark *et al.,* 1981; Bareyre *et al.,* 2004; Courtine *et al.,* 2008) or from intrinsic reorganization of intraspinal circuits (Barriere *et al.,* 2008). For the latter, Barrière and colleagues impressively demonstrated that cats with a thoracic lateral hemisection recovered robust hindlimb locomotion. By performing a subsequent complete transection caudal to the hemisection, the authors could show immediate functional hindlimb stepping in the trained cats. This indicates intrinsic reorganization of the lumbar CPG networks after the first hemi-lesion, probably by remaining supraspinal input, as a key element of functional recovery. Given the very different functional outcome observed in the present study after unilateral hemisection, the mechanisms of functional recovery must differ substantially between fore- and hindlimbs, in the quadrupedal rat as the bipedal human.

To investigate direct damage of motor circuits by the cut lesion, histological analysis of cervical motoneuron numbers and morphology were performed. The extent of the lesions was limited affecting motoneurons over a rostrocaudal distance of only 1 mm, which roughly corresponds to half a cervical spinal segment. Since most motoneuron pools innervating particular forelimb muscles span 2 or more segments (McKenna *et al.,* 2000), direct damage of motoneurons is unlikely to be a major reason for

the severe motor deficits of the forelimb after injury. This is further supported by the observation that patients with cervical SCI at different spinal levels often show very similar motor impairments of arm/hand functions, regardless of the exact location of the lesion (Levi *et al.,* 1996). Moreover, cervical CPG networks operating rhythmic locomotor activity in rats are located predominately in spinal segments C7-T1 (Ballion *et al.,* 2001), well below our C4/5 lesion.

Interestingly, recent data from retrograde neuroanatomical tracing of descending tracts from the cervical and lumbar spinal cord in intact adult rats revealed that most supraspinal descending systems such as the corticospinal and most bulbospinal tracts reveal a considerably higher fibre number ending in the cervical than in the lumbar enlargement (Björn Zörner*,* in preparation). Similar observations were reported for reticulospinal fibres in humans (Nathan, 1994). The major exceptions were the monoaminergic nuclei (raphe nuclei, locus coeruleus), which displayed denser innervation of the lumbar spinal cord, as also shown in the present study. These anatomical data strongly suggest that forelimb movements, contrary to the hindlimbs, require more supraspinal commands controlling motor function, which is reflected in the locomotor deficits after unilateral SCI. Hindlimb circuits, in contrast, function more autonomously based on a prominent CPG controlled by commissural interneurons, some midline crossing fibres from the spared tracts, and remaining sensory afferents (Barriere *et al.,* 2008).

Monoamines are key regulators of motoneuron and local circuit excitability in the spinal cord. In intact animals, the density of 5-HT and TH-positive fibres was 2 to 5 times higher in the lumbar than the cervical spinal cord (this study; for 5-HT see also Hadjiconstantinou *et al.,* 1984; Colado *et al.,* 1988). After cervical unilateral hemisection, the 5-HT and TH-positive fibres were highly reduced in the cervical and lumbar hemicord. In agreement with Golder and Bregman (C2 and mid thoracic unilateral hemisection) but in contrast to Saruhashi and colleagues (unilateral T8 hemisection), we did not observe a restoration of the ipsilesional 5-HT and TH fibre plexus up to 4 weeks after the lesion, but even found a further reduction of the 5-HT and TH signals from 4 days to 28 days after the lesion (Bregman, 1987; Saruhashi *et al.,* 1996; Golder *et al.,* 2001). The lack of monoaminergic regrowth after cervical hemisection in this study indicates that monoaminergic fibre sprouting is not a key component of locomotor recovery observed in this lesion model.

After complete transection of the lower spinal cord, monoaminergic agonists have a potent facilitatory effect on hindlimb CPGs in mice, rats, cats and monkeys (Forssberg and Grillner, 1973; Barbeau and Rossignol, 1991; Fedirchuk *et al.,* 1998; Feraboli-Lohnherr *et al.,* 1999; Antri *et al.,* 2003 and 2005;

Guertin, 2004; Landry and Guertin, 2004). Clonidine application in SCI patients revealed unclear results, varying from detrimental to beneficial for locomotion (Stewart *et al.,* 1991; Dietz *et al.,* 1995). When we injected agonists of the different monoaminergic systems intrathecally in the chronic phase after the C4/5 hemisection, particular parameters of hindlimb locomotion were modulated by specific receptor agonists, but mostly in a negative, non-functional direction (increase in dragging, reduction in weight support, deterioration of inter-hindlimb coordination, and reduction of hindlimb protraction). The rigid and non-functional forelimb showed almost no reaction to the monoaminergic agonists; an increase in shoulder height and limb stiffness after application of the dopaminergic agonist apomorphine was the only drug-induced modulation observed. The α2-noradrenergic receptor agonist clonidine showed various detrimental effects on hindlimb locomotion ranging from increased paw dragging, to deteriorated left-right alternation. Similar adverse effects of clonidine on hindlimb locomotion were also found in cats with incomplete thoracic SCI (Brustein and Rossignol, 1999). The 5-HT_2 receptor agonist quipazine, which has been shown to be highly potent in facilitating locomotion of completely spinalised rats (Antri *et al.,* 2003 and 2005; Gerasimenko *et al.,* 2007; Ichiyama *et al.,* 2008; Courtine *et al.,* 2009), had only minor effects on hindlimb locomotion in our rats with a unilateral C4/5 hemisection. Injections of the selective 5-HT_1 receptor agonist 8-OHDPAT induced a significant reduction of weight support, which is well known as $5HT_1$-induced flat body posture in the serotonin syndrome (Darmani and Ahmad, 1999). The dopaminergic agonist apomorphine did not elicit any modulation of hindlimb locomotion.

Our results suggest that the monoaminergic drive may be more important for hindlimb networks, whereas forelimb locomotor networks, which need to flexibly target different muscle groups to execute motor tasks (Harel *et al.,* 2008), are more precisely controlled and driven by supraspinal centres, requiring specific descending input instead of the rather global monoaminergic stimulation. This is further supported by the higher density of monoaminergic fibres in the lumbar compared to the cervical spinal cord, which is also reflected in the respective receptor densities (5-HT_1 receptors, (Marlier *et al.,* 1991); D1 receptors, (Dubois *et al.,* 1986). However, the exact site of drug actions (i.e. segmental level and cell type) can not be identified by the present study.

A second important conclusion of our results concerns the big differences seen in the drug effects between the incomplete and the complete or ventral SCI models. In the C4/5 unilateral hemisection model, the locomotor responses to the monoaminergic agonists were minor and, importantly, mostly negative for the hindlimbs. In contrast, rats with complete or large ventral thoracic SCI reacted to

monoaminergic agonists with substantial and mostly positive locomotor responses (Feraboli-Lohnherr *et al.,* 1999; Antri *et al.,* 2003 and 2005; Courtine *et al.,* 2009; unpublished observations) especially when in combination with epidural spinal cord stimulation (Gerasimenko *et al.,* 2007; Courtine *et al.,* 2009). One reason for these surprising discrepancies might be the differing number, sensitivity and distribution (pre- versus post-synaptic) of monoaminergic receptors in SCI models of different severity (Rossignol *et al.,* 2001): Hayshi and colleagues postulated that a certain threshold denervation of monoaminergic fibres must be present in order to induce post-synaptic receptor changes; upregulation of lumbar 5-HT_{2C} receptors was only seen after severe, but not moderate contusion injury in the thoracic spinal cord (Hayashi *et al.,* 2010). Moreover, monoaminergic drugs applied after complete or large ventral SCI act exclusively on post-synaptic receptors, whereas in our lesion model, the drugs can affect pre-synaptic (unlesioned terminals) and post-synaptic receptors. Since the function of these receptors could be different depending on their location (i.e. negative feedback role for pre-synaptic receptors), the differing pre-/post-synaptic receptor balance is likely to affect the pharmacological effects on locomotion. Murray et al. showed that transcriptional changes after complete spinal cord transection led to the production of 5-HT_{2C} receptors, which are spontaneously active without 5-HT (Murray *et al.,* 2010). These constitutively active receptors are thought to act as functional compensation for the severe loss of descending serotonergic fibres from the brainstem. Hence, the appearance of these receptors is likely to be dependent again on the severity of the lesion. Lastly, monoaminergic stimulation could negatively interfere with spared locomotor commands, which are present after unilateral hemisection, but absent after complete or large ventral SCI.

In conclusion, the present study demonstrates a clearly different response of fore- versus hindlimb spinal circuitries upon unilateral ablation of supraspinal commands. As observed in primates and humans, spontaneous motor recovery after cervical unilateral hemisection (leading to the Brown-Séquard syndrome) is considerable for the lower limbs, but often marginal or absent for the ipsilesional upper extremity. Responsiveness to monoaminergic drugs was absent in the forelimb and higher, although mainly functionally negative, in the hindlimbs. Monoaminergic stimulation, which exerts positive locomotor effects in animals with complete or ventral SCI, interfered with the remaining supraspinal command systems in rats with incomplete SCI. The present study illustrates the urgent need to model cervical incomplete SCI as a frequent SCI type in humans, to better understand the differing control systems of upper and lower extremities as well as potential therapeutic options like the stimulation of spinal monoamine receptors.

Supplementary material

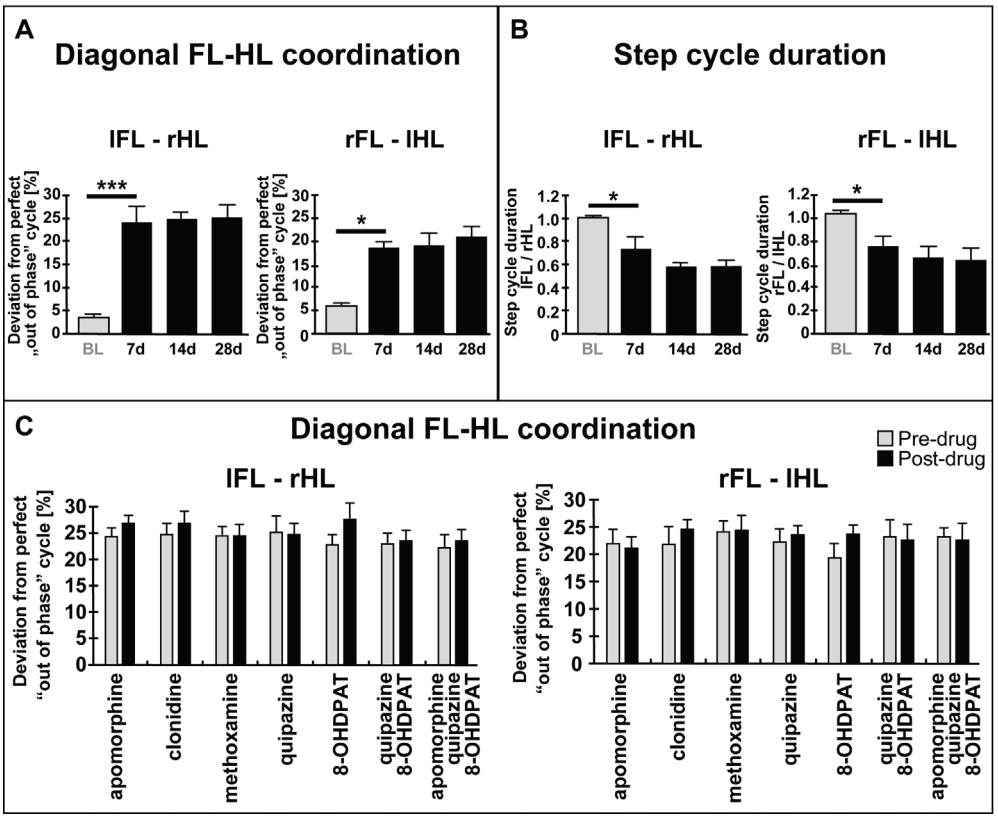

Supplementary Figure 1 Diagonal forelimb/hindlimb coupling. (A) Forelimb/hindlimb coupling shows a nearly perfect "in phase" rhythm in intact animals. The deviation from a perfect "in phase" is 3.7 percent for the left forelimb/right hindlimb (lFL/rHL), and 6.0 percent for the right forelimb/left hindlimb (rFL/lHL). Both diagonals (lFL/rHL and rFL/lHL) showed massive coordinative impairment after the lesion. The deficits in antero-posterior coordination persisted over the whole experimental period and were similar for the both diagonals. (B) The step cycle duration for the forelimbs (impaired and unimpaired) was clearly shorter compared to the step cycle duration of the hindlimbs. The increased stepping frequency of the forelimbs distorted the forelimb/hindlimb coordination, since almost 2 forelimb steps were performed during a single hindlimb step. (C) Intrathecal injections of diverse monoaminergic agonists did not significantly modulate forelimb/hindlimb coupling. Data are presented as mean ± SEM. Statistical evaluation was done with One-way ANOVA repeated measures with Bonferroni *post hoc* test comparing BL with 7d (lesion deficit) and 7d with 28d (functional recovery). * $P < 0.05$; ** $P < 0.01$; *** $P < 0.001$.

References

Alstermark B, Isa T, Lundberg A, Pettersson LG, Tantisira B. The effect of low pyramidal lesions on forelimb movements in the cat. Neurosci Res. 1989; 7(1): 71-5.

Alstermark B, Lindstrom S, Lundberg A, Sybirska E. Integration in descending motor pathways controlling the forelimb in the cat. 8. Ascending projection to the lateral reticular nucleus from C3-C4 propriospinal also projecting to forelimb motoneurones. Exp Brain Res. 1981; 42(3-4): 282-98.

Antri M, Barthe JY, Mouffle C, Orsal D. Long-lasting recovery of locomotor function in chronic spinal rat following chronic combined pharmacological stimulation of serotonergic receptors with 8-OHDPAT and quipazine. Neurosci Lett. 2005; 384(1-2): 162-7.

Antri M, Mouffle C, Orsal D, Barthe JY. 5-HT1A receptors are involved in short- and long-term processes responsible for 5-HT-induced locomotor function recovery in chronic spinal rat. Eur J Neurosci. 2003; 18(7): 1963-72.

Ballermann M, Fouad K. Spontaneous locomotor recovery in spinal cord injured rats is accompanied by anatomical plasticity of reticulospinal fibers. Eur J Neurosci. 2006; 23(8): 1988-96.

Ballion B, Morin D, Viala D. Forelimb locomotor generators and quadrupedal locomotion in the neonatal rat. Eur J Neurosci. 2001; 14(10): 1727-38.

Balter JE, Zehr EP. Neural coupling between the arms and legs during rhythmic locomotor-like cycling movement. J Neurophysiol. 2007; 97(2): 1809-18.

Barbeau H, Rossignol S. Initiation and modulation of the locomotor pattern in the adult chronic spinal cat by noradrenergic, serotonergic and dopaminergic drugs. Brain Res. 1991; 546(2): 250-60.

Bareyre FM, Kerschensteiner M, Raineteau O, Mettenleiter TC, Weinmann O, Schwab ME. The injured spinal cord spontaneously forms a new intraspinal circuit in adult rats. Nat Neurosci. 2004; 7(3): 269-77.

Barriere G, Leblond H, Provencher J, Rossignol S. Prominent role of the spinal central pattern generator in the recovery of locomotion after partial spinal cord injuries. J Neurosci. 2008; 28(15): 3976-87.

Bregman BS. Development of serotonin immunoreactivity in the rat spinal cord and its plasticity after neonatal spinal cord lesions. Brain Res. 1987; 431(2): 245-63.

Brustein E, Rossignol S. Recovery of locomotion after ventral and ventrolateral spinal lesions in the cat. II. Effects of noradrenergic and serotoninergic drugs. J Neurophysiol. 1999; 81(4): 1513-30.

Colado MI, Arnedo A, Peralta E, Del Rio J. Unilateral dorsal rhizotomy decreases monoamine levels in the rat spinal cord. Neurosci Lett. 1988; 87(3): 302-6.

Courtine G, Bunge MB, Fawcett JW, Grossman RG, Kaas JH, Lemon R, Maier I, Martin J, Nudo RJ, Ramon-Cueto A, Rouiller EM, Schnell L, Wannier T, Schwab ME, Edgerton VR. Can experiments in nonhuman primates expedite the translation of treatments for spinal cord injury in humans? Nat Med. 2007; 13(5): 561-6.

Courtine G, Gerasimenko Y, van den Brand R, Yew A, Musienko P, Zhong H, Song B, Ao Y, Ichiyama RM, Lavrov I, Roy RR, Sofroniew MV, Edgerton VR. Transformation of nonfunctional spinal circuits into functional states after the loss of brain input. Nat Neurosci. 2009; 12(10): 1333-42.

Courtine G, Roy RR, Hodgson J, McKay H, Raven J, Zhong H, Yang H, Tuszynski MH, Edgerton VR. Kinematic and EMG determinants in quadrupedal locomotion of a non-human primate (Rhesus). J Neurophysiol. 2005; 93(6): 3127-45.

Courtine G, Song B, Roy RR, Zhong H, Herrmann JE, Ao Y, Qi J, Edgerton VR, Sofroniew MV. Recovery of supraspinal control of stepping via indirect propriospinal relay connections after spinal cord injury. Nat Med. 2008; 14(1): 69-74.

Darmani NA, Ahmad B. Long-term sequential determination of behavioral ontogeny of 5-HT1A and 5-HT2 receptor functions in the rat. J Pharmacol Exp Ther. 1999; 288(1): 247-53.

Dietz V, Colombo G, Jensen L, Baumgartner L. Locomotor capacity of spinal cord in paraplegic patients. Ann Neurol. 1995; 37(5): 574-82.

Dietz V, Fouad K, Bastiaanse CM. Neuronal coordination of arm and leg movements during human locomotion. Eur J Neurosci. 2001; 14(11): 1906-14.

Dietz V, Harkema SJ. Locomotor activity in spinal cord-injured persons. J Appl Physiol. 2004; 96(5): 1954-60.

Drew T. Functional organization within the medullary reticular formation of the intact unanesthetized cat. III. Microstimulation during locomotion. J Neurophysiol. 1991; 66(3): 919-38.

Dubois A, Savasta M, Curet O, Scatton B. Autoradiographic distribution of the D1 agonist [3H]SKF 38393, in the rat brain and spinal cord. Comparison with the distribution of D2 dopamine receptors. Neuroscience. 1986; 19(1): 125-37.

Duysens J, Van de Crommert HW. Neural control of locomotion; The central pattern generator from cats to humans. Gait Posture. 1998; 7(2): 131-41.

Eidelberg E. Consequences of spinal cord lesions upon motor function, with special reference to locomotor activity. Prog Neurobiol. 1981; 17(3): 185-202.

Fedirchuk B, Nielsen J, Petersen N, Hultborn H. Pharmacologically evoked fictive motor patterns in the acutely spinalized marmoset monkey (Callithrix jacchus). Exp Brain Res. 1998; 122(3): 351-61.

Feraboli-Lohnherr D, Barthe JY, Orsal D. Serotonin-induced activation of the network for locomotion in adult spinal rats. J Neurosci Res. 1999; 55(1): 87-98.

Forssberg H, Grillner S. The locomotion of the acute spinal cat injected with clonidine i.v. Brain Res. 1973; 50(1): 184-6.

Gerasimenko YP, Ichiyama RM, Lavrov IA, Courtine G, Cai L, Zhong H, Roy RR, Edgerton VR. Epidural spinal cord stimulation plus quipazine administration enable stepping in complete spinal adult rats. J Neurophysiol. 2007; 98(5): 2525-36.

Giroux N, Rossignol S, Reader TA. Autoradiographic study of alpha1- and alpha2-noradrenergic and serotonin1A receptors in the spinal cord of normal and chronically transected cats. J Comp Neurol. 1999; 406(3): 402-14.

Golder FJ, Reier PJ, Bolser DC. Altered respiratory motor drive after spinal cord injury: supraspinal and bilateral effects of a unilateral lesion. J Neurosci. 2001; 21(21): 8680-9.

Grillner S. The motor infrastructure: from ion channels to neuronal networks. Nat Rev Neurosci. 2003; 4(7): 573-86.

Grillner S, Wallen P. Central pattern generators for locomotion, with special reference to vertebrates. Annu Rev Neurosci. 1985; 8: 233-61.

Guertin PA. Synergistic activation of the central pattern generator for locomotion by l-beta-3,4-dihydroxyphenylalanine and quipazine in adult paraplegic mice. Neurosci Lett. 2004; 358(2): 71-4.

Hadjiconstantinou M, Panula P, Lackovic Z, Neff NH. Spinal cord serotonin: a biochemical and immunohistochemical study following transection. Brain Res. 1984; 322(2): 245-54.

Harel R, Asher I, Cohen O, Israel Z, Shalit U, Yanai Y, Zinger N, Prut Y. Computation in spinal circuitry: lessons from behaving primates. Behav Brain Res. 2008; 194(2): 119-28.

Hayashi Y, Jacob-Vadakot S, Dugan EA, McBride S, Olexa R, Simansky K, Murray M, Shumsky JS. 5-HT precursor loading, but not 5-HT receptor agonists, increases motor function after spinal cord contusion in adult rats. Exp Neurol.; 221(1): 68-78.

Ichiyama RM, Gerasimenko Y, Jindrich DL, Zhong H, Roy RR, Edgerton VR. Dose dependence of the 5-HT agonist quipazine in facilitating spinal stepping in the rat with epidural stimulation. Neurosci Lett. 2008; 438(3): 281-5.

Jahn K, Deutschlander A, Stephan T, Kalla R, Hufner K, Wagner J, Strupp M, Brandt T. Supraspinal locomotor control in quadrupeds and humans. Prog Brain Res. 2008; 171: 353-62.

Kloos AD, Fisher LC, Detloff MR, Hassenzahl DL, Basso DM. Stepwise motor and all-or-none sensory recovery is associated with nonlinear sparing after incremental spinal cord injury in rats. Exp Neurol. 2005; 191(2): 251-65.

Küchler M, Fouad K, Weinmann O, Schwab ME, Raineteau O. Red nucleus projections to distinct motor neuron pools in the rat spinal cord. J Comp Neurol. 2002; 448(4): 349-59.

Kuerzi J, Brown EH, Shum-Siu A, Siu A, Burke D, Morehouse J, Smith RR, Magnuson DS. Task-specificity vs. ceiling effect: step-training in shallow water after spinal cord injury. Exp Neurol. 2010; 224(1): 178-87.

Landry ES, Guertin PA. Differential effects of 5-HT1 and 5-HT2 receptor agonists on hindlimb movements in paraplegic mice. Prog Neuropsychopharmacol Biol Psychiatry. 2004; 28(6): 1053-60.

Lawrence DG, Kuypers HG. The functional organization of the motor system in the monkey. II. The effects of lesions of the descending brain-stem pathways. Brain. 1968; 91(1): 15-36.

Lee JK, Johnson CS, Wrathall JR. Up-regulation of 5-HT2 receptors is involved in the increased H-reflex amplitude after contusive spinal cord injury. Exp Neurol. 2007; 203(2): 502-11.

Lemon RN. Descending pathways in motor control. Annu Rev Neurosci. 2008; 31: 195-218.

Levi AD, Tator CH, Bunge RP. Clinical syndromes associated with disproportionate weakness of the upper versus the lower extremities after cervical spinal cord injury. Neurosurgery. 1996; 38(1): 179-83; discussion 83-5.

Little JW, Halar E. Temporal course of motor recovery after Brown-Sequard spinal cord injuries. Paraplegia. 1985; 23(1): 39-46.

Marlier L, Teilhac JR, Cerruti C, Privat A. Autoradiographic mapping of 5-HT1, 5-HT1A, 5-HT1B and 5-HT2 receptors in the rat spinal cord. Brain Res. 1991; 550(1): 15-23.

Martinez M, Brezun JM, Zennou-Azogui Y, Baril N, Xerri C. Sensorimotor training promotes functional recovery and somatosensory cortical map reactivation following cervical spinal cord injury. Eur J Neurosci. 2009; 30(12): 2356-67.

Martinez M, Delcour M, Russier M, Zennou-Azogui Y, Xerri C, Coq JO, Brezun JM. Differential tactile and motor recovery and cortical map alteration after C4-C5 spinal hemisection. Exp Neurol. 2010; 221(1): 186-97.

McKenna JE, Prusky GT, Whishaw IQ. Cervical motoneuron topography reflects the proximodistal organization of muscles and movements of the rat forelimb: a retrograde carbocyanine dye analysis. J Comp Neurol. 2000; 419(3): 286-96.

McKinley W, Santos K, Meade M, Brooke K. Incidence and outcomes of spinal cord injury clinical syndromes. J Spinal Cord Med. 2007; 30(3): 215-24.

Muir GD, Whishaw IQ. Complete locomotor recovery following corticospinal tract lesions: measurement of ground reaction forces during overground locomotion in rats. Behav Brain Res. 1999; 103(1): 45-53.

Murray KC, Nakae A, Stephens MJ, Rank M, D'Amico J, Harvey PJ, Li X, Harris RL, Ballou EW, Anelli R, Heckman CJ, Mashimo T, Vavrek R, Sanelli L, Gorassini MA, Bennett DJ, Fouad K. Recovery of motoneuron and locomotor function after spinal cord injury depends on constitutive activity in 5-HT2C receptors. Nat Med. 2010; 16(6): 694-700.

Nathan PW. Effects on movement of surgical incisions into the human spinal cord. Brain. 1994; 117 (Pt 2): 337-46.

Pettersson LG, Alstermark B, Blagovechtchenski E, Isa T, Sasaski S. Skilled digit movements in feline and primate--recovery after selective spinal cord lesions. Acta Physiol (Oxf). 2007; 189(2): 141-54.

Rosenzweig ES, Courtine G, Jindrich DL, Brock JH, Ferguson AR, Strand SC, Nout YS, Roy RR, Miller DM, Beattie MS, Havton LA, Bresnahan JC, Edgerton VR, Tuszynski MH. Extensive spontaneous plasticity of corticospinal projections after primate spinal cord injury. Nat Neurosci. 2010; 13(12): 1505-10.

Rossignol S, Giroux N, Chau C, Marcoux J, Brustein E, Reader TA. Pharmacological aids to locomotor training after spinal injury in the cat. J Physiol. 2001; 533(Pt 1): 65-74.

Roth EJ, Park T, Pang T, Yarkony GM, Lee MY. Traumatic cervical Brown-Sequard and Brown-Sequard-plus syndromes: the spectrum of presentations and outcomes. Paraplegia. 1991; 29(9): 582-9.

Saruhashi Y, Young W, Perkins R. The recovery of 5-HT immunoreactivity in lumbosacral spinal cord and locomotor function after thoracic hemisection. Exp Neurol. 1996; 139(2): 203-13.

Stewart JE, Barbeau H, Gauthier S. Modulation of locomotor patterns and spasticity with clonidine in spinal cord injured patients. Can J Neurol Sci. 1991; 18(3): 321-32.

Taylor RG, Gleave JR. Incomplete spinal cord injuries; with Brown-Sequard phenomena. J Bone Joint Surg Br. 1957; 39-B(3): 438-50.

Vilensky JA. Locomotor behavior and control in human and non-human primates: comparisons with cats and dogs. Neurosci Biobehav Rev. 1987; 11(3): 263-74.

Webb AA, Muir GD. Compensatory locomotor adjustments of rats with cervical or thoracic spinal cord hemisections. J Neurotrauma. 2002; 19(2): 239-56.

Webb AA, Muir GD. Sensorimotor behaviour following incomplete cervical spinal cord injury in the rat. Behav Brain Res. 2005; 165(2): 147-59.

Weidner N, Ner A, Salimi N, Tuszynski MH. Spontaneous corticospinal axonal plasticity and functional recovery after adult central nervous system injury. Proc Natl Acad Sci U S A. 2001; 98(6): 3513-8.

Wirz M, Zörner B, Rupp R, Dietz V. Outcome after incomplete spinal cord injury:central cord versus Brown-Sequard syndrome. Spinal Cord. 2010; 48(5): 407-14.

Zörner B, Filli L, Starkey ML, Gonzenbach R, Kasper H, Röthlisberger M, Bolliger M, Schwab ME. Profiling locomotor recovery: comprehensive quantification of impairments after CNS damage in rodents. Nat Methods. 2010; 7(9): 701-8.

Chapter 4

Rewiring of reticulospinal fibers onto relaying C3-C4 propriospinal neurons after unilateral C4/C5 hemisection in adult rats

Linard Filli, Anne Engmann, Björn Zörner, Lukas Bachmann, Miriam Gullo and Martin E. Schwab

Ongoing research project

Abstract

Although long-distance regeneration is absent in the central nervous system, spinal cord injured patients and respective animal models show some recovery of motor functions. Neuronal plasticity at several levels of the central nervous system is thought to be a major component of this functional recovery.

Here, anatomical plasticity of different supraspinal brain areas was investigated after a unilateral C4/C5 hemisection using neuroanatomical tracing techniques. Retrograde tracer injection at the ipsilesional spinal level C3/C4 identified specific descending brain systems showing persistent anatomical plasticity up to 43 days after spinal cord injury. Region-specific anterograde tracing verified the gigantocellular reticular nucleus as highly plastic bulbospinal system, showing massive fiber sprouting rostral to the lesion. These fibers were colocalized with the synaptic vesicular glutamate transporter 2 (vGLUT2), indicating their synaptic integration. Additionally, the sprouting fibers from the gigantocellular reticular nucleus were shown to form close apposition-like contacts with propriospinal neurons located at the ipsilesional spinal level C3/C4. The propriospinal neurons innervated sublesional target areas by midline re-crossing fibers, as revealed by retrograde tracer injections in the ipsilesional cervical enlargement. After the C4/5 hemisection the number of re-crossing propriospinal fibers was highly increased in the cervical enlargement below the lesion, demonstrating anatomical plasticity at the intraspinal level. These results suggest spontaneous anatomical plasticity at different levels oft the central nervous system, leading to a relay of reticulospinal commands to the denervated spinal areas below the lesion.

Introduction

Spinal cord injury (SCI) most often affects descending motor, ascending sensory and autonomic fiber tracts leading to devastating impairments in patients (Schwab and Bartholdi, 1996). Deficits resulting from SCI often include paralysis/paresis of extremities, sensory loss, chronic pain and problems with bladder and bowl function (Rossignol *et al.,* 2007). The segmental location and the severity of the spinal lesion determine the neurological deficits and the prognosis of functional outcome (Schwab, 2002; Zörner *et al.,* 2010).

Plasticity and re-growth of neuronal fibers is limited in the adult mammalian central nervous system (CNS; Raineteau and Schwab, 2001). Long-distance regeneration of axotomized fibers is absent under spontaneous conditions. Different extrinsic factors such as myelin-associated proteins (Schwab and Caroni, 1988; Raineteau and Schwab, 2001, Liu *et al,* 2002) and extracellular matrix molecules (i.e. CSPGs; Oohira *et al.,* 1991; Silver and Miller, 2004) exert growth inhibiting effects on neuronal axons. Moreover, adult CNS neurons discard limited intrinsic potential to extend and re-grow after injury (Rossi *et al.,* 2001; Afshari *et al.,* 2009). After spinal trauma, the glial scar and processes embraced as secondary damage (altered blood pressure, changed ion concentrations, inflammation ect.) negatively influence anatomical plasticity of spared and severed fibers (Bunge *et al.*, 1993; Norenberg *et al.,* 2004, Schwab *et al.,* 2006). Nevertheless, patients and animal models usually show a certain extent of spontaneous functional recovery after incomplete SCI (Tator *et al.,* 1995). Early improvement of functions after SCI is mainly accredited to the reversion of the severely pathological circumstances within and around the lesion site (e.g. spinal shock, local ischemia etc.). Subsequent restorations of motor functions are attributed to diverse adaptations of the CNS generally embraced as plasticity. These plastic processes can take place in neurons and glial cells, as well as at different levels ranging from molecular and cellular adaptations to anatomical reorganizations of entire neuronal circuits (Zörner and Schwab, 2010; Raineteau, 2008).

Neuroanatomical plasticity includes processes such as sprouting of severed fibers (regenerative plasticity) or structural changes of intact fibers (compensatory plasticity). Spontaneous anatomical rearrangements were shown for several descending motor systems after spinal injury: corticospinal (Fouad *et al.,* 2001), rubrospinal (Lawrence and Kuypers, 1968a,b), and reticulospinal projections (Ballermann and Fouad, 2006) revealed neuroanatomical adaptations subsequent to spinal trauma.

Besides anatomical plasticity in descending supraspinal systems, adaptations following SCI were also found in intraspinal networks. Indeed, propriospinal networks have gained increased interest due to

their considerable plastic potential after SCI. There is growing evidence that the formation of intraspinal detour pathways is an important substrate for functional recovery after SCI (Flynn *et al.,* 2011). Propriospinal neurons (PSNs) play, as already mentioned by Sir Charles Sherrington, a critical role in performing motor reflexes, voluntary movements and sensory processing (Sherrington and Laslett, 1903; Kostyuk and Vasilenko, 1979; Jankowska, 1992; Foreman, 2000; Alstermark *et al.,* 2007; Conta, 2009; Cowley *et al.,* 2010). Propriospinal networks are critical to integrate and modulate inputs from different supraspinal descending systems and peripheral afferents and to synchronize the activity in spinal motor circuits (Flynn *et al.,* 2011).

The probably most investigated PSN pool is the C3-C4 propriospinal system. In the cat this pool has been shown to receive input from the cortex, the red nucleus and the reticular formation, which is integrated and transmitted to motoneurons located in the cervical enlargement innervating the forelimb (Alstermark *et al.,* 1984; Illert and Lundberg, 1978; Illert *et al.,* 1977 and 1981). The C3-C4 propriospinal system seems to form a feedback loop to the cerebellum (via the brainstem) providing supraspinal systems with a copy of the C3-C4 activity patterns, thereby enabling motor error correction (Illert and Lundberg, 1978; Alstermark *et al.,* 1981).

Previous studies displayed the plastic potential of PSNs after spinal injury in adult rats (Bareyre *et al.,* 2004; Courtine *et al.,* 2008). Subsequent to a thoracic dorsal hemisection, corticospinal projections were shown to contact long-propriospinal neurons in the cervical enlargement, which bypassed the lesion site and increasingly innervated motor neurons caudal to the lesion (Bareyre *et al.,* 2004). These anatomical reorganizations were accompanied by functional recovery. Courtine *et al.* revealed that axotomy of all descending projections by a thoracic staggered lesion paradigm was followed by significant recovery of hindlimb function, but only if the single hemisections were separated by 10 weeks. The conclusion was that the intrinsic spinal network in between the lesions was able to relay supraspinal information to the denervated lumbar target sites, which resulted in recovery of stepping. This was confirmed by intraspinal excitotoxic ablation of the interneurons which abolished the restoration of stepping (Courtine *et al.,* 2008). However, this study did not provide information on which particular supraspinal commands were bypassed by the PSN pool in order to evoke the remarkable recovery of stepping performance.

The aim of this study was to investigate anatomical plasticity at different levels of the CNS after a unilateral C4/C5 spinal cord hemisection. We were interested in sprouting of severed supraspinal fibers rostral to the lesion. Moreover, this study investigated the connections between plastic

bulbospinal systems and PSN networks by the combined approach of antero- and retrograde tracing and immunohistochemical synaptic staining. The anatomical investigation of intraspinal circuits is of importance given their promising plastic capacity and their potential to restore motor functions upon partial SCI.

Methods

Experimental setup

All studies were performed with the approval of, and in accordance with the guidelines of the Veterinary Office of the Canton Zurich, Switzerland. Female adult Lewis rats (180 - 220 g, Centre d'`Elevage R.Janvier) were used for all experiments. They were housed in groups of three to four animals per cage, at a 12:12 h light:dark cycle, with water and food *ad libitum*. For all experiments three different time points were defined relative to the SCI: intact, acute (17 days after SCI), and subchronic (43 days after SCI). Detailed descriptions of the study design and particular sub-experiments can be found in Fig 1.

Surgical procedures

Surgeries were performed under systemic anesthesia (Hypnorm, 120 mg per 200 g body weight, Janssen Pharmaceutics; Dormicum, 0.75 mg per 200 g body weight, Roche Pharmaceuticals). Eyes were protected with Vitamin A cream (Chauvin Novopharma AG) and the skin around the incision was desinfected using standardized iodine solution (Betadine, B.Brown). After surgery the rats were returned to a heating blanket for recovery. Postoperative care included two health checks per day. Analgesics (Rimadyl: 2.5 mg per kg body weight, Pfizer AG) were applied for two days after the surgery and antibiotics (Baytril: 5 mg per kg body weight, Bayer AG) were applied for one week after surgery to prevent bladder or wound infections. Subcutaneous injections of Glucose-Ringer Solution (Fresenius) were given to counter dehydration after the surgical procedures. Bladders were checked and manually emptied twice a day, until normal bladder control had returned.

Spinal cord injury

The skin above vertebral level C2 to T2 was shaved, disinfected and opened with a scalpel. Connective tissue between skin and muscle was removed by blunt dissection. The superficial muscle layers overlying the vertebral column were carefully separated along the midline and the vertebral laminae were cleared from the deepest muscle layer and surrounding connective tissue. A laminectomy was performed at C4 vertebral level and the dura mater was opened. 5 drops of the anesthetic lidocaine (Lidoject 1% solution, Hexal AG Germany) were applied to the dorsal surface of the spinal cord to avoid movement during lesioning. A complete unilateral hemisection was performed on the right hemicord at the caudal end of spinal level C4, using a sharp sapphire knife (World

Precision Instruments). To ensure the completeness of the hemisection the cut was repeated several times. The C4 dorsal root was spared and left intact. Immediately after the lesion, 0.2 ml of the opioid antagonist Naloxon (OrPha Swiss GmbH) was injected subcutaneously to accelerate awakening, therefore reducing the mortality rate.

Neuroanatomical tracing

A laminectomy or craniectomy was performed to expose the desired region of the spinal cord or brain. Tracer injections were performed using a stereotaxic apparatus (Kopf AG). Tracers were injected with a velocity of 6 nl/sec using a UltraMicroPump (World Precision Instruments). 2 different tracer were used: the green-fluorescent Miniemerald (ME, 10'000 MW dextran: Molecular Probes, Invitrogen) and the red-fluorescent Tetramethylrhodamine (TMR, 3'000 MW dextran: Molecular Probes, Invitrogen). Both tracers were injected as 10% (w/V) solutions, diluted in dH2O.

Tracing of spinal segments C3/C4

The cervical vertebral column was exposed and the vertebral lamina C4 and parts of C3 was removed. The rat's vertebral column was fixed using stereotaxic clamps placed on the prominent processes of the vertebrae C2 and T2. 4 ME injections with a volume of 100 nl each were performed (mediolateral (ML): 0.9 mm, dorsoventral (DV): 1.6 mm). The injections started at the middle of spinal segment C4 and were placed in intervals of 500 µm in rostral direction. The tracer was transported for 14 days until the animals were perfused.

Retrograde tracing of cervical enlargement (C6-C8)

To retrogradely label C3-C4 PSN somata projecting to the cervical enlargement, 10 ipsilesional TMR injections were performed at spinal level C6 to C8 with a volume of 225 nl each (ML: 0.9 mm, DV: 1.6 mm). The tracer was transported for 7 days until the animals were perfused.

Anterograde tracing of brainstem nuclei

A craniectomy was performed using a dental drill and the animal was head-fixed in the stereotaxic frame. The position of the skull was adjusted so that bregma and lambda were on the same DV and ML level. The dura mater was locally opened and 50 nl of ME were injected in the gigantocellular reticular nucleus (ML: 1.05 mm, RC: 4.5 mm caudal from lambda, DV: 7.8 mm) and the caudal pons

(ML: 0.8 mm; RC: 4.75 mm caudal from lambda; DV: 9.64 mm). Due to a prominent blood vessel overlying the pontine target area, tracer injections in this region were performed at an angle of 14°in the sagittal plane pointing in the rostral direction. The tracer was transported for 21 days until the animals were perfused.

Tissue processing

14 days after the last tracing, animals were sacrificed by an overdose of pentobarbital (Esconarcon, 250 ml/100 g body weight, i.p.). Rats were perfused transcardially with 50 ml of 1% Heparin-Ringer solution (Heparin: B.Brown, Ringer: Fresenius), followed by a perfusion with 300 ml of a 4% para-formaldehyde (PFA, Sigma Aldrich) solution containing 5% sucrose (Sigma Aldrich). The spinal cord and the brain were extracted, postfixed in 4% PFA at 4°C for 24 hours and finally transferred into 30% sucrose solution at 4°C for 2-3 days for cryoprotection. Spinal cords and brains were embedded and frozen separately in O.C.T. Compound (Tissue-Tek) at -40°C. The frozen tissue was cut in 40 µm thick coronal sections at the cryostat (Microm HM560), taken up on Superfrost plus glass slides (Thermo Scientific) and coverslipped with Mowiol (Merck). Free-floating sections for immunohistochemical stainings were collected in 0.1 M PB directly after cutting and stored in Antifreeze solution (150 g Glucose, 500 ml 50 mM PB, 300 ml Ethylenglycol) at -20°C until further processing.

Nissl staining

The sections were quickly immersed in water twice for 2 sec, and then incubated in a cresyl violet solution (1 g cresyl violet acetate (Aldrich Chemical Company Inc.) in 200 ml dH2O) for 3 min. The sections were dehydrated in an increasing series of alcohol (70% EtOH, 80% EtOH, 90% EtOH, 100% EtOH) until the non-specific Nissl-staining was removed and the white matter of the spinal cord appeared in a bright color. The slides were immersed in Xylol and coverslipped with Eukitt (O. Kindler GmbH & CO).

Immunohistochemistry

Free-floating sections were washed in PBS for 5 min and permeabilized for 30 min with TNB containing 5% NGS (Normal Goat Serum) and 0.4% TritonX-100. The sections were washed again in PBS for 1 min and immersed in hypotonic buffer (PB 0.01 M) containing the primary antibody (rabbit-antivGlut2 1:750, Synaptic Systems), 0.1% TritonX-100 and 2% NGS. After incubation at 4°C on a

shaker for 2-3 days, the slides were washed in PBS three times for 5 min each. The sections were blocked in TNB for 10 min and then incubated in hypotonic buffer (PB 0.01 M) containing the respective secondary antibody (DyLight649 goat-anti-rabbit IgG 1:200, Jackson ImmunoResearch Laboratories Inc.; DyLight488-Streptavidin 1:1000, Jackson ImmunoResearch Laboratories Inc.), 0.1% TritonX-100 and 2% NGS on a shaker at 4°C over night. Finally, the sections were washed in PBS three times, mounted on Superfrost glass slides, air dried over night and coverslipped with Mowiol (Merck).

Quantification of neuroanatomical tracings

Retrograde cell counts in defined brain regions

The number of ME-positive cells was counted on every fourth brain section using a fluorescence microscope (Axioskop 2, Zeiss) with 10-fold magnification. Only traced neurons revealing bright fluorescence and a good morphology were selected to minimize autofluorescence artefacts. To count labeled cells in specific brain areas, sections were fitted into a template using defined, anatomical landmarks (anterior commissure, red nucleus, complete facial nerve, inferior olive, pyramidal decussation). The template was based on the rat brain atlas (”The rat brain in stereotaxic coordinates” George Paxinos & Charles Watson [Paxinos & Watson (2009)]). Seven different brain regions were defined and quantified: motor cortex (M1/M2), red nucleus magnocellular part (RMC), locus coeruleus (LC), oral pons (PnO), caudal pons (PnC), gigantocellular reticular nucleus (Giganto) and medullary reticular nucleus ventral part (MdV).

Anterogradely traced descending fibers

Coronal spinal cord sections were photographed at 10-fold magnification with a fluorescent microscope (Axioskop 2 MOT, Zeiss) using the Neurolucida software (Neurolucida 8.0, mbf bioscience MicroBrightField Inc.). Image acquisition in the subchronic animals was started at the rostral end of the lesion and continued for 4 mm in rostral direction, covering the spinal segments C3 and C4. In intact tissue image acquisition was started 1 mm caudal to the rostral end of C4 and was continued for 4 mm in rostral direction. In every animal, each sixth section was photographed. A grid (5x7) was overlaid as shown in Fig 4d, whose position and expansion was defined by the size and shape of the grey matter. Every intersection of a fiber with the medial and ventral side of a panel was counted. The three dimensional data volume in the rostro-caudal, dorso-ventral and medio-lateral direction was analyzed

using Matlab R2010b. Projections of the data in the dorso-ventral and mediolateral axis were done using the whole data set. For projections along the rostro-caudal axis only the three most ventral segments along the dorso-ventral axis were pooled. Absolute fiber counts were normalized by measuring the optical density of traced fibers in the lateral and ventral funiculi of the spinal segment C1 using Photoshop CS3.

Confocal characterization of close apposition-like contacts and synaptic stainings

Close apposition-like structures and colocalizations of anterogradely labelled Giganto fibers with the synaptic marker vGLUT2 were investigated using a confocal microscope with the lasers pretuned to 488 nm (ME, DyLight488), 543 nm (TMR) and 633 nm (DyLight649). Confocal image acquisition was performed using the spectral confocal microscope TCS SP2 AOBS (Leica Microsystems) with a 40-fold oil immersion objective (HCX PL APO Oil, 1.25 numerical aperture) at 4-fold zoom. The synaptic staining was investigated at maximal antibody penetration depth. Image size was defined as 1024x1024 pixels. The pinhole was set at 1 Airy unit. Triple-immunofluorescence staining was visualized with sequential acquisition of separate color channels to avoid bleed-through of fluorochromes.

Quantification of re-crossing fibers originating from C3/C4 PSNs

Coronal spinal cord sections in the cervical enlargement (spinal segment C6-C8) were photographed at 10-fold magnification with a fluorescent microscope (Axioskop 2 MOT, Zeiss) using the Neurolucida software (Neurolucida 8.0, mbf bioscience Micro- BrightField Inc.). The midline was defined by determining the middle of the central canal in each section. Fiber intersections with this midline were quantified in every sixth section. Absolute fiber counts were normalized using densitometry, as described in the previous section.

Statistics

Statistical analysis was performed using the program GraphPad Prism 4. Statistical comparison between two unrelated groups was performed using an unpaired, two-tailed Student's *t*-test. Analyses between more than two groups were done using a one-way ANOVA combined with the Bonferroni *post hoc* test. Statistics between several related groups were done using a one-way ANOVA for repeated measurements, combined with the Bonferroni *post hoc* test. Data are presented as animal

group mean values with error bars representing s.e.m. in all graphs. * $P < 0.05$; ** $P < 0.01$; *** $P < 0.001$.

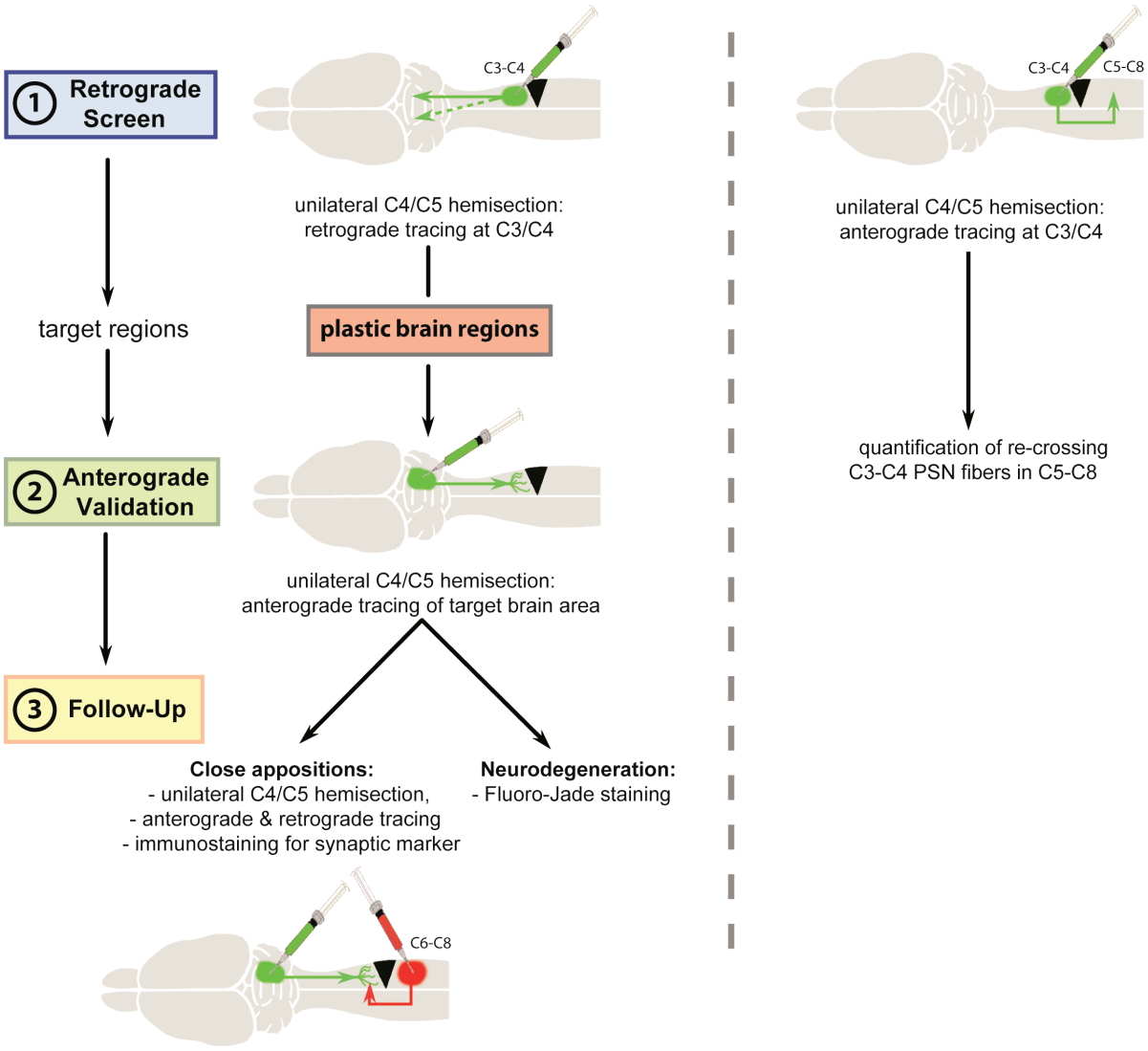

Figure 1: Experimental design of the study. In a first step, various spinally projecting brain areas were investigated for their plastic potential after a unilateral C4/C5 hemisection. A tracer was injected at the ipsilesional level C3/C4. Its retrograde component was used for the retrograde screen (1. Retrograde screen), whereas its anterograde transport was used to investigate the plastic response of propriospinal neurons (PSNs) located at spinal level C3/C4 (right side of figure). Plastic target regions from the retrograde screen were investigated in more detail by precise region-specific anterograde tracing in the brainstem (2. Anterograde validation). In follow-up experiments (3. Follow-Up), the identified regions revealing fiber plasticity rostral to the SCI were investigated in more detail by performing additional tracings and different stainings.

Results

Histological assessment of lesion completeness and tracer injections

The size and completeness of the unilateral hemisections were investigated in Nissl-stained coronal spinal cord sections in all lesioned animals. Animals with significant over- or underhemisection were excluded from the study. This is true for all sub-experiments of the study. A representative Nissl-stained C4/C5 lesion site is depicted in Fig 2b. Tracer injection sites in the brainstem and spinal cord were checked and animals with inappropriately positioned injection sites were excluded from the study.

Retrograde analysis of supraspinal projections to the ipsilesional spinal segments C3/C4

To screen distinct supraspinal descending systems for anatomical plasticity rostral to a C4/C5 unilateral hemisection, the tracer ME was injected in the spinal segments C3/C4 ipsilateral to the lesion (Fig 2c). Retrogradely labelled cell bodies were counted in distinct brain areas of intact (n = 6), acute (17 dpi, n = 7) and subchronic (43 dpi, n = 8) animals. Animals of the acute group were traced 3 days after injury, animals of the subchronic group 29 days after SCI. Cell numbers were investigated in the motor cortex (M1/M2), red nucleus (RMC), oral pons (PnO), caudal pons (PnC), gigantocellular reticular nucleus (Giganto), medullary reticular nucleus (MdV), and locus coeruleus (LC) (Fig 2d-g). The absolute cell counts for intact, acute and subchronic animals for M1/M2, RMC, PnO, PnC, Giganto, MdV and LC are shown in Fig 3 a-g.

PnC, Giganto and MdV revealed persistent anatomical plasticity in the retrograde screen

Two descending systems revealed significant plastic changes subsequent to SCI. The amount of labelled neurons in the contralesional RMC was increased in the acute phase after injury, but significantly decreased back to intact levels in subchronic animals (Fig 3b). The second system revealing significant fiber plasticity after injury was the LC. On its ipsilesional side, cell counts significantly dropped in the acute phase but increased again to nearly intact levels 43 days after injury (Fig 3g). PnC, Giganto and MdV showed persistent changes in the number of ME-positive neurons which, however, were not statistically significant. Cell numbers on the ipsilesional side of the PnC were considerably increased in subchronic animals compared to the intact and acute situation (Fig 3d). In the ipsilesional Giganto, the number of neurons in acute and subchronic animals was increased in

comparison to intact animals (Fig 3e). Cell counts in the ipsilesional MdV were unchanged between intact and acute animals, but dropped considerably in the subchronic situation (Fig 3f). The number of labelled cells in the area M1/M2 (Fig 3a) and PnO (Fig 3c) was unchanged at all time points. Although statistically not significant, the most interesting descending systems identified were the PnC, the Giganto and the MdV, as these descending systems showed persistent fiber plasticity in the C3/C4 gray matter, which correlates with the time course of motor recovery.

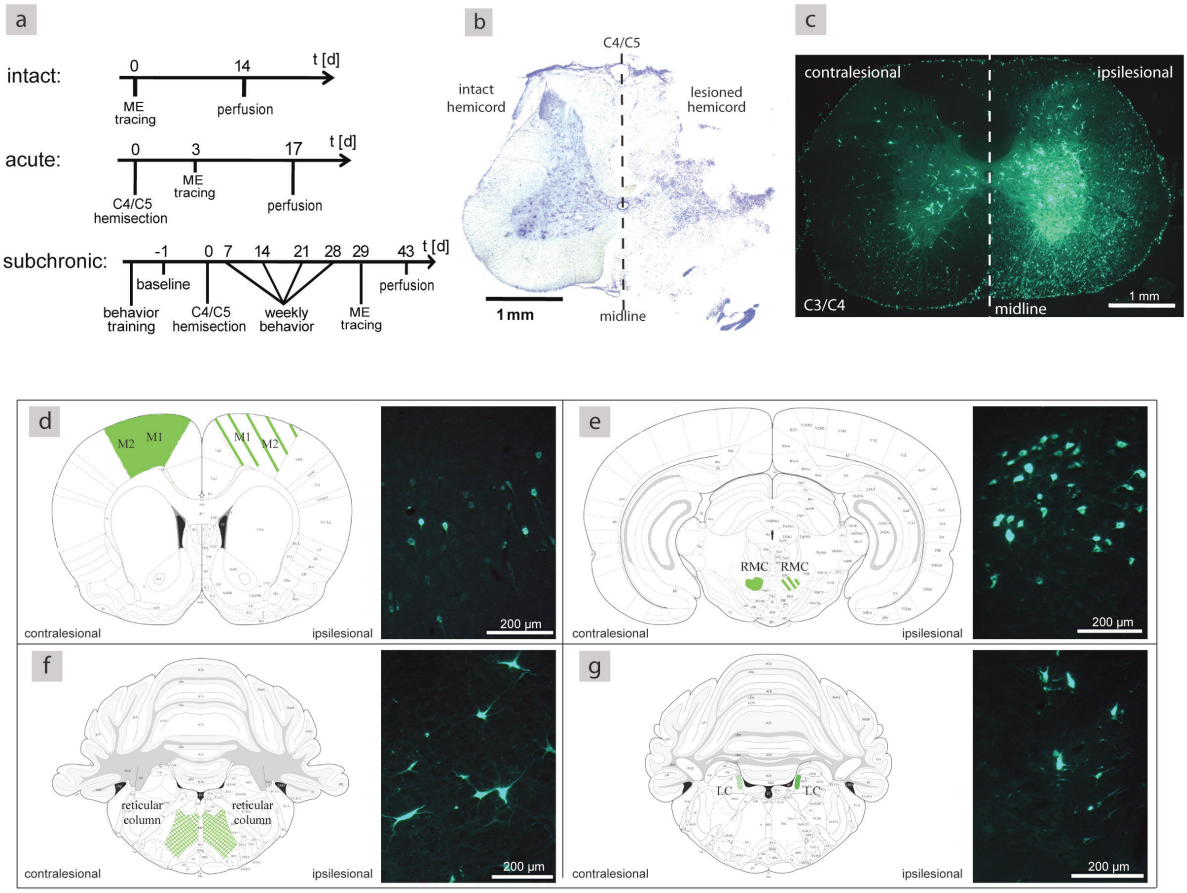

Figure 2: Retrograde tracing at ipsilesional spinal level C3/C4 to screen for plastic descending brain areas. (a) Three different animal groups (intact, acute, subchronic) were used for the retrograde screen. Intact animals were perfused 14 days after the tracing at spinal level C3/C4. Animals in the acute group were traced 3 days after a unilateral C4/C5 hemisection, whereas animals in the subchronic group were traced 29 days after injury. The animals were perfused 14 days after the tracing. In the subchronic group, behavioral analysis was performed in addition. **(b)** Representative Nissl-stained section showing a lateral C4/C5 hemisection. One hemicord is completely transected leaving the contralesional side spared. The dashed line indicates the midline. **(c)** Representative fluorescent picture of a ME injection at spinal level C3/C4. The dashed line indicates the midline. The needle penetration is positioned strictly ipsilesionally with the main injection in the intermediate and ventral portion of the gray matter. **(d-g)** Definition of counting areas in the brain. **(d)** Primary and secondary motorcortex (M1/M2) with pyramidal neurons in cortical layer V. **(e)** Red nucleus (RMC) showing traced cell bodies with mainly contralateral spinal projections. **(f)** Reticular column (RetCol). Typical ME-positive neurons in the Giganto nucleus with their large cell bodies. **(g)** Locus coeruleus (LC) showing the rather small amount of cells projecting to the spinal cord.

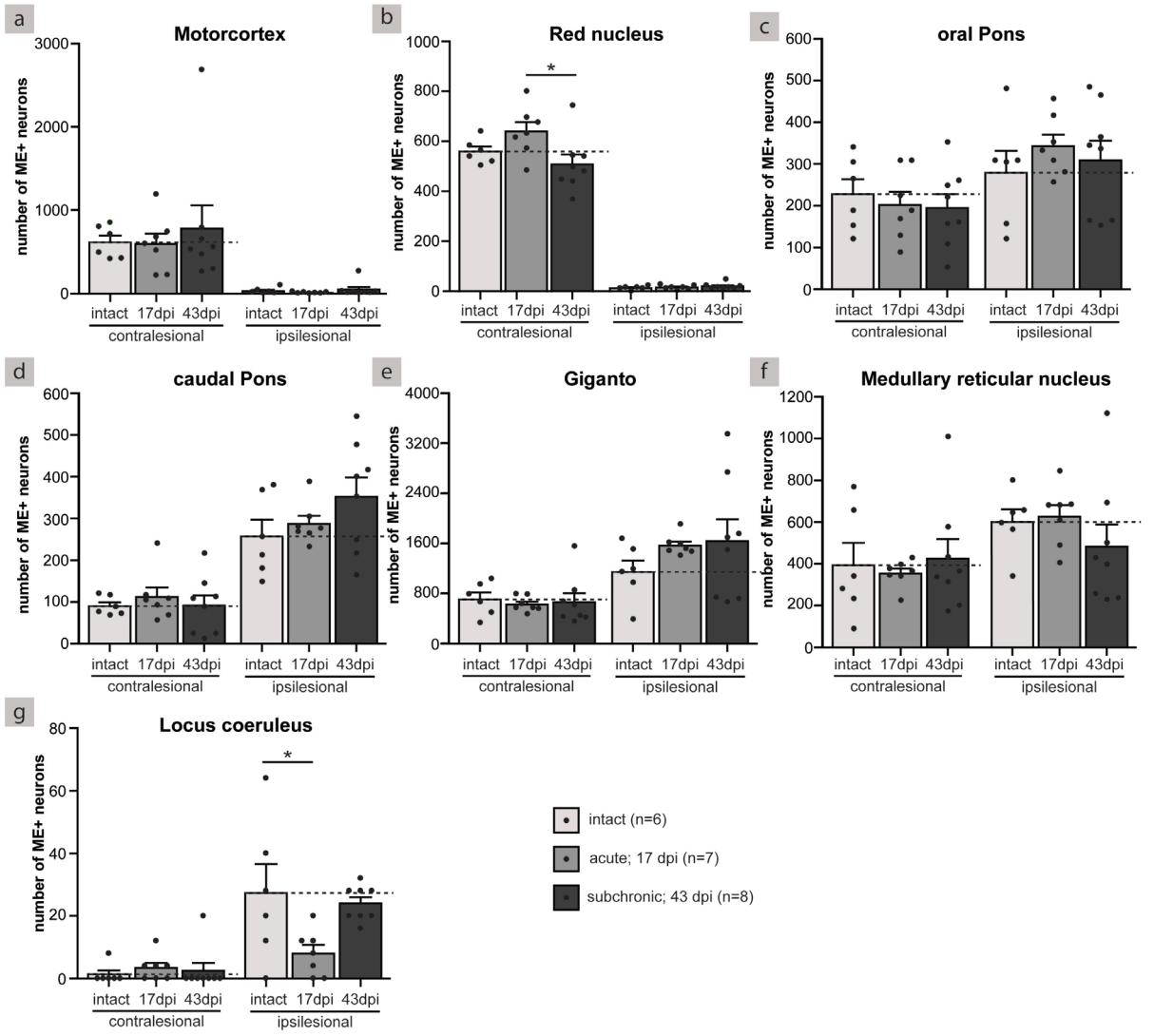

Figure 3: Quantification of ME-positive neurons in specific supraspinal brain regions. Each panel illustrates the number of ME-positive neurons on the contra- and ipsilesional side in a specific brain region in intact, acute (17 dpi) and subchronic (43 dpi) animals. Cell numbers were extrapolated to reflect the total number of cells in the specific brain area. Bar graphs are overlaid with scatter dot plots of the single animals' values. The color code and the number of animals per group are indicated in the bottom right corner. **(a)** The motorcortex revealed mainly crossing projections, showing only few cells on the ipsilesional side. There were no changes in cell counts on the contra- or ipsilesional side after the lesion compared to the intact situation. **(b)** The red nucleus (magnocellular part) also projected mainly to the contralateral hemicord. There was no change in cell numbers after the lesion on the ipsilesional side. The cell counts on the contralesional side were increased in acute animals when compared to the intact situation, but significantly decreased again in subchronic animals. **(c)** The oral pons showed a bilateral projection pattern to the spinal cord. No considerable changes in the amount of ME-positive cells occurred on the contra- and ipsilesional side after injury. **(d)** The contralesional side of the caudal pons showed no difference in the number of traced neurons over time. On the ipsilesional side there was an increase in cell numbers in subchronic animals. **(e)** The gigantocellular reticular nucleus revealed no change in the number of ME-positive neurons on the contralesional side. The amount of traced cells on the ipsilesional side was increased in acute and subchronic animals. **(f)** The contralesional side of the medullary reticular nucleus showed equal cell numbers over all time points. The amount of labelled cells on the ipsilesional side was unchanged from intact to acute animals, but was decreased in subchronic animals. **(g)** The locus coeruleus showed a strongly ipsilateral projection pattern. No change could be detected on the contralesional side over time. On the ipsilesional side, there was a decreased number of labelled neurons compared to the intact situation. The amount of cells significantly recovered back to intact level in subchronic animals. Statistical evaluation was done by One-way ANOVA with Bonferroni *post hoc* test comparing intact, 17dpi (acute) and 43 dpi (subchronic) animals on each hemisphere. All indicated error bars indicate s.e.m. * $P < 0.05$. dpi = days post injury.

Anterograde neuroanatomical tracing of PnC and Giganto

To validate the anatomical plasticity observed in the retrograde screen, precise tracer injections were performed in the identified brainstem areas. The tracer ME was injected either in the PnC or the Giganto. In order to identify appropriate injection sites in the PnC and Giganto, the retrogradely labelled cell numbers (from the retrograde screen) of intact and chronic animals were plotted over the rostro-caudal axis of the reticular column (Fig 4a). The difference in cell counts between subchronic and intact animals was used as measure of persistent fiber plasticity of the particular brainstem structure. Maximal fiber sprouting was found in rostral parts of the PnC and throughout the Giganto. Accordingly, the injection sites for the PnC and the Giganto were determined to further investigate the anatomical plasticity of these bulbospinal systems. Tracer injections were performed in intact animals ($n_{Giganto}$=4, n_{PnC}=5) and subchronic animals 29 days after SCI ($n_{Giganto}$=3, n_{PnC}=4).

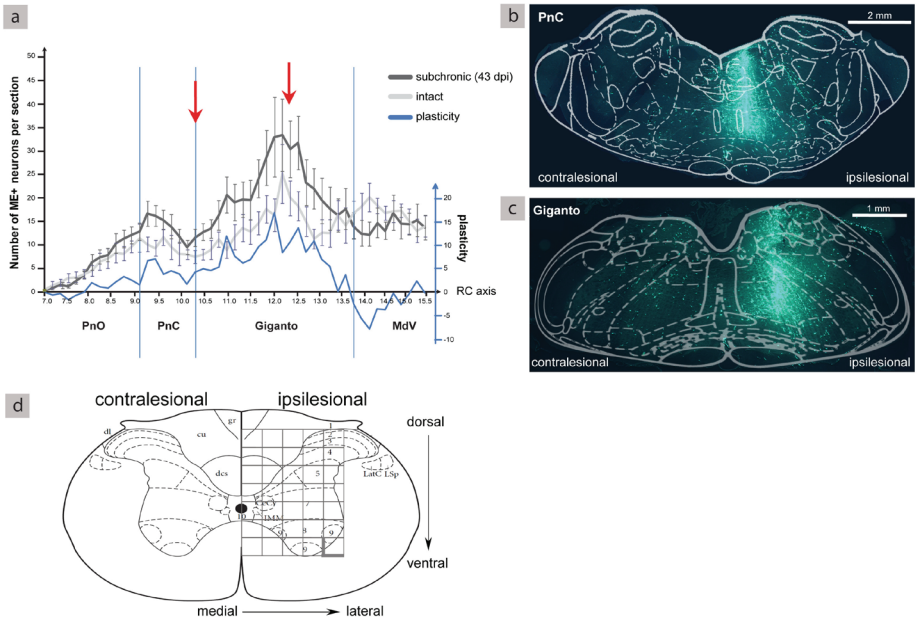

Figure 4: Anterograde bulbospinal tracing to confirm fiber sprouting rostral to the SCI. (a) Number of retrogradely labeled neurons per section along the rostro-caudal axis of the reticular column revealed by the retrograde C3/C4 tracing. The x-axis corresponds to the rostro-caudal coordinates of the Rat Brain atlas (Paxinos and Watson, 2009). The light and dark gray lines represent the number of ME-positive neurons in intact and subchronic animals respectively. The blue y-axis on the right illustrates the plasticity as difference between the number of ME-positive neurons in subchronic and intact animals (blue curve). According to these plastic maxima, the sites for the anterograde tracer injection were determined (red arrows). **(b)** Representative picture of an ipsilesional ME injection in the PnC. The fluorescent photograph is overlaid with a schematic illustration of the brainstem from the Rat Brain atlas (Paxinos and Watson, 2009). The tracer penetration is positioned strictly ipsilesionally with the main injection in the medial to upper ventral portion of the PnC. **(c)** Representative picture of an ipsilesional ME injection in the Giganto. The tracer penetration is positioned strictly ipsilesionally with the main injection in the medial to upper ventral portion of the Giganto. **(d)** Schematic representation of the grid used for quantification of fiber sprouting. The ipsilesional side of a coronal section of spinal level C3-C4 is overlayed with a 5x7 grid. The grid's expansion and positioning was defined by the maximal medio-lateral extent of the gray matter at the ventral horn and the general dorsal/ventral expansion of the gray matter. dpi = days post injury.

Histological assessment of lesion completeness and tracer injections

Size and completeness of the lesion were checked as described before. The tracer injections in the brainstem had to be positioned strictly ipsilesionally with the main injection in the medial to upper ventral portion of the PnC and Giganto (Fig 4b/c). The mean rostro-caudal injection coordinates (in relation to bregma) were 10.17 ± 0.12 mm for the PnC and 12.3 ± 0.14 mm for the Giganto.

Descending PnC fibers did not reveal sprouting rostral to the spinal lesion

Descending PnC fibers were mainly localized in the ventral and lateral portion of the ipsilesional white matter with only a few traced fibers running in the contralesional white matter. The PnC fibers mainly innervated the lateral/intermediate portion of the ventral horn (Fig 5c/e). PnC fibers were quantified over a rostro-caudal distance of 4mm starting from the rostral end of the lesion (Fig 5a). There was no significant difference in fiber density between intact and subchronic animals in any dimension (Fig 5a/c/e/g). Only a minor sprouting response of PnC fibers was detected in the medial/intermediate zone of the gray matter in subchronic animals (Fig 5e/g). Moreover, subchronic animals revealed a decreased innervation in the rostral parts of the spinal segments C3/C4 being in vicinity of the lesion. The number of fibers reached a plateau at 2.4 mm distance from the rostral lesion end, which was significantly higher than in close proximity to the lesion. However, there was no significant difference between subchronic and intact animals when directly comparing corresponding points along the rostro-caudal axis (Fig 5a). The absence of major plastic changes was further confirmed by quantification of fibers in the dorso-ventral (Fig 5c) and medio-lateral (Fig 5e) axis. A heating plot summarizing the 4 mm rostro-caudal distance rostral to the lesion depicted also only a minor sprouting response of PnC fibers (= ME-positive fibers in subchronic animals - ME-positive fibers in intact animals) upon SCI (Fig 5g). The only significant increase in sprouting was found in the dorsal horn at the border between gray and white matter, but the absolute fiber changes were minor (blue color).

Giganto fibers showed massive sprouting rostral to the lesion

Descending Giganto fibers were found to run mainly in the ventral and lateral portion of the ipsilesional white matter. In contrast to the PnC, a considerable fraction of traced fibers descended also in the ventral and dorsolateral funiculi of the contralesional white matter, which is in line with the projection pattern found in the retrograde screen. The innervation pattern of the descending Giganto fibers covered the lateral portion of the ventral horn, which is similar to PnC projections (Fig 5d/f).

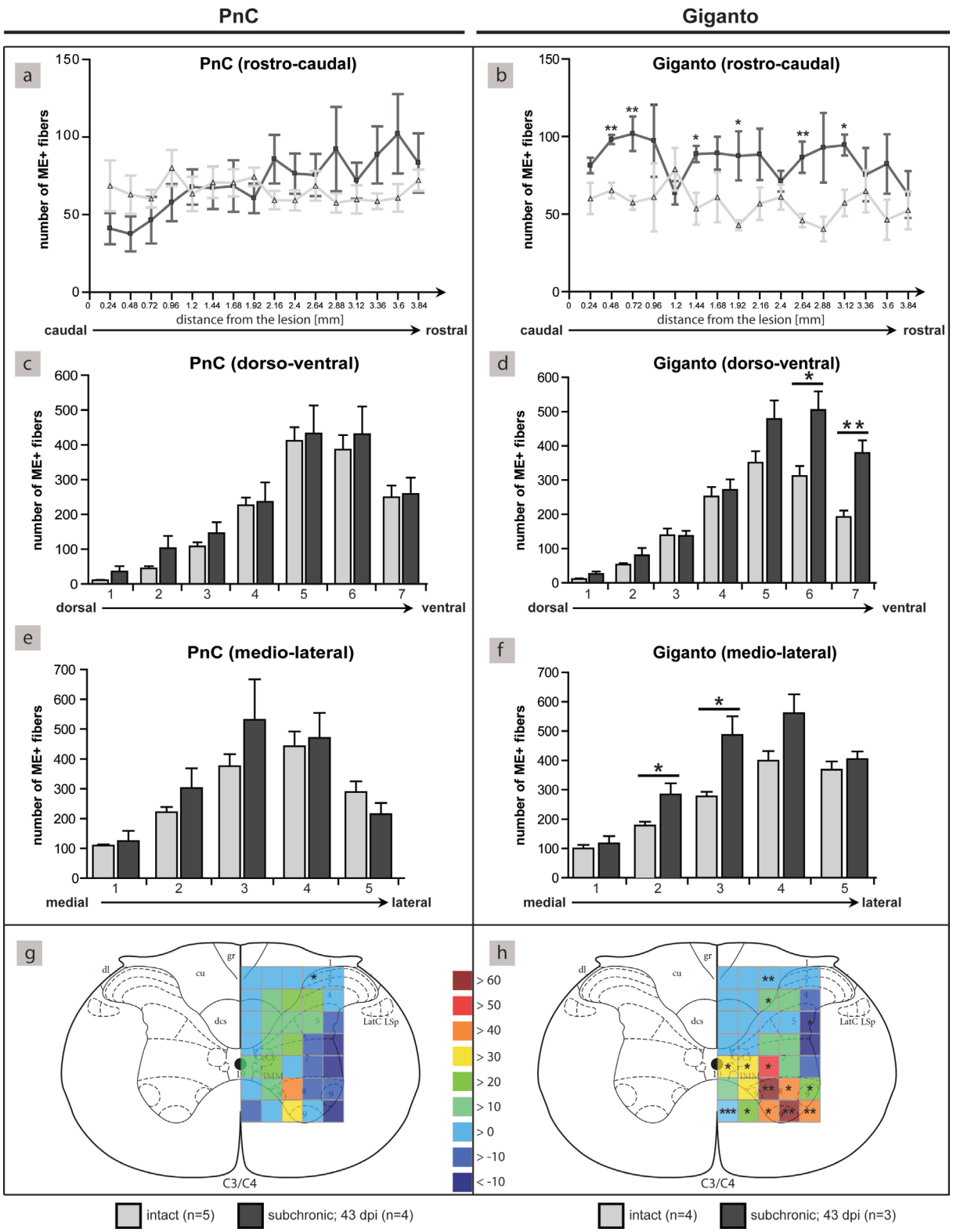
PnC
Giganto
a
PnC (rostro-caudal)
number of ME+ fibers
distance from the lesion [mm]
caudal
rostral
b
Giganto (rostro-caudal)
c
PnC (dorso-ventral)
dorsal
ventral
d
Giganto (dorso-ventral)
e
PnC (medio-lateral)
medial
lateral
f
Giganto (medio-lateral)
g
h
dl
cu
gr
dcs
LatC LSp
IMM
C3/C4
> 60
> 50
> 40
> 30
> 20
> 10
> 0
> -10
< -10
intact (n=5)
subchronic; 43 dpi (n=4)
intact (n=4)
subchronic; 43 dpi (n=3)

Figure 5: Quantification of fiber sprouting at spinal level C3/C4. The left column of this figure depicts projections of the data volume in the three single dimensions for PnC fiber density. The right column shows the corresponding results for the Giganto. Light gray represents the intact and dark gray the subchronic situation (43 dpi). **(a)** Quantification of PnC fiber sprouting along the rostro caudal axis at spinal level C3/C4. The x-coordinate 0 was aligned to the rostral end of the lesion. There was no significant change in the number of PnC fibers between intact and subchronic animals. **(b)** Quantification of Giganto fiber sprouting at spinal level C3/C4 along the rostro-caudal axis. Fiber counts were increased along the rostro-caudal axis with several significant differences (indicated by stars). **(c)** Quantification of PnC fibers along the dorso-ventral axis. There was no significant change in the fiber counts in the dorso-ventral dimension. **(d)** Quantification of Giganto fibers along the dorso-ventral axis. The dorso-ventral segments 5, 6 and 7 of the grid revealed increased levels of fibers in subchronic animals. **(e)** Quantification of PnC fibers in the medio-lateral dimension. No significant changes in the number of PnC fibers were detected between intact and subchronic animals. **(f)** Quantification of Giganto fibers in the medio-lateral dimension. Segments 2, 3 and 4 showed increased fiber sprouting in chronic animals. **(g)** Heating plot summarizing the changes in the number of PnC fibers in the medio-lateral and dorso-ventral dimension at spinal level C3/C4. Absolute changes in the number of fibers per region were minor. **(h)** Heating plot of Giganto fibers at spinal level C3/C4. Absolute changes in the number of fibers were much more pronounced compared to the PnC. A large and statistically significant increase in the number of Giganto fibers occurred throughout the whole ventral horn. Statistical evaluation was done by Student`s *t*-test (two tailed, paired) comparing corresponding data between intact and subchronic animals. Error bars indicate s.e.m. * $P < 0.05$, ** $P < 0.01$, *** $P < 0.001$. dpi = days post injury.

There was a pronounced sprouting of Giganto fibers rostral to the lesion in subchronic animals when compared to intacts (Fig 5b/d/f/h). The fiber innervation was significantly increased in ventral and medial/intermediate segments of the gray matter in subchronic animals (Fig 5d/f). The heating plot displayed a maximal sprouting response of Giganto fibers in the ventro-lateral gray matter, coinciding with the primary entry zone of descending Giganto fibers (Fig 5h). Additionally a slight increase in sprouting could be observed at the gray/white matter border in the dorsal column and in the white matter of the ventral funiculus. However, the absolute changes in these areas were small, as indicated by the blue coloring.

Sprouting Giganto fibers were colocalized with the synaptic marker vGLUT2

Retrograde and anterograde tracing revealed a persistent increase in sprouting Giganto fibers rostral to the lesion. In order to investigate the functional properties of these fibers, an anterograde tracing of the Giganto nucleus was combined with immunohistochemical stainings for the synaptic marker vGLUT2. Colocalization of vGLUT2 with ME-positive fibers was frequently found in the spinal segments C3/C4 (Fig 6c/f). Colocalizations were identified both along running fibers (en passant) and on terminals of labelled fibers.

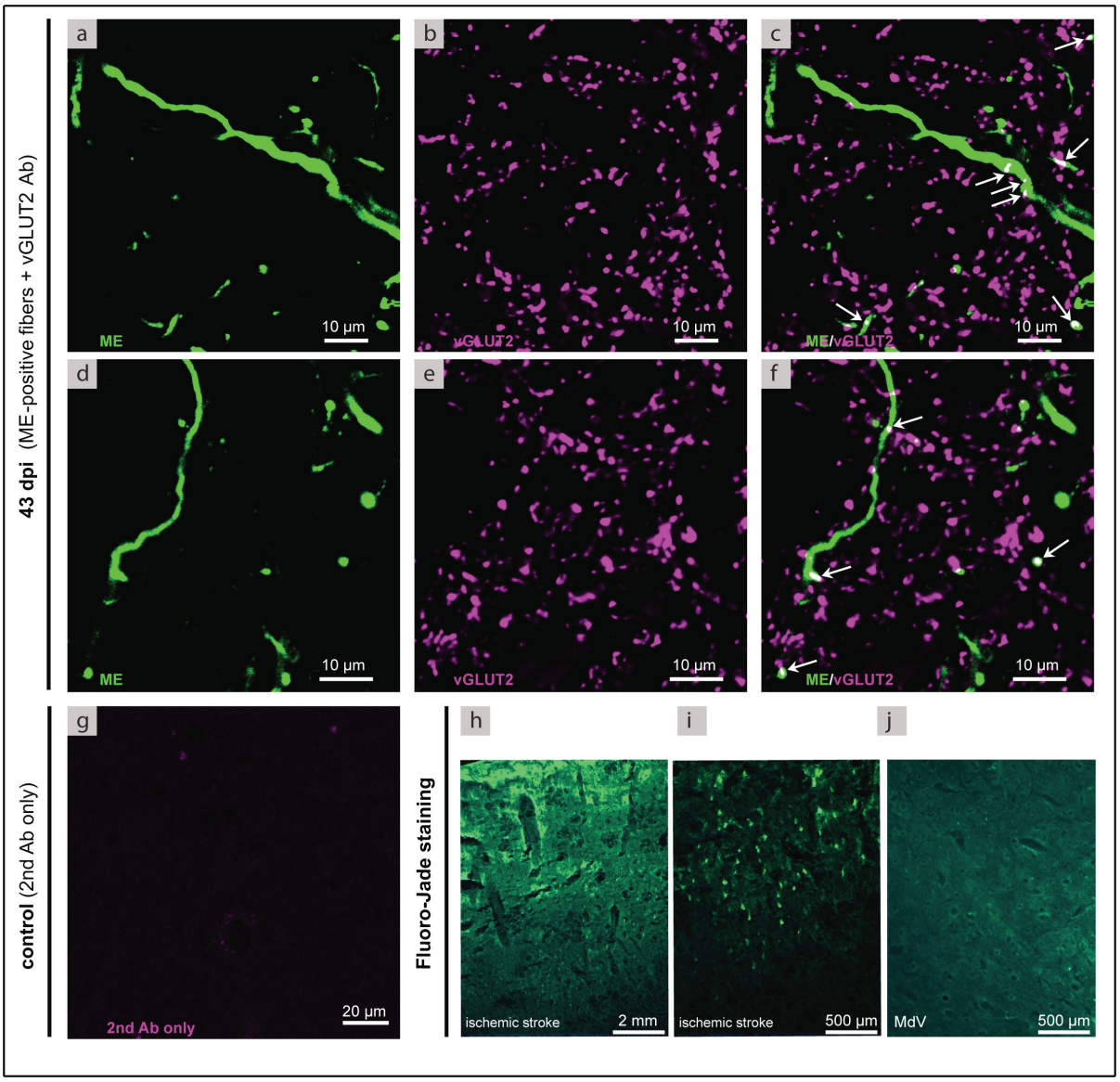

Figure 6: Colocalization of descending Giganto fibers with vGLUT2 at spinal level C3/C4. (a,d) Anterogradely traced Giganto fibers in the ventral horn at spinal level C3/C4. In order to see continuous fibers, the ME tracing was reinforced with a Dylight488 Streptavidin. **(b,e)** Immunohistochemical staining against vGLUT2. The staining results in specifically labelled synaptic terminals with minimal background. **(c,f)** Merged representative pictures showing ME-positive Giganto fibers (green) and the staining against vGLUT2 (purple). Colocalizations of the synaptic staining with ME-positive fibers resulted in white dots (indicated by white arrows). Colocalizations could be identified along fibers (en passant) and at fiber endings (terminals). **(g)** Negative control staining with secondary antibody only. No signal was obtained in the control, showing high specificity of the secondary antibody. **(h)** Fluoro-Jade staining of ischemic penumbra tissue after an endothelin-1 induced stroke in M1/M2. A high background can be seen directly in the ischemic tissue. **(i)** Higher magnification of the ischemic penumbra revealed multiple Fluoro-Jade positive cell bodies and axons. **(j)** No Fluoro-Jade positive cells were found in the MdV 43 days after a cervical unilateral C4/C5 hemisection. dpi = days post injury.

Sprouting Giganto fibers form close apposition-like contacts with C3-C4 PSNs

Immunohistochemical stainings against vGLUT2 indicated a synaptic integration of sprouting Giganto fibers at spinal level C3/C4 (Fig 6). To investigate the possible cellular targets of the sprouting Giganto

fibers, the tracer TMR was injected ipsilesionally on spinal levels C6 to C8 (Fig 7a). The injections in the cervical enlargement (C6 to C8) were positioned in the medial to ventral portion of the gray matter (Fig 7a). This tracing was performed in the same animals which received a ME injection in the Giganto nucleus. The combination of the anterograde tracing (ME) and a retrograde tracing (TMR) allowed a direct assessment of close appositions between descending Giganto fibers and PSNs, which bridge the lesion site and innervate the ipsilesional cervical enlargement. First, the localization of traced PSN somata was determined in coronal sections of spinal level C3/C4. TMR-positive cells were located in the ventral horn, primarily in Rexed's laminae VII, VIII and IX. Interestingly, this is the region of maximal Giganto sprouting after SCI (Fig 7b). Close apposition-like contacts between descending ME-positive fibers and TMR-positive dendrites or somata were frequently found. Most colocalizations were positioned on apical dendrites (Fig 7h). Only few connections were localized directly on the cell soma (Fig 7e). To assess the functional integration of the close apposition-like structures, ME/TMR doubled traced sections were stained for vGLUT2 (Fig 7i-l). Triple colocalization of the tracers TMR and ME with the antibody directed against vGLUT2 was evident in most cases of TMR/ME double colocalizations (Fig 7l).

C3-C4 PSNs increased their re-crossing fibers to the ipsilesional spinal segments C5 to C8

After showing a direct innervation of C3-C4 PSNs by Giganto fibers, the projection pattern of the PSNs was investigated in more detail. The anterograde aspect of the ME tracing in the spinal segments C3/C4 was analyzed for this purpose. ME-positive midline crossing fibers were counted in the spinal segments C5 to C8 caudal to the hemisection in acute (17 dpi, n = 8) and subchronic (43 dpi, n = 6) animals. Quantification revealed a strong and statistically significant increase in the number of midline re-crossing fibers in subchronic animals (Fig 7m). A more detailed analysis of midline re-crossing fibers showed no differences between specific cervical spinal segments (Fig 7n). Midline re-crossings C3-C4 PSN fibers were significantly increased at every investigated spinal level.

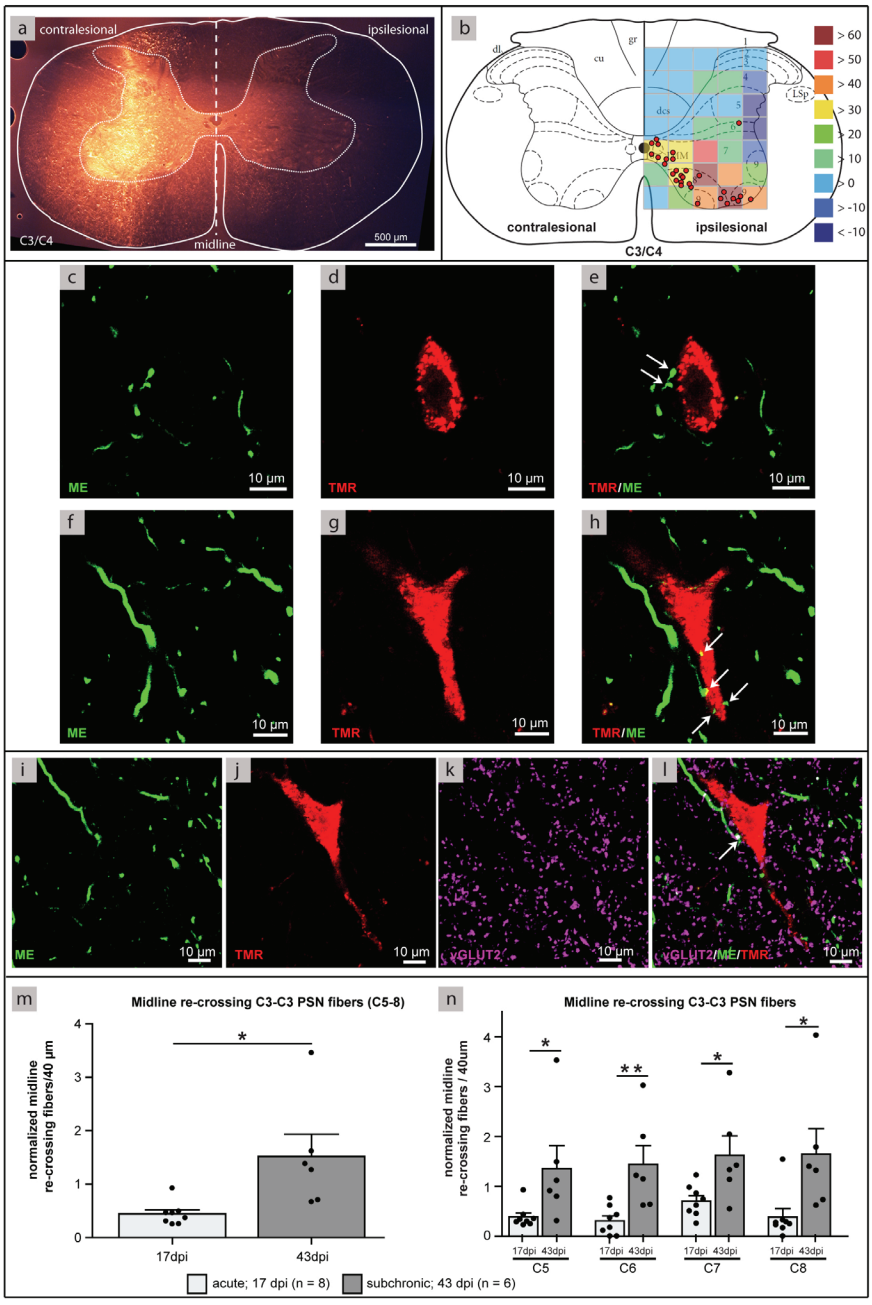

Figure 7: Recrossing C3-C4 PSNs are innervated by sprouting Giganto fibers. **(a)** Representative TMR injection site at spinal level C6. The TMR penetration was positioned strictly ipsilesionally with the main injection in the intermediate and ventral portion of the gray matter. **(b)** Overlay of the re-crossing C3-C4 PSNs with the heating plot displaying the Giganto fiber sprouting at spinal level C3/C4. Almost all re-crossing C3-C4 PSNs were locate in the ventral gray matter (Redex's lamina VII, VIII and IX), strongly correlating with the area of maximal sprouting of Giganto fibers in subchronic animals. **(c-h)** Representative pictures revealing close appositions between ME-positive Giganto fibers (green) and TMR-positive re-crossing PSNs (red) at spinal level C3/C4 in subchronic animals. **(c,f)** Anterogradely traced Giganto fibers in the ventral horn at spinal level C3/C4. **(d,g)** TMR positive re-crossing PSN cell body located in the ventral horn at spinal level C3/C4. **(e,h)** Merged pictures of ME-positive Giganto fibers and TMR-positive PSNs. Close apposition-like contacts of Giganto fibers onto re-crossing C3-C4 PSNs were frequently found (indicated by white arrows) on the apical dendrites, but also directly on the soma. **(i-l)** Staining of close apposition-like contacts with vGLUT2. **(i)** Representative picture of Giganto fibers and **(j)** TMR-positive re-crossing PSN cell body located in the ventral horn at spinal level C3/C4. **(k)** Staining against vGLUT2 resulted in specifically labelled synaptic terminals with minor background. **(l)** Merged pictures showing colocalization of the close apposition-like contacts with vGLUT2 (white arrows) demonstrating synaptic connections between Giganto fibers and re-crossing C3-C4 PSNs. **(m-n)** Quantification of midline re-crossing PSNs fibers at spinal level C5 to C8 in acute (17 dpi) and subchronic (43 dpi) animals. **(m)** The number of midline re-crossing C3-C4 PSN fibers was highly increased in the cervical enlargement of subchronic animals when compared to the acute situation. **(n)** Segment-specific analysis of midline re-crossing C3-C4 PSN fibers. No segment-specific differences in midline re-crossing fibers can be detected. Statistical evaluation was performed by Student`s *t*-test (two-tailed, paired) comparing corresponding data between acute and subchronic animals. Error bars indicate s.e.m. * $P < 0.05$, ** $P < 0.01$. dpi = days post injury.

No neurodegeneration occurred in the MdV

The retrograde screen identified an obvious decay in the number of labelled neurons in the MdV. A Fluoro-Jade staining was performed to investigate neurodegenerative processes as possible reason for the decrease of labelled MdV cells. Coronal sections of ischemic stroke tissue (positive control for the staining) and the MdV were stained with Fluor-Jade. Fluoro-Jade staining in MdV sections revealed no labeled cells or axons in subchronic animals (Fig 6j). In the ischemic stroke tissue, however, Fluoro-Jade staining resulted in specifically labelled cells in the penumbra (Fig 6i). The lesion site itself was characterized by a massive non-specific background (Fig 6h). Therefore, although the staining protocol seemed to work in ischemic tissue, no Fluoro-Jade positive neurons were found in the MdV.

Discussion

The present study investigated the anatomical plasticity of descending supraspinal systems and intraspinal circuitries after incomplete cervical SCI. Neuroanatomical tracings revealed an increased sprouting of severed Giganto fibers rostral to a unilateral C4/C5 hemisection. These sprouts were still apparent 43 days after axotomy and seemed to be synaptically integrated, as revealed by immunostainings for vGLUT2. The sprouting Giganto fibers were frequently found to contact apical dendrites or somata of PSNs located at spinal level C3/C4. These PSNs were shown to form re-crossing fibers around the lesion site and to innervate the ipsilesional cervical enlargement. Interestingly these re-crossing projections were significantly increased in subchronic animals when compared to acute ones. Therefore we hypothesize that the sprouting Giganto fibers connect to PSNs rostral to the lesion, which in turn bridge the information to denervated spinal regions.

Retrograde screening identified persistent anatomical plasticity in specific supraspinal descending systems following incomplete cervical SCI

Seven supraspinal regions (M1/M2, RMC, PnO, PnC, Giganto, MdV and LC) were screened for anatomical plastic responses following SCI by retrograde tracer injection rostral to the lesion. To confirm the unilaterality of tracer injections and the validity of the defined brain regions, the absolute cell numbers and projection patterns of single nuclei were compared with the literature. Considering the different tracing efficiencies, the results obtained in the retrograde screen corresponded well to counts from former studies (B.Zörner, unpublished data) and to the literature (Ghosh *et al.,* 2010). The projection patterns of the investigated supraspinal systems were also in line with the literature (CST: Weidner *et al.,* 2001; RST: Kuchler *et al.,* 2002; LC: Nygren and Olson, 1977; unpublished observations).

The investigated brain regions displayed different reactions in response to a unilateral spinal cord hemisection. Variable plastic responses (i.e. atrophy/cell death of soma; sprouting/retraction of fibers) of different systems to axotomy are well described in the literature and are usually hypothesized to result from different intrinsic properties of the respective neurons (Plunet *et al.,* 2002). Regeneration-associated proteins, trophic factors and their receptors have variable expression patterns in different supraspinal systems (Tobias *et al.,* 2003). Moreover, various studies have also shown that the plasticity of a particular system strongly depends on the distance to the lesion site, which could also differently affect the various supraspinal systems (Fernandes *et al.,* 1999; Giehl and Tetzlaff, 1996).

M1/M2 and PnO showed no plastic response after the spinal injury. Generally, the CST has been shown to be a rather plastic system in the rat (Fouad *et al.,* 2001; Weidner *et al.,* 2001; Ghosh *et al.,* 2009) and non-human primate (Kaeser *et al.,* 2010; Rosenzweig *et al.,* 2010). Sprouting of CST fibers in rats has been detected spontaneously (Ghosh *et al.,* 2009; Bareyre *et al.,* 2004; Pallini *et al.,* 1988) and after treatment (inhibition of Nogo (Ghosh *et al.,* 2009; Wiessner *et al.,* 2003); exogenous neurotrophic factors (Zhou and Shine, 2003); training (Maier *et al.,* 2008); electrical stimulation (Brus-Ramer *et al.,* 2007)). The studies which demonstrated spontaneous sprouting of axotomized CST fibers (Ghosh *et al.,* 2009; Bareyre *et al.,* 2004), however, used different lesion paradigms, different areas of investigation and distance from the lesion, rendering a direct comparison of the results difficult. Moreover, it has been shown that CST fibers display a pronounced progressive retraction after axotomy, resulting in about 2.5 mm distance retraction from the lesion after 56 days (Pallini *et al.,* 1988). Due to a massive retraction of CST fibers, the region of tracer injection might have missed the area of the main CST sprouting. To our knowledge, there are no studies which have investigated the plastic potential of the PnO after any type of CNS lesion.

In the contralesional RMC the cell counts were increased in acute animals when compared to the intact situation. In subchronic animals, however, the number of ME-positive neurons was significantly decreased again (back to intact levels). These results might indicate an initial sprouting response of the RMC acutely after the lesion. The newly formed sprouts, however, did not persist up to the subchronic phase after injury. This pruning effect might be activity-dependent due to missing functional connections (Luo and O'Leary, 2005; Maier and Schwab, 2006). The absence of persistent plasticity in the RMC is in line with the literature, where no spontaneous sprouting response of rubrospinal fibers was detected up to 31 weeks after injury (Hendriks *et al.,* 2006). Due to their very chronic point of investigation, Hendriks *et al.* probably missed the transient sprouting response acutely after SCI, as detected in this study.

The LC revealed a significantly decrease in cells in acute animals, which recovered back to intact levels in the subchronic phase after SCI. The LC is a neuromodulatory, noradrenergic, globally projecting system (Nygren and Olson, 1977). Several studies have identified the LC as plastic system after different forms of CNS insults (Nygren and Olson, 1977; Fritschy and Grzanna, 1992). Due to the ipsilateral projection pattern of the LC to the spinal cord, a hemisection at C4/C5 would axotomize a large fraction of the nucleus' spinal projections. The high impact of the lesion on this system might explain the acutely very pronounced decrease in labelled cells as 'initial shock' of the system. The

observed recovery of cell numbers at the subchronic time point might reflect the plastic potential of the LC. However, the results obtained for the LC have to be interpreted with caution, since the number of cells in the LC is limited and the nucleus reveals some degree of autofluorescence, which can impede specific cell counting.

Even though cell counts of the ipsilesional PnC, Giganto and MdV showed no statistically significant changes, these supraspinal regions were the most interesting ones regarding their persistent anatomical plasticity. It is assumed that sprouts which are functionally integrated into neural networks are more stable. Unspecific connections might be removed and retracted again, according to the activity-dependent pruning paradigm (Luo and O'Leary, 2005). The Giganto is mainly thought to control parameters of basic locomotion such as muscle tonus, balance and rhythmicity (Peterson, 1979; Wang, 2009). The pontine reticular nuclei (PnC and PnO) are also thought to play a major role in the guidance of crude motor functions. Studies performing electrical stimulation have proven that both systems produce motor-relevant output (Siegel, 1979). However, there is no knowledge about the plastic response of these descending systems upon SCI.

Labelled neurons in the ipsilesional MdV decreased to about 80% of intact levels in subchronic animals. This could be explained by different mechanisms: Different supraspinal tracts show different susceptibilities to axonal retraction after axotomy. To our knowledge, this has not yet been specifically investigated for MdV projections. The tract could retract very far, and thus a potential sprouting response was not targeted by the retrograde tracing. Alternatively the MdV fibers could undergo excessive activity-dependent pruning, leading to a strongly diminished tracer uptake. Neurodegenerative processes of ipsilaterally descending MdV neurons (i.e. cell death) were not observed, as revealed by the Fluoro-Jade staining. However, Fluoro-Jade is probably not sensitive for all types of neurodegeneration (Schmued *et al.,* 1997; Schmued and Hopkins, 2000).

Anterograde tracing confirmed increased sprouting of Giganto fibers, but not of PnC fibers after injury

The neuroanatomy of the descending PnC and Giganto fibers and their spinal innervation patterns were in line with the previous literature (Matsuyama *et al.,* 2004a; Ballermann and Fouad, 2006).

Quantification of anterogradely traced PnC fibers revealed no significant changes in the innervation or density of fibers rostral to the lesion. A single significant sprouting response could be detected at the border between gray and white matter in the dorsal horn. Since the PnC in fact does not project to the

dorsal column, this effect is most probably an artefact, which could be supported by the small change in absolute cell numbers.

A possible reason for the varying results of the retrograde and anterograde tracing is that the tracer injection in the PnC was localized at the very caudal end of the PnC, which disclosed less fiber sprouting in the retrograde screen. The difference between the theoretical and the actual penetrations in the pons was probably mainly due to a deflection of the canula by membranes covering the cerebellum and the brainstem. In summary the anterograde tracing data did not confirm the increased sprouting of PnC fibers after SCI, which was observed after the retrograde C3/C4 tracing. Therefore it has to be concluded that the caudal PnC does not display anatomical plasticity in response to an incomplete cervical SCI.

Quantification of Giganto fibers rostral to the lesion displayed a massive sprouting reaction in subchronic animals. Fiber counts were nearly doubled within the ventral gray matter throughout the whole rostro-caudal distance of 4 mm above the lesion site, thus confirming the results obtained in the retrograde screen. Data projection in the dorso-ventral axis revealed nearly doubled fiber counts in the ventral horn of subchronic animals, but no plasticity of fibers in the dorsal and intermediate segments of the gray matter. The heating plot confirmed the sprouting pattern already obtained from the single dimension graphs. The main sprouting response of severed Giganto fibers was located in the intermediate region of the ventral horn. As for the PnC, changes in the dorsal horn are difficult to interpret, since Giganto fibers usually do not descend in the dorsal column. Despite the statistical significance, there were only low changes of absolute fiber numbers in these areas. In summary, the anterograde tracing of the Giganto nucleus confirmed the increased fiber innervation rostral to the injury revealed by the retrograde tracing.

Sprouting Giganto fibers synaptically integrate into the spinal circuitry

In order to investigate the functionality of the sprouting Giganto fibers, spinal cord sections of subchronic animals were stained for the presynaptic marker vGLUT2. Several publications showed that vGLUT2 is expressed by most bulbospinal neurons (Hagglund *et al.,* 2010). Additionally, the Allen Brain Atlas (Paxinos and Watson, 2009) confirmed the presence of the corresponding mRNA in the Giganto. The synaptic staining resulted in specific and intense labelling of presynaptic terminals whose size (about 1 µm) corresponded to the literature (Maier *et al.,* 2008). Indeed colocalizations of vGLUT2

boutons with Giganto fibers were frequently detected in the ventral gray matter of the spinal segments C3/C4. In general two different types of colocalizations were visible: On the one hand synapses were localized along running fibers, representing en-passant boutons. On the other hand collocalizatinos were localized at the end of fibers, indicating synaptically active axon terminals. The synaptic colocalization of Giganto fibers indicate that these fibers not only sprout upon a spinal insult, but that they functionally integrate into the spinal network.

Rewiring of Giganto fibers onto relaying C3-C4 PSNs

To disclose the cellular targets of the vGLUT2-positive Giganto fibers, a retrograde tracing of the ipsilesional cervical spinal segments C6 to C8 was performed in subchronic animals. Since the lesions were checked for their completeness, the labelled PSNs in the ipsilesional spinal segments C3/C4 had to be re-crossing fibers, which cross the midline rostral to the lesion, bypass the lesion site and cross the midline again caudally, thereby forming a bridge around the hemisection. Interestingly, the localization of these traced PSNs in the gray matter matched exactly the area of major sprouting of descending Giganto fibers. The detected localization of PSNs in the gray matter is in agreement with previous findings (Vavrek *et al*., 2006*)*. Confocal analysis revealed frequent close apposition-like contacts between Giganto fibers and the PNSs, mostly on its apical dendrites. These close appositions were often colocalized with vGLUT2, suggesting the formation of synaptic contacts. The concept of intraspinal bridging was previously observed for different descending tract systems (Bareyre *et al.,* 2004; Vavrek *et al.,* 2006; Courtine *et al.,* 2008). Bareyre *et al.* showed that a thoracic dorsal hemisection led to collateral sprouting of severed hindlimb CST fibres within the cervical enlargement. The sprouts formed specific connections with long descending PSNs, which innervated the lumbar spinal enlargement, thereby bridging cortical commands around the lesion site to their former target areas. After a more severe thoracic spinal cord injury (only sparing the ventral quadrant), Vavrek *et al.* observed the same effect as Bareyre, but only after intracortical application of the neurtrophic factor BDNF. Courtine *et al.* observed that PSNs directly rostral to a thoracic unilateral hemisection sprouted within the ipsilesional lumbar spinal cord caudal to the lesion. However, a specific rewiring of locomotor-relevant bulbospinal fibers onto intraspinal networks has not been shown so far.

Relaying C3-C4 PSNs enhance their midline re-crossing fibers upon hemisection

The main message by Courtine and colleagues was that intraspinal relays were crucial to induce spontaneous locomotor hindlimb recovery in the absence of direct supraspinal command to the lumbar spinal cord. Therefore we investigated the question, if the C3-C4 PSNs not only received specific Giganto input, but also showed plastic changes themselves. After anterograde tracing of the ipsilesional C3/C4 spinal cord, we counted midline re-crossing fibers in the cervical enlargement (C5 to C8). The averaged values of midline re-crossing fibers were strikingly increased in the cervical enlargement of subchronic animals when compared to acute animals. This increase in midline re-crossing C3-C4 PSNs fibers might further amplify the transmission of supraspinal commands to the ipsilesional spinal segments C5 to C8. In contrast, only minor projections from the C3-4 PSNs were found in the lumbar spinal cord (data not shown) indicating that the C3-C4 neurons relay supraspinal commands mainly to the cervical enlargement.

Correlation to spontaneous motor recovery after SCI

Spontaneous functional recovery of animals with a cervical unilateral hemisection is well investigated in the literature (Webb and Muir, 2002; Filli *et al.,* 2011). This lesion leads to a Brown-Séquard syndrome, which is characterized by ipsilesional motor weakness or paralysis and loss of proprioception with contralesional deficits in pain and temperature sensation (Little and Halar, 1985; Roth *et al.,* 1991). The crude pattern of functional recovery in rats consists of substantial recovery of hindlimb functions, but only marginal motor recovery of forelimb functions, leaving the upper extremities severely impaired or fully paralyzed. The timeline of plastic anatomical changes in this study is well correlated with the time course of functional recovery. However, the anatomical plasticity does not directly match the pattern of functional recovery in that the relay primarily leads to an innervation of the ipsilesional cervical enlargement, but the motor recovery of the respective forelimb is limited. The exact innervation pattern of C3-C4 PSN fibers have not been investigated in detail yet. It appeared as if the re-crossing PSN fibers innervated the ventro-medial portions of the ipsilesional gray matter in spinal segments C5 to C8. This would correlate to the location of long-projecting PSNs which project to the lumbar spinal cord (Vavrek *et al.,* 2006). Direct innervation of motoneurons by PSN fibers was not observed. Therefore, we can not exclude that C3-C4 PSNs reconnect to long descending PSNs within the cervical enlargement, which in turn project to lumbar spinal areas relevant

for hindlimb locomotion. Further electrophysiological and anatomical investigations are planned to disclose the spinal connections and their relevance for motor recovery.

Besides the C3-C4 PSN bridge, our lab has shown that alternative mechanisms such as spontaneous compensatory sprouting of contralesional descending Giganto fibers can lead to motor improvements in rats with the C4/C5 unilateral spinal cord hemisection (B. Zörner, unpublished data). Thus, in order to make specific statements about the functional role of the C3-C4 PSN relay, this neuronal pool has to be investigated using more sensitive techniques, such as electrophysiology or specific functional ablation of this neuronal population.

Conclusion

Anatomical plasticity was shown to occur at two different levels in the CNS following cervical unilateral hemisection in adult rats. A combination of retro- and anterograde tracing demonstrated massive persistent sprouting of severed descending reticulospinal fibers rostral to the lesion site up to 43 days after injury. These sprouts were colocalized with vGLUT2, indicating their synaptic integration into the spinal network. The fibers originating from the Giganto rewired to ipsilesional C3-C4 PSNs, which projected re-crossing fibers to the sublesional cervical enlargement. Close apposition-like structures between Giganto fibers and C3-C4 PSNs were found on the apical dendrites and somata. Most of these contacts were colocalized with vGLUT2, suggesting the formation of synaptic connections. This remodelling of supra- and intraspinal networks leads to a relay of Giganto commands to the denervated target areas via PSNs. A direct bridging of supraspinal commands through re-crossing PSN fibers has the advantage that the numerous supraspinal systems do not have to undergo massive reorganizations of their spinal projection after the unilateral SCI. Their severed fibers can innervate the intraspinal relay which in turn bridges the commands around the lesion site. Anatomical plasticity was further disclosed at the intraspinal level. Ipsilesional C3-C4 PSNs increased their re-crossing projections to the cervical enlargement in subchronic animals as compared to acute animals, thereby amplifying the bridging effect. The functional relevance of this newly formed detour pathway has to be investigated by further experiments.

References

Afshari FT, Kappagantula S & Fawcett JW. Extrinsic and intrinsic factors controlling axonal regeneration after spinal cord injury. Expert Rev Mol Med. 2009; 11, e37.2.

Alstermark B, Isa T, Pettersson LG & Sasaki S. The C3-C4 propriospinal system in the cat and monkey: a spinal pre-motoneuronal centre for voluntary motor control. Acta Physiol (Oxf). 2007; 189(2), 123–140.

Alstermark B, Lindstrom S, Lundberg A & Sybirska E. Integration in descending motor pathways controlling the forelimb in the cat. 8. Ascending projection to the lateral reticular nucleus from C3-C4 propriospinal also projecting to forelimb motoneurones. Exp Brain Res. 1981; 42, 282–298.

Alstermark B, Lundberg A & Sasaki S. Integration in descending motor pathways controlling the forelimb in the cat. 10. Inhibitory pathways to forelimb motoneurones via C3-C4 propriospinal neurones. Exp Brain Res. 1984; 56(2), 279–292.

Ballermann M & Fouad K. Spontaneous locomotor recovery in spinal cord injured rats is accompanied by anatomical plasticity of reticulospinal fibers. Eur J Neurosci. 2006; 23(8), 1988–1996.

Bareyre FM, Kerschensteiner M, Raineteau O, Mettenleiter TC, Weinmann O & Schwab ME. The injured spinal cord spontaneously forms a new intraspinal circuit in adult rats. Nat Neurosci. 2004; 7(3), 269–277.

Brus-Ramer M, Carmel JB, Chakrabarty S & Martin JH. Electrical stimulation of spared corticospinal axons augments connections with ipsilateral spinal motor circuits after injury. J Neurosci. 2007; 27(50),13793–13801.

Bunge RP, Puckett WR, Becerra JL, Marcillo A & Quencer RM. Observations on the pathology of human spinal cord injury. A review and classification of 22 new cases with details from a case of chronic cord compression with extensive focal demyelination. Adv Neurol. 1993; 59, 75-89.

Courtine G, Song B, Roy RR, Zhong H, Herrmann JE, Ao Y, Qi J, Edgerton VR, Sofroniew MV. Recovery of supraspinal control of stepping via indirect propriospinal relay connections after spinal cord injury. Nat Med. 2008; 14(1), 69–74.

Cowley KC, Zaporozhets E & Schmidt BJ. Propriospinal transmission of the locomotor command signal in the neonatal rat. Ann NY Acad Sci. 2010; 1198, 42–53.

Fernandes KJ, Fan DP, Tsui BJ, Cassar SL & Tetzlaff W. Influence of the axotomy to cell body distance in rat rubrospinal and spinal motoneurons: differential regulation of GAP-43, tubulins, and neurofilament-M. J Comp Neurol. 1999; 414(4), 495–510.

Filli L, Zörner B, Weinmann O, Schwab ME. Motor deficits and recovery in rats with unilateral spinal cord hemisection mimic the Brown-Sequard syndrome. Brain. 2011; 134(Pt8), 2261-2273.

Flynn JR, Graham BA, Galea MP & Callister RJ. The role of propriospinal interneurons in recovery from spinal cord injury. Neuropharmacology. 2011; 60(5), 809–822.

Foreman RD. Integration of viscerosomatic sensory input at the spinal level. Prog Brain Res. 2000; 122, 209–221.

Fouad K, Pedersen V, Schwab ME & Brosamle C. Cervical sprouting of corticospinal fibers after thoracic spinal cord injury accompanies shifts in evoked motor responses. Curr Biol. 2001; 11(22), 1766– 1770.

Fritschy JM & Grzanna R. Restoration of ascending noradrenergic projections by residual locus coeruleus neurons: compensatory response to neurotoxin-induced cell death in the adult rat brain. J Comp Neurol. 1992; 321(3), 421–441.

Ghosh A, Haiss F, Sydekum E, Schneider R, Gullo M, Wyss MT, Mueggler T, Baltes C, Rudin M, Weber B, Schwab ME. Rewiring of hindlimb corticospinal neurons after spinal cord injury. Nat Neurosci. 2010; 13(1), 97–104.

Ghosh A, Sydekum E, Haiss F, Peduzzi S, Zörner B, Schneider R, Baltes C, Rudin M, Weber B, Schwab ME. Functional and anatomical reorganization of the sensory-motor cortex after incomplete spinal cord injury in adult rats. J Neurosci. 2009; 29(39), 12210–12219.

Giehl KM & Tetzlaff W. BDNF and NT-3, but not NGF, prevent axotomy-induced death of rat corticospinal neurons in vivo. Eur J Neurosci. 1996; 8(6), 1167–1175.

Hagglund M, Borgius L, Dougherty KJ & Kiehn O. Activation of groups of excitatory neurons in the mammalian spinal cord or hindbrain evokes locomotion. Nat Neurosci. 2010; 13(2), 246–252.

Hendriks WT, Eggers R, Ruitenberg MJ, Blits B, Hamers FP, Verhaagen J & Boer GJ. Profound differences in spontaneous long-term functional recovery after defined spinal tract lesions in the rat. J Neurotrauma. 2006;. 23(1), 18–35.

Illert M, Jankowska E, Lundberg A & Odutola A. Integration in descending motor pathways controlling the forelimb in the cat. 7. Effects from the reticular formation on C3-C4 propriospinal neurones. Exp Brain Res. 1981; 42(3-4), 269–281.

Illert M & Lundberg A. Collateral connections to the lateral reticular nucleus from cervical propriospinal neurones projecting to forelimb motoneurones in the cat. Neurosci Lett. 1978; 7(2-3), 167–172.

Illert M, Lundberg A & Tanaka R. Integration in descending motor pathways controlling the forelimb in the cat. 3. Convergence on propriospinal neurones transmitting disynaptic excitation from the corticospinal tract and other descending tracts. Exp Brain Res. 1977; 29(3-4), 323–346.

Jankowska E. Interneuronal relay in spinal pathways from proprioceptors. Prog Neurobiol. 1992; 38(4), 335–378.

Kaeser M, Wyss AF, Bashir S, Hamadjida A, Liu Y, Bloch J, Brunet JF, Belhaj-Saif A, Rouiller EM. Effects of unilateral motor cortex lesion on ipsilesional hand's reach and grasp performance in monkeys: relationship with recovery in the contralesional hand. J Neurophysiol. 2010; 103(3), 1630–1645.

Kostyuk PG & Vasilenko DA. Spinal interneurons. Annu. Rev. Physiol. 1979 ; 41, 115–126.

Kuchler M, Fouad K, Weinmann O, Schwab ME & Raineteau O. Red nucleus projections to distinct motor neuron pools in the rat spinal cord. J Comp Neurol. 2002; 448(4), 349–359.

Lawrence DG & Kuypers HG. The functional organization of the motor system in the monkey. I. The effects of bilateral pyramidal lesions. Brain. 1968a, 91(1), 1–14.

Lawrence DG & Kuypers HG. Brain. The functional organization of the motor system in the monkey. II. The effects of lesions of the descending brain-stem pathways. Brain. 1968b;. 91(1), 15–36.

Little JW & Halar E. Temporal course of motor recovery after Brown-Sequard spinal cord injuries. Paraplegia. 1985; 23(1), 39–46.

Liu BP, Fournier A, GrandPré T, Strittmatter SM. Myelin-associated glycoprotein as a functional ligand for the Nogo-66 receptor. Science. 2002; 297(5584):1190-3.

Luo L & O'Leary DD. Axon retraction and degeneration in development and disease. Annu Rev Neurosci. 2005; 28, 127–156.

Maier IC, Baumann K, Thallmair M, Weinmann O, Scholl J & Schwab ME. Constraint-induced movement therapy in the adult rat after unilateral corticospinal tract injury. J Neurosci. 2008; 28(38), 9386–9403.

Maier IC & Schwab ME. Sprouting, regeneration and circuit formation in the injured spinal cord: factors and activity. Philos Trans R Soc Lond., Biol Sci. 2006; 361(1473), 1611–1634.

Matsuyama K, Mori F, Nakajima K, Drew T, Aoki M & Mori S. Locomotor role of the corticoreticular-reticulospinal-spinal interneuronal system. Prog Brain Res. 2004; 143, 239–249.

Norenberg MD, Smith J & Marcillo A. The pathology of human spinal cord injury: defining the problems. J Neurotrauma. 2004; 21(4), 429-440.

Nygren LG & Olson L. A new major projection from locus coeruleus: the main source of noradrenergic nerve terminals in the ventral and dorsal columns of the spinal cord. Brain Res. 1977. 132(1), 85–93.

Oohira A, Matsui F & Katoh-Semba R. Inhibitory effects of brain chondroitin sulfate proteoglycans on neurite outgrowth from PC12D cells. J Neurosci. 1991; 11(3), 822-827.

Pallini R, Fernandez E & Sbriccoli A. Retrograde degeneration of corticospinal axons following transection of the spinal cord in rats. A quantitative study with anterogradely transported horseradish peroxidase. J Neurosurg. 1988 ; 68(1), 124–128.

Paxinos G & Watson C. Elsevier Inc. 2009; 6, 12145–12158.

Peterson BW. Reticulospinal projections to spinal motor nuclei. Annu Rev Physiol. 1979; 41, 127–140.

Plunet W, Kwon BK & Tetzlaff W. Promoting axonal regeneration in the central nervous system by enhancing the cell body response to axotomy. J Neurosci. 2002; 68(1), 1–6.

Raineteau O & Schwab ME. Nat Rev Neurosci. 2001; 2(4), 263–273.

Rosenzweig ES, Courtine G, Jindrich DL, Brock JH, Ferguson AR, Strand SC, Nout YS, Roy RR, Miller DM, Beattie MS, Havton LA, Bresnahan JC, Edgerton VR, Tuszynski, MH. Extensive spontaneous plasticity of corticospinal projections after primate spinal cord injury. Nat Neurosci. 2010; 13(12), 1505–1510.

Rossi F, Buffo A & Strata P. Regulation of intrinsic regenerative properties and axonal plasticity in cerebellar Purkinje cells.Restor. Neurol Neurosci. 2001 ; 19(1-2), 85–94.

Rossignol S, Schwab M, Schwartz M & Fehlings MG. Spinal cord injury: time to move? J Neurosci. 2007; 27(44), 11782–11792.

Roth EJ, Park T, Pang T, Yarkony GM & Lee MY. Traumatic cervical Brown-Sequard and Brown-Sequard-plus syndromes: the spectrum of presentations and outcomes. Paraplegia. 1991; 29(9), 582–589.

Schmued LC, Albertson C & Slikker W. Fluoro-Jade: a novel fluorochrome for the sensitive and reliable histochemical localization of neuronal degeneration. Brain Res. 1997; 751(1), 37–46.

Schmued LC & Hopkins KJ. Fluoro-Jade B: a high affinity fluorescent marker for the localization of neuronal degeneration. Brain Res. 2000; 874(2), 123–130.

Schwab JM, Brechtel K, Mueller CA, Failli V, Kaps HP, Tuli SK, Schluesener HJ. Experimental strategies to promote spinal cord regeneration--an integrative perspective. Prog Neurobiol. 2006; 78(2), 91-116.

Schwab ME & Caroni P. J. Oligodendrocytes and CNS myelin are nonpermissive substrates for neurite growth and fibroblast spreading in vitro. J Neurosci. 1988; 8(7): 2381-93.

Schwab ME. Repairing the injured spinal cord. Science. 2002; 295(5557), 1029–1031.

Schwab ME & Bartholdi D. Degeneration and regeneration of axons in the lesioned spinal cord. Physiol Rev. 1996; 76(2), 319–370.

Sherrington C & Laslett E. Observations on some spinal reflexes and the interconnection of spinal segments. J. Physiol. 1903. 29(1), 58–96.

Siegel JM. Behavioral functions of the reticular formation. Brain Res. 1979; 180(1), 69–105.

Silver J & Miller JH. Regeneration beyond the glial scar. Nat Rev. Neurosci. 2004; 5(2), 146–156.

Tobias CA, Shumsky JS, Shibata M, Tuszynski MH, Fischer I, Tessler A, Murray M. Delayed grafting of BDNF and NT-3 producing fibroblasts into the injured spinal cord stimulates sprouting, partially rescues axotomized red nucleus neurons from loss and atrophy, and provides limited regeneration. Exp Neurol. 2003; 184(1), 97–113.

Vavrek R, Girgis J, Tetzlaff W, Hiebert GW & Fouad K. BDNF promotes connections of corticospinal neurons onto spared descending interneurons in spinal cord injured rats. Brain. 2006; 129(Pt6), 1534–1545.

Wang D. Reticular formation and spinal cord injury. Spinal Cord. 2009; 47(3), 204–212.

Webb AA & Muir GD. Compensatory locomotor adjustments of rats with cervical or thoracic spinal cord hemisections. J Neurotrauma. 2002; 19(2), 239–256.

Weidner N, Ner A, Salimi N & Tuszynski MH. Spontaneous corticospinal axonal plasticity and functional recovery after adult central nervous system injury. Proc Nat Acad Sci. U.S.A. 2001; 98(6), 3513–3518.

Wiessner C, Bareyre FM, Allegrini PR, Mir AK, Frentzel S, Zurini M, Schnell L, Oertle T, Schwab ME. Anti-Nogo-A antibody infusion 24 hours after experimental stroke improved behavioral outcome and corticospinal plasticity in normotensive and spontaneously hypertensive rats. J Cereb Blood Flow Metab. 2003; 23(2), 154–165.

Zhou L & Shine HD. Neurotrophic factors expressed in both cortex and spinal cord induce axonal plasticity after spinal cord injury. J Neurosci. Res. 2003; 74(2), 221–226.

Zörner B & Schwab ME. Anti-Nogo on the go: from animal models to a clinical trial. Ann NY Acad Sci. 2010; 1198 Suppl 1, 22–34.

Conclusion and Outlook

This thesis provides detailed information about motor physiology and neuronal network plasticity in adult rats upon unilateral cervical transection of the spinal cord. In this section, the results of the different projects will be discussed in relation to each another and will be put into the broad context of the existing literature. Moreover, potential supplementary experiments are suggested and discussed.

Comprehensive assessment of motor ability in rodents after central nervous system injury

In the first project, we constructed a behavioral setup enabling objective and quantitative profiling of rodent locomotion after different forms of neuropathology. Transgenic mice as well as rats with different spinal cord injuries and endothelin-1-induced stroke were tested in a battery of 4 different locomotor tests including skilled locomotion, overground walking, wading through shallow water, and swimming. The kinematic analysis of the recorded locomotor performance allowed objective and sensitive quantification of specific locomotor parameters. The evaluation of different types of locomotion has been shown to yield an overall locomotor profile which is highly specific for a particular type of lesion. Roughly summarized, dorsal hemisection of the thoracic cord revealed severe and persistent deficits in skilled locomotion, but relatively mild deficits in basic locomotor hindlimb parameters. In contrast, ventral transection of the thoracic spinal cord displayed much more severe dysfunctions in hindlimb locomotion, including partial or even total paralysis. Unilateral spinal cord hemisection at cervical spinal level resulted in robust recovery of hindlimb locomotion, but major persistent deficits in forelimb motor functions. These lesion outcomes were in line with earlier findings from different laboratories (Kiehn, 2006; Goulding, 2009; Grillner *et al.,* 2008; Eidelberg, 1981; Brustein and Rossignol, 1999; Webb and Muir, 2002 and 2005; Martinez *et al.,* 2009). However, the battery of tests generated lots of additional quantitative readouts which allowed a detailed quantification of lesion deficits and characterization of transgenic animals. The locomotor tests providing partial body weight support (wading, swimming) enabled very early assessment of locomotion even after severe forms of spinal cord injury. Such acute locomotor assessment is infeasible with common locomotor tests such as overground walking. The behavioral system demonstrated high sensitivity in that real restoration of locomotor function could be distinguished from compensatory strategies such as overuse of intact limbs. Finally it could be shown that particular locomotor parameters were better suited to quantify a certain lesion model than other parameters. Therefore, a list of accurate locomotor parameters best suited to quantify specific types of nervous

system injuries was generated. The implementation of such a comprehensive battery of locomotor tests is important as it can lead to more reliable and accurate functional assessments in the field of animal research.

Future experiments should use the growing data base of detailed locomotor parameters to perform mathematical cross-correlations (e.g. principal component analysis) between different locomotor parameters occurring after particular types of central nervous system injury. This optimized data analysis might lead to a better understanding of the global locomotor pattern resulting from specific forms of neuropathology, to detect complex functional effects of treatments, and to improve the value of the locomotor analysis to predict functional outcome.

Motor physiology of rats with C4/C5 unilateral spinal cord hemisection

Based on the behavioral setup described above, a detailed investigation of quadrupedal locomotion was performed in rats after unilateral C4/C5 hemisection. The locomotor analysis revealed substantial recovery of hindlimb locomotion which was clearly superior to the minor spontaneous recovery of the ipsilesional forelimb. Interestingly, this disproportional motor recovery pattern mimicked the primate (Rosenzweig *et al.,* 2010) and the human situation (Levi *et al.,* 1996). In order to elucidate potential reasons accounting for the asymmetric recovery of upper and lower limbs, we investigated the damage of cervical motor circuits by the cut lesion. Histological analysis revealed only a minor rostro-caudal lesion extent, which rendered direct damage of motor circuits (including cervical CPG networks) unlikely to account for the meager forelimb recovery. Retrograde neuroanatomical tracing of lumbar and cervical spinal segments revealed that the cervical spinal cord is more densely innervated by most descending supraspinal systems than the lumbar spinal cord, which is in line with anatomical findings in humans (Nathan, 1994). This anatomical result indicates that forelimb spinal circuits require more supraspinal control to exert motor function compared to the lumbar spinal circuits, which seem to be more autonomous from descending commands. This hypothesis is supported by recent experiments in cats which found that hindlimb motor circuits strongly depend on the spinal CPG networks and on sensory afferents, even if supraspinal inputs were present (Barrière *et al.,* 2008).

To facilitate locomotor performance in rats with unilateral C4/C5 hemisection, we applied different monoaminergic agonist intrathecally in animals 31 days post injury. In previous experiments, monoaminergic treatment has been demonstrated to be a potent facilitator of locomotion after total transection of the thoracic spinal cord in mice, rats, cats and monkeys (Forsberg and Grillner, 1973;

Barbeau and Rossignol, 1991; Fedirchuk *et al.,* 1998; Feraboli-Lohnherr *et al.,* 1999; Guertin, 2004; Antri *et al.,* 2003). Different to these results, application of monoaminergic agonist seemed to interfere with remaining supra- or proprio-spinal inputs in our experiment. Monoaminergic stimulation led to minor, often negative locomotor modulations of the hindlimbs, whereas the forelimbs were not affected by the agonists. Similar deteriorating effects upon monoaminergic application were observed in cats and rat models with incomplete thoracic spinal cord injury (Brustein and Rossignol, 1999; Hayashi *et al.,* 2010).

Summarized, these experiments indicate that fore- and hindlimb functionality differ considerably in response to unilateral ablation of descending tracts and to monoaminergic stimulation. Strongly simplified, forelimb motor physiology seems to be primarily optimized to flexibly target different muscle groups in order to execute complex motor tasks, whereas hindlimb functionality is mainly suited to exert stereotypic rhythmic locomotion. After unilateral cervical transection, forelimb motor function is permanently impaired and cannot be modulated by, for instance, the rather global monoaminergic drive, which is in contrast to the more autonomous hindlimb networks. Detailed neurophysiological investigations, as extensively performed for lumbar CPG networks (Barbeau and Rossignol, 1991; Duysens and van de Crommert, 1998; Courtine *et al*., 2009; Frigon *et al.,* 2010; Lungu *et al.,* 2010) are crucial for cervical motor circuits in order to understand forelimb physiology (e.g. role of sensory input for locomotor performance etc.). Moreover, the effects of restricted electrolytic lesions of specific motor brain areas on the motor performance of the forelimb (including skilled reaching tasks) could shed new light on the control of forelimb function. Lesioning defined motor brain systems would provide more precise conclusions about forelimb motor control than lesions at the level of the spinal cord, where the descending tracts can be scattered across the white matter. New insight into the neurophysiology and anatomy of cervical motor circuits will be important to design therapeutic interventions for enhanced arm/hand recovery after incomplete cervical spinal cord injury.

Finally, this project demonstrated that a particular treatment can affect functions very differently depending on the location and severity of the spinal cord injury. A detailed investigation of the lesion severity and location is required to understand and improve the efficacy of a given therapeutic intervention.

Neuroanatomical plasticity of bulbo- and propriospinal systems upon unilateral C4/C5 spinal cord hemisection

In addition to motor physiology, we investigated the spontaneous neuroanatomical rearrangements in supra- and intra-spinal neuronal circuits upon C4/C5 hemisection. Retrograde tracer injections were performed in the ipsilesional spinal segments C3/C4 to screen different supraspinal systems for anatomical plastic responses after axotomy. The screen revealed that the distinct descending systems react differently to axotomy. This is probably correlated with the cell-specific expression of growth-associated proteins, neurotrophic factors and other cell-specific properties (Tobias *et al.,* 2003). Descending fibers from the nucleus reticularis gigantocellularis (Giganto) and the caudal pons (PnC) displayed increased fiber sprouting rostral to the lesion which persisted up to 43 days post injury. Specific anterograde tracing of the Giganto and the PnC nucleus confirmed the massive sprouting response of axotomized Giganto fibers. The sprouting of Giganto fibers was selectively increased in the ventral laminae of the gray matter in the ipsilateral segments C3/C4. The colocalization of these fibers with the presynaptic marker vGLUT2 suggested their synaptic integration into the cervical spinal network. Retrograde tracing of the ipsilesional cervical enlargement (C6-C8) below the lesion revealed labelled neurons in the ipsilesional spinal segments C3/C4, suggesting re-crossing propriospinal C3-C4 neurons which innervate the denervated cervical enlargement. The location of these re-crossing propriospinal neurons in the gray matter matched the area of maximal sprouting of Giganto fibers. Indeed, confocal analysis showed close appositions of Giganto fibers onto apical dendrites (and less frequent onto the soma) of re-crossing propriospinal neurons, which in turn bridged the lesion site. Anterograde anatomical tracing at C3/C4 demonstrated that C3-C4 propriospinal fibers significantly increased their re-crossing projections to the ipsilesional cervical enlargement in response to the injury. Thus, the propriospinal relay of reticulospinal commands is amplified by direct sprouting of severed Giganto fibers and by increased re-crossing projections of C3-C4 propriospinal neurons around the lesion site.

There is rising evidence that the formation of intraspinal detour pathways is an important substrate for functional recovery after incomplete spinal cord injury (Flynn *et al.,* 2011). Bareyre and colleagues showed that axotomized corticospinal fibers specifically innervated long-propriospinal fibers, which projected to the lumbar spinal cord (Bareyre *et al.,* 2004). These anatomical rearrangements were associated with functional improvement and changed electrophysiological measurements. Moreover, Courtine and colleagues demonstrated in a model of thoracic staggered hemisections that, in the

absence of direct supraspinal projections to the lumbar spinal cord, intraspinal detour pathways were required to enable substantial hindlimb recovery in mice (Courtine *et al.,* 2008).

In this study we were able to specifically identify reticulospinal projections to rewire onto C3-C4 relaying neurons. Plasticity of reticulospinal fibers is particularly interesting, as these fibers are known to exert locomotor commands (Peterson, 1979; Wang, 2009). Thus, bridging of reticulospinal inputs might be associated with motor recovery after incomplete spinal cord injury.

Investigating the functional relevance of the observed propriospinal detour pathway is crucial. In future electrophysiological experiments we aim to specifically stimulate the nucleus reticularis gigantocellularis and to record evoked field potentials from specific areas in the cervical enlargement of acutely and chronically injured animals. This will allow us to state whether the relay truly conducts information from the ipsilesional brainstem to the denervated cervical enlargement. An increase of conduction from acute to chronic time points after the injury would strongly infer that the relay is not only of anatomical, but also of physiological relevance.

Moreover, specific functional ablation of the re-crossing C3-C4 population would clarify the physiological relevance of this cell population for motor performance. This might be achieved by injection of retrograde transsynaptic viral constructs in the ipsilesional segments C6-C8, which then could specifically label the re-crossing C3-C4 neuron population. Optogenetic inhibition or stimulation could modify the activity of these neurons, thereby disclosing their functional relevance.

Summarized, this dissertation provides new information about motor physiology and neuroanatomical plastic adaptations upon incomplete cervical spinal cord injury in adult rats. Interestingly, the motor physiology of fore- and hindlimb differ upon cervical spinal insult; spontanous motor recovery and effects of exogenously applied neuromodulators were very different in hindlimb and forelimb networks post injury. Further experiments including electrophysiology and ablation or functional blockade of specific supraspinal centres are needed to further analyze the differential motor control circuits of fore- and hindlimbs. Anatomical investigations in this thesis showed neuronal plasticity at different levels of the central nervous system following unilateral hemisection of the cervical spinal cord. Descending reticulospinal fibers and propriospinal neurons rostral to the lesion rearranged anatomically post injury, thus relaying supraspinal information to the denervated cervical enlargement. Electrophysiological experiments are currently performed to elucidate the functional relevance of this plastic propriospinal

relay. More refined methods including viral constructs and optogenetic manipulations will allow to draw specific conclusions about the functional role of the observed anatomical rearrangements.

References for conclusion and outlook

Antri M, Mouffle C, Orsal D, Barthe JY. 5-HT1A receptors are involved in short- and long-term processes responsible for 5-HT-induced locomotor function recovery in chronic spinal rat. Eur J Neurosci. 2003; 18(7): 1963-72.

Barbeau H, Rossignol S. Initiation and modulation of the locomotor pattern in the adult chronic spinal cat by noradrenergic, serotonergic and dopaminergic drugs. Brain Res. 1991; 546(2): 250-60.

Bareyre FM, Kerschensteiner M, Raineteau O, Mettenleiter TC, Weinmann O & Schwab ME. The injured spinal cord spontaneously forms a new intraspinal circuit in adult rats. Nat Neurosci. 2004; 7(3), 269–277.

Barriere G, Leblond H, Provencher J, Rossignol S. Prominent role of the spinal central pattern generator in the recovery of locomotion after partial spinal cord injuries. J Neurosci. 2008; 28(15): 3976-87.

Brustein E, Rossignol S. Recovery of locomotion after ventral and ventrolateral spinal lesions in the cat. II. Effects of noradrenergic and serotoninergic drugs. J Neurophysiol. 1999; 81(4): 1513-30.

Courtine G, Song B, Roy RR, Zhong H, Herrmann JE, Ao Y, Qi J, Edgerton VR, Sofroniew MV. Recovery of supraspinal control of stepping via indirect propriospinal relay connections after spinal cord injury. Nat Med. 2008; 14(1), 69–74.

Courtine G, Gerasimenko Y, van den Brand R, Yew A, Musienko P, Zhong H, Song B, Ao Y, Ichiyama RM, Lavrov I, Roy RR, Sofroniew MV, Edgerton VR. Transformation of nonfunctional spinal circuits into functional states after the loss of brain input. Nat Neurosci. 2009; 12(10): 1333-42.

Duysens J, Van de Crommert HW. Neural control of locomotion; The central pattern generator from cats to humans. Gait Posture. 1998; 7(2): 131-41.

Eidelberg E. Consequences of spinal cord lesions upon motor function, with special reference to locomotor activity. Prog Neurobiol. 1981; 17(3): 185-202.

Fedirchuk B, Nielsen J, Petersen N, Hultborn H. Pharmacologically evoked fictive motor patterns in the acutely spinalized marmoset monkey (Callithrix jacchus). Exp Brain Res. 1998; 122(3): 351-61.

Feraboli-Lohnherr D, Barthe JY, Orsal D. Serotonin-induced activation of the network for locomotion in adult spinal rats. J Neurosci Res. 1999; 55(1): 87-98.

Flynn JR, Graham BA, Galea MP & Callister RJ. The role of propriospinal interneurons in recovery from spinal cord injury. Neuropharmacology. 2011; 60(5), 809–822.

Forssberg H, Grillner S. The locomotion of the acute spinal cat injected with clonidine i.v. Brain Res. 1973; 50(1): 184-6.

Frigon A, Barrière G, Leblond H, Rossignol S. Asymmetric changes in cutaneous reflexes after a partial spinal lesion and retention following spinalization during locomotion in the cat. J Neurophysiol. 2009; 102(5), 2667-80.

Guertin PA. Synergistic activation of the central pattern generator for locomotion by l-beta-3,4-dihydroxyphenylalanine and quipazine in adult paraplegic mice. Neurosci Lett. 2004; 358(2): 71-4.

Goulding, M. Circuits controlling vertebrate locomotion: moving in a new direction. Nat Rev Neurosci 2009; 10, 507-518.

Grillner, S., Wallen, P., Saitoh, K., Kozlov, A. & Robertson, B. Neural bases of goal-directed locomotion in vertebrates--an overview. Brain Res Rev 2008; 57, 2-12.

Hayashi Y, Jacob-Vadakot S, Dugan EA, McBride S, Olexa R, Simansky K, Murray M, Shumsky JS. 5-HT precursor loading, but not 5-HT receptor agonists, increases motor function after spinal cord contusion in adult rats. Exp Neurol. 2010; 221(1): 68-78.

Kiehn, O. Locomotor circuits in the mammalian spinal cord. Annu Rev Neurosci 2006; 29, 279-306.

Levi AD, Tator CH, Bunge RP. Clinical syndromes associated with disproportionate weakness of the upper versus the lower extremities after cervical spinal cord injury. Neurosurgery. 1996; 38(1): 179-83; discussion 83-5.

Lungo O, Frigon A, Piché M, Rainville P, Rossignol S, Doyon J. Changes in spinal reflex excitability associtiated with motor sequence learning. J Neurophysiol. 2010; 103(5), 2675-83.

Martinez M, Brezun JM, Zennou-Azogui Y, Baril N, Xerri C. Sensorimotor training promotes functional recovery and somatosensory cortical map reactivation following cervical spinal cord injury. Eur J Neurosci. 2009; 30(12): 2356-67.

Nathan PW. Effects on movement of surgical incisions into the human spinal cord. Brain. 1994; 117 (Pt 2): 337-46.

Peterson BW. Reticulospinal projections to spinal motor nuclei. Annu Rev Physiol. 1979; 41, 127–140.

Rosenzweig ES, Courtine G, Jindrich DL, Brock JH, Ferguson AR, Strand SC, Nout YS, Roy RR, Miller DM, Beattie MS, Havton LA, Bresnahan JC, Edgerton VR, Tuszynski MH. Extensive spontaneous plasticity of corticospinal projections after primate spinal cord injury. Nat Neurosci. 2010; 13(12): 1505-10.

Tobias CA, Shumsky JS, Shibata M, Tuszynski MH, Fischer I, Tessler A, Murray M. Delayed grafting of BDNF and NT-3 producing fibroblasts into the injured spinal cord stimulates sprouting, partially rescues axotomized red nucleus neurons from loss and atrophy, and provides limited regeneration. Exp Neurol. 2003; 184(1), 97–113.

Wang D. Reticular formation and spinal cord injury. Spinal Cord. 2009; 47(3), 204–212.

Webb AA, Muir GD. Compensatory locomotor adjustments of rats with cervical or thoracic spinal cord hemisections. J Neurotrauma. 2002; 19(2): 239-56.

Webb AA, Muir GD. Sensorimotor behaviour following incomplete cervical spinal cord injury in the rat. Behav Brain Res. 2005; 165(2): 147-59.

Appendix

Author's contribution:

Chapter 1:

LF prepared the review. MES supervised the writing.

Chapter 2:

BZ and LF designed the study, developed the testing setup, performed surgeries, collected and analyzed data, made the figures and prepared the manuscript. MLS developed stroke lesions, performed surgeries and prepared the manuscript. RG developed the EMG setup, performed the recordings and collected data. HK developed the testing setup and the software. MR performed surgeries, and collected and analyzed data. MB developed the software and collected and analyzed data. MES designed the study, prepared the manuscript, and conceived and supervised the study.

Chapter 3:

LF designed the experiment, performed surgical and histological procedures, collected and analyzed data and prepared the manuscript. BZ designed the experiment and performed surgery. OW performed histological procedures. MES designed the experiment and prepared the manuscript.

Chapter 4:

LF designed the experiment, performed surgical and histological procedures and analyzed data. AKE performed surgical and histological procedures and anlalyzed data. BZ designed the study and performed surgeries. LB and MG performed surgeries. MG performed histological processing. Most parts of this study were performed during the master thesis of AKE, which was supervised by LF. Data are identical to this master thesis. The figures are, except from figures 1 and 4, unchanged. The text has been rewritten and reformulated.

Curriculum Vitae

Linard Peider Filli

Born: March 12th 1984 in Zürich

Citizen of Davos, Graubünden, Switzerland

Education:

09.2008 - 11.2011	PhD student at the laboratory of Prof. Martin E. Schwab; Brain Research Institute of the University of Zurich and the ETH Zurich. Title of doctoral thesis: *Motor physiology and neural network anatomy in rats following incomplete cervical spinal cord injury*
10.2006 - 06.2008	Master of Science ETH in Biology; Major in Neuroscience Master thesis supervised by Dr. Björn Zörner in the lab of Prof. Martin E. Schwab. Title of master thesis: *Structural plasticity of spared reticulospinal projections is associated with locomotor recovery after incomplete spinal cord injury in rats*
01.2006 – 07.2006	Student Exchange Program; Northwestern University Evanston/Chicago Biology Department; Research project in the lab of Assistant Professor MD Jaime Grutzendler about endocytotic processes in cortical neurons.
10.2003 – 09.2006	Bachelor of Science ETH in Biology
08.1997 - 06.2003	Gymnasium Schweizerische Alpine Mittelschule Davos

Academic honors:

2002 Award of „Schweizer Jugend forscht“ for the work about:

Die Winterruhe des Dachses in der Region Davos-Horlauben

Talks, Posters and Tutorials:

03.2009 - 08.2011 Associate member of the Christopher and Dana Reeve Foundation (CDRF). Active participation in meetings in San Diego (2x), Chicago, New Jersey, Ittingen (Switzerland) and Cambridge.

10. 2009 L. Filli, B. Zörner, M. Röthlisberger and M. E. Schwab: *Modulation of forelimb locomotor function by serotonergic treatment after incomplete cervical spinal cord injury in adult rats.* Poster at Society for Neuroscience (SFN) meeting, Chicago, 2009.

11.2010 L. Filli, B. Zörner, A. Engmann, O. Weinmann, M. E. Schwab: *Locomotor responsiveness to monoamines differs between fore- and hindlimb networks in rats after incomplete cervical spinal cord injury.* Poster at Society for Neuroscience (SFN) meeting, San Diego, 2010.

07.2010 TOPEA (**T**ranseuro, **O**ptistem, **P**lasticise, **E**ndostem, **A**ngioscaff) Meeting in Barcelona. Talk: *Neuronal regeneration and plasticity after spinal cord injury*

08.2010 Measuring Behavior 2010 in Eindhoven. Tutorial: *The MotoRater: A new, standardized testing system for quantification of locomotor impairment in rodents with CNS damage*

Publications:

Profiling locomotor recovery: comprehensive quantification of impairments after CNS damage in rodents. Filli L[*], Zörner B[*], Starkey ML, Gonzenbach R, Kasper H, Röthlisberger M, Bolliger M, Schwab ME. [*] contributed equally to this work.

Nature Methods. 2010 7:701-8.

Motor deficits and recovery in rats with unilateral spinal cord hemisection mimic the Brown-Séquard syndrome. Filli L, Zörner B, Weinmann O, Schwab ME.

Brain. 2011 134:2261-73.

Acknowledgement

It is hardly feasible to thank everyone who supported me during the period of my doctoral thesis. In this acknowledgement I want to thank at least the most important people who helped me during this time.

First I want to thank Professor Martin Schwab. Martin was an excellent PhD supervisor, who always found time if I needed his scientific advice. He showed me how to design, to organize and perform goal-directed research without neglecting interesting and unexpected results in the periphery of the project. The huge enthusiasm which Martin daily exemplified fascinated my throughout my whole thesis and was an important drive for my PhD.

Dr. Björn Zörner was a very important person during my thesis. Björn fostered me from the very beginning of my time at the Brain Research Institute. As supervisor of my master thesis, he instructed me in diverse laboratory techniques, basic theoretical knowledge and scientific discussion during my master thesis and throughout large parts of my PhD. Thank you very much Björn!

I want to thank the "Spinal cord injury - mini group" including Lukas Bachmann, Miriam Gullo, Anne Engmann and Sandra Kapitza. Without the internal group support, the performance of *in vivo* experiments is hardly feasible. Also outside of the institute it was always great to spend time with you.
I want to thank Dr. Lisa Schnell for proofreading parts of my doctoral thesis. Special thanks to Anne Engmann, who performed her master thesis under me supervision. Our team work was very pleasant and productive. It was great fun to supervise you.

Thanks for the technical support (Oliver Weinmann, Miriam Gullo, Hansjörg Kaspar and Regula Schneider), for the support in the thesis coordination (Anita Buchli) and administration (Minou Nadjafpour, Tanya Bülbül-Aydinalp), and for the support in animal care (Gisep Bazzell and his team).

Thank you to all the members of the lab. It was very nice to spend time in the great atmosphere of the lab.

Besides the direct support in the lab, I enjoyed also a lot of support in my private environment. Thanks to my lab colleagues and to all of my friends with whom I spent a lot of time outside of the lab.
Speziellen Dank an meine ganze Familie, die grosses Verständnis dafür aufbrachte, dass ich oft sehr mit meinen Doktoratsstudien beschäftigt war. Meine Eltern und meine Geschwister unterstützten mich vorbildlich in allen Lebenssituationen und stand mir jederzeit mit gutem Rat zur Seite. Danke vielmals, das ist alles andere als selbstverständlich!

Speziellen Dank auch an Julia, die mich besonders in den letzten Zügen meiner Doktorarbeit sehr oft mental unterstützt hat und mich täglich motivierte weiter zu machen. Ohne sie wäre mir das Ganze sicherlich schwerer gefallen.